HAL
archives-ouvertes.fr

Slab fragmentation beneath the Aegean/Anatolia transition zone: Insights from the tectonic and metamorphic evolution of the Eastern Aegean region

Vincent Roche, Laurent Jolivet, D. Papanikolaou, Erdin Bozkurt, Armel Menant, G. Rimmelé

▶ **To cite this version:**

Vincent Roche, Laurent Jolivet, D. Papanikolaou, Erdin Bozkurt, Armel Menant, et al.. Slab fragmentation beneath the Aegean/Anatolia transition zone: Insights from the tectonic and metamorphic evolution of the Eastern Aegean region. Tectonophysics, Elsevier, 2019, 754, pp.101-129. 10.1016/j.tecto.2019.01.016 . insu-02012398

HAL Id: insu-02012398
https://hal-insu.archives-ouvertes.fr/insu-02012398

Submitted on 19 Feb 2019

HAL is a multi-disciplinary open access archive for the deposit and dissemination of scientific research documents, whether they are published or not. The documents may come from teaching and research institutions in France or abroad, or from public or private research centers.

L'archive ouverte pluridisciplinaire **HAL**, est destinée au dépôt et à la diffusion de documents scientifiques de niveau recherche, publiés ou non, émanant des établissements d'enseignement et de recherche français ou étrangers, des laboratoires publics ou privés.

Accepted Manuscript

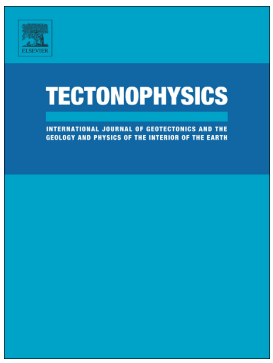

Slab fragmentation beneath the Aegean/Anatolia transition zone: Insights from the tectonic and metamorphic evolution of the Eastern Aegean region

V. Roche, L. Jolivet, D. Papanikolaou, E. Bozkurt, A. Menant, G. Rimmelé

PII: S0040-1951(19)30009-5
DOI: https://doi.org/10.1016/j.tecto.2019.01.016
Reference: TECTO 128039

To appear in: *Tectonophysics*

Received date: 8 August 2018
Revised date: 15 January 2019
Accepted date: 17 January 2019

Please cite this article as: V. Roche, L. Jolivet, D. Papanikolaou, et al., Slab fragmentation beneath the Aegean/Anatolia transition zone: Insights from the tectonic and metamorphic evolution of the Eastern Aegean region, Tectonophysics, https://doi.org/10.1016/j.tecto.2019.01.016

This is a PDF file of an unedited manuscript that has been accepted for publication. As a service to our customers we are providing this early version of the manuscript. The manuscript will undergo copyediting, typesetting, and review of the resulting proof before it is published in its final form. Please note that during the production process errors may be discovered which could affect the content, and all legal disclaimers that apply to the journal pertain.

ACCEPTED MANUSCRIPT

Slab fragmentation beneath the Aegean/Anatolia transition zone: insights from the tectonic and metamorphic evolution of the Eastern Aegean region

V. Roche[1, 2, 3*], L. Jolivet[4], D. Papanikolaou[5], E. Bozkurt[6, 7], A. Menant[8] and G. Rimmelé[9]

[1]*Université d'Orléans, ISTO, UMR 7327, 45071, Orléans, France*
[2]*CNRS/INSU, ISTO, UMR 7327, 45071 Orléans, France*
[3]*BRGM, ISTO, UMR 7327, BP 36009, 45060 Orléans, France*
[4] *Sorbonne Université, CNRS-INSU, Institut des Sciences de la Terre Paris, ISTeP UMR 7193, F-75005 Paris, France*
[5] *Department of Geology and Geoenvironment, National & Kapodistrian University of Athens, Zografou 15784, Greece*
[6]*Middle East Technical University, Department of Geological Engineering, Üniversiteler Mahallesi, Dumlupınar Bulvarı No: 1, 06800 Ankara, Turkey*
[7]*Center for Global Tectonics & State Key Laboratory of Geological Processes and Mineral Resources, China University of Geosciences, Wuhan, 388 Lumo Road, Hongshan District, Wuhan 430074, Hubei Province, China*
[8]*Institut de Physique du Globe de Paris, Sorbonne Paris Cité, Univ. Paris Diderot, CNRS, F-75005 Paris, France*
[9]*Total SA - CSTJF, Avenue Larribau, 64000 Pau, France*

* Corresponding author: Vincent Roche: vincent.roche@cnrs-orleans.fr (vincent.roche@sorbonne-universite.fr from 2019).

ACCEPTED MANUSCRIPT

1. Introduction

Slab rollback and tearing are common features in subduction zones and have a strong impact on the tectonic and metamorphic evolution of the overriding plate [e.g. Dewey, 1988; Royden, 1993; Wortel & Spakman, 2000; Govers & Wortel, 2005; Jolivet et al., 2013; Sternai et al., 2014]. One of the best examples to study consequences of this slab dynamics is located in the Eastern Mediterranean region, where numerous mantle tomography studies elucidate the deeper lithosphere structures [Bijward et al., 1998; De Boorder et al., 1998; Piromallo & Morelli, 2003; Wortel & Spakman, 2004; Li et al., 2008; Berk Biryol et al. 2011; Salaün et al., 2012; Delph et al., 2015]. Although results show a clear ~ 200 km-depth low-velocity anomaly below western Turkey interpreted as a major tear in the Hellenic slab, there is no consensus about the causes of this tearing and its consequences on the time-space tectonic and metamorphic evolution in the overriding plate [e.g. Dilek & Altunkaynak, 2009; Papanikolaou, 2013; Jolivet et al., 2015; Menant et al., 2016a; Gover & Fichtner 2016]. Some studies suggest the existence of (i) a wide sinistral lithospheric-scale shear zone accommodating different finite rates of back-arc extension due to the slab tear [Gessner et al., 2013; Jolivet et al., 2015], (ii) a localized NE-SW striking transfer zone [e.g. Uzel et al., 2015], and (iii) regional variations (e.g. Samos) induced by a sinistral wrench component that was superimposed on the regional NNE-SSW extension [Ring et al., 2017]. However, few field observations of ductile and brittle markers and their link with the metamorphic evolution exist in the Eastern Mediterranean domain that occupies a key-position at the transition between the Aegean domain and western Turkey.

ACCEPTED MANUSCRIPT

To better understand the crustal consequences of tearing, and thus the geodynamic evolution of the Eastern Mediterranean domain, it appears therefore crucial to clarify (i) the geological correlations between the Cyclades and the Menderes Massif that have often been disputed due to significant lithological differences [e.g. Ring et al., 1999a; Jolivet et al., 2004a] and (ii) the distribution of kinematic indicators and the extent of metamorphic events in this region since the initiation of the tear. However, apart from the recent work of Ring et al. [2017] focusing on brittle deformation, very few geological studies [e.g. Franz & Okrusch, 1992; Franz et al., 2005; Roche et al., 2018a] were devoted so far to those islands located in the western Aegean domain (e.g. Fourni, Arki, Lipsi and Leros) (Fig. 1). We therefore focus on these islands, by describing for the first time a complete regional scheme of ductile kinematic indicators and associated pressure-temperature (P-T) conditions. We thus shed light on the possible relations between the Cyclades and the Menderes Massif and, finally, we discuss the evolution of the tear in the subducting African lithosphere and its consequences on the upper plate tectonic history.

2. Geological setting

2.1. Geodynamic evolution of the eastern mediteranean region

Since the early Cenozoic at least, a single lithospheric slab has been continuously subducting northward below the Aegean region and the Anatolides - Taurides, accommodating most of the slow convergence between Africa and Eurasia during the closure of the Neotethys oceanic realm [e.g. Spakman et al., 1988; Faccenna et al., 2003; Jolivet et al., 2003; Van Hinsbergen et al., 2005; 2010a; Jolivet & Brun, 2010; Papanikolaou, 2013; Pourteau et al.,

ACCEPTED MANUSCRIPT

2013]. After the closure of the Vardar Ocean in the late Cretaceous-Paleocene, subduction of Africa-derived continental blocks below Eurasia led to the formation of a crustal-scale orogenic wedge (i.e. the Hellenides and the Taurides) [Brunn, 1956; Aubouin, 1959; Brunn et al., 1970; Jacobshagen et al., 1978], by decoupling tectonic nappes from the subducting lithosphere [Brunn et al., 1976; Bonneau & Kienast, 1982; Jolivet et al., 2003; van Hinsbergen et al., 2005; Brun & Faccenna, 2008; Jolivet & Brun, 2010; Ring et al., 2010]. These nappes consist of coherent stratigraphic sequences and sedimentary facies, each characterizing a paleogeographic environment. Most of these nappes have also recorded different pressure-temperature (P-T) metamorphic conditions such as (i) high-pressure and low-temperature metamorphism (HP-BT) (e.g. in the Tavşanlı Zone [Okay, 1984; 2002; Plunder et al., 2013]; in the Afyon Zone [e.g. Candan et al., 2005; Pourteau et al., 2014] and its equivalent in the southwestern part of Turkey, i.e. the HP Lycian Nappe [e.g. Oberhänsli et al., 2001; Rimmelé et al., 2003a] recently renamed Ören unit by Pourteau et al. [2013] (see Appendix for more information); the Cycladic Blueschists Unit (CBU) [e.g Blake et al., 1981; Bonneau & Kienast, 1982; Trotet et al., 2001]) and (ii) barrovian-type metamorphism (e.g. in the Tavşanlı Zone [e.g. Seaton et al., 2009]; in the Menderes Massif [e.g. Sengör et al., 1984; Régnier et al., 2003] (see Appendix)). Despite the importance of the post-orogenic overprint on orogenic architecture, various correlations (e.g. stratigraphy, tectono-metamorphic history) have been proposed between Greece and Turkey in the Aegean region [Brunn et al., 1976; Dürr et al., 1978; Papanikolaou & Demirtasli, 1987; Robertson et al., 1991; Papanikolaou, 1997; Göncüoğlu et al., 1997; Ring et al., 1999a; Jolivet et al., 2004b].

ACCEPTED MANUSCRIPT

Since the Early Oligocene, the collapse of the Hellenides-Taurides belt and post-orogenic extension in this region have been mainly controlled by the progressive southward retreat of the African slab [e.g. Le Pichon & Angelier, 1979; Lister et al., 1984; Jolivet & Faccenna, 2000; Jolivet & Brun, 2010], but also by the tear below western Turkey (e.g. see tomographic studies of Spakman et al. [1988], Govers & Wortel [2005] and Berk Biryol et al. [2011]). The nappe stack was cut by extensional low-angle normal faults leading to the exhumation of a series of metamorphic core complexes (MCCs) along a warm geotherm, leading to crustal anatexy [Lister et al., 1984; Avigad & Garfunkel, 1989; 1991; Gautier & Brun, 1994; Jolivet et al., 2004b]. For instance, in the Aegean domain, top-to-the-NE detachments described in the northern part of the Cyclades link up to form the crustal-scale North Cycladic Detachment System [NCDS, Jolivet et al., 2010]. In addition, the Naxos-Paros Detachment System (NPDS) exhumed magmatic gneiss, metapelites and marbles through a top-to-the-NE shearing event in the central part of Cyclades [e.g. Urai et al., 1990; Buick, 1991; Gautier et al., 1993]. Top-to-the-SW kinematics was also described in the western part of the Cyclades linked into a single major detachment system named the West Cycladic Detachment System (WCDS [Grasemann et al., 2012]). In western Anatolia, the exhumation of the Menderes Massif Core Complex is also mainly accommodated by three detachments: (i) the top-to-the-S Büyük Menderes detachment [e.g. Hetzel et al., 1995a; Gessner et al., 2001], (ii) the top-to-the-NNE Gediz detachment (also named Alaşehir or Kuzey detachment) [e.g. Hetzel et al., 1995a; 1995b; Gessner et al., 2001; Lips et al., 2001] and (iii) the top-to-the-NE the Simav detachment [e.g. Işık & Tekeli, 2001].

The present-day context is characterized by a more localized extension, notably in the central part of the Menderes Massif [Seyítoğlu et al., 1992; Seyítoğlu & Scott, 1996; Aktug et

ACCEPTED MANUSCRIPT

al., 2009]. The Cyclades and the Menderes Massif are also part of the Anatolia-Aegean domain that is currently extruding at a fast rate along the dextral North Anatolian Fault (NAF) since 5 Ma (Fig. 1) [McKenzie, 1972; Barka, 1992; Le Pichon et al., 1995; McClusky et al., 2000; Reilinger et al., 2006; 2010]. In addition, instantaneous GPS velocities further show that the Aegean domain moves faster to the southwest than the Anatolian plate, the difference being accommodated by the active extension [Le Pichon et al., 1995; Armijo et al., 1999; McClusky et al., 2000; Jolivet, 2001].

To sum-up, the Aegean-Western Turkey area has recorded the complete succession of tectonic episodes from the Late Cretaceous subduction to the Paleocene-Eocene continental accretion and crustal thickening, and the Late Oligocene to Present back-arc extension [e.g. Le Pichon & Angelier, 1981; Bonneau, 1982; Papanikolaou, 1987; Jolivet & Faccenna, 2000; Jolivet et al., 2004a]. Most of the history of this region is thus controlled by regional stresses imposed by the retreating and tearing subducting lithosphere [e.g. Le Pichon & Angelier, 1979; Mercier et al., 1989; Faccenna et al., 2006; Jolivet et al., 2013; Sternai et al., 2014]. In the following, we present only the main units across the Eastern Aegean domain, other units belonging to the western and central Aegean domain and to Western Turkey are presented in Appendix.

2.2. Geology of the Eastern Aegean islands

2.2.1. Samos

ACCEPTED MANUSCRIPT

Several studies were devoted to Samos Island that occupies a key-position at the transition between Aegean domain and western Turkey (Figs. 1, 2a and 2c) [Mposkos, 1978; Papanikolaou, 1979; Theodoropoulos, 1979; Mposkos & Perdikatsis, 1984; Weidmann et al., 1984; Mezger & Okrusch, 1985; Okrusch et al., 1984; Chen, 1995; Will et al., 1998; Ring et al., 1999b; Ring et al., 2007]. The metamorphic succession of Samos consists of four distinct tectono-metamorphic units, from the base to the top. (i) The Kerketeas marbles crop out in the western part of the island in a tectonic window below the overlying Ampelos unit [Papanikolaou, 1979; Theodoropoulos, 1979; Ring et al., 1999b]. The tectonic contact between these units is named Pythagoras Thrust. The Kerketeas unit consists in a monotonous sequence of dolomitic marbles with local schist on top that can be correlated with the Basal Unit [Ring et al., 2001], i.e. the Gavrovo-Tripolitza nappe. Iincipient HP-LT metamorphism and a subsequent greenschist overprint is recorded [Mposkos, 1978]. (ii) The Ampelos unit outcrops over the central part of the island (Fig. 2a). We include in this unit the Agios Nikolaos unit distinguished by some authors [Ring et al., 1999b]. It is mainly made of metasediments (e.g. schists and marbles) with minor occurrences of metabasites. The lower part contains slices of gneiss that provided Carboniferous and Triassic radiometric ages on zircons [Ring et al., 1999b]. This unit can be correlated with the lower part of the CBU [Ring et al., 1999b]. The Ampelos nappe underwent an Eocene blueschist-facies metamorphic event (520 °C, 19 kbar), followed by an Oligo-Miocene overprint under greenschist-facies conditions (455 – 485 °C, 6 – 7 kbar) [Okrusch et al., 1984; Chen, 1995; Chen et al., 1995; Will et al., 1998]. (iii) The Selçuk nappe crops out in the center of the island as discontinuous outcrops of metabasites (Fig. 2a) [Ring et al., 1999b]. It is similar in terms of lithology to the ophiolitic mélange metamorphosed in HP-LT conditions in the upper

ACCEPTED MANUSCRIPT

part of the CBU, for instance in Syros and Sifnos (Fig. 2a) [Okrusch & Bröcker, 1990]. (iv) The Vourliotes nappe crops out in the eastern part of the island where it is mainly made of schists and marbles (Fig. 2a). The upper marble formation has been dated as Upper Cretaceous on the basis of rudists found within the metabauxite outcrops at the eastern part of the island [Papanikolaou, 1979]. It recorded the same metamorphic conditions as the Ampelos nappe [Ring et al., 1999b]. (v) The Kallithea nappe and the Katavasis Complex are only found in the westernmost part of the island, on top of Kerketeas marbles. Here, we merged both units in the Kallithea nappe that can be correlated with the Upper Cycladic Nappe where no evidence for a Cenozoic HP-LT metamorphism is observed. The Kallithea nappe is made of sandstones, serpentinized peridotite lenses, spilite and diabase with red radiolarites and fossiliferous ammonitico rosso-type limestones overlain by an Upper Triassic to Jurassic massive limestone series [Papanikolaou, 1979; Theodoropoulos, 1979]. The underthrusted Katavasis Complex is mainly composed of marbles, amphibolites and quartzites, formed under amphibolite-facies conditions [Mezger & Okrusch, 1985; Chen, 1995]. It is locally intruded at ~10 Ma by igneous dykes cut by a distinct low-angle normal fault [Ring et al., 1999b], suggesting a younger activity of this fault that is interpreted as an extension of the NCDS [Jolivet et al., 2010].

A large surface of Samos is covered by Mio-Pliocene sedimentary basins [Theodoropoulos, 1979; Weidmann et al., 1984] (Fig. 2a). K-Ar age data (on sanidine and biotite in tuffaceous rocks) of Weidmann et al. [1984] provide age constraints for sedimentary rocks. From 12 Ma and 9 Ma one can observe conglomerates with locally-derived pebbles of basement, then the freshwater limestones Pythagorion formation, volcanoclastic rocks (i.e. basalt and tuff), formed 11 Myrs ago, overlain by the Hora formation grading from thick-bedded

ACCEPTED MANUSCRIPT

limestones to thin-bedded diatomaceous shales and, finally, thinly bedded limestones deposited some 9 Ma ago. The upper cycle, formed between 8.6 and 6.2 Ma, starts with the Mytilini formation, made of conglomerates and tuffaceous marls that rests unconformably above the Hora or the Pythagorion formation. The upper cycle ends with the Kokkari formation made of lacustrine limestones attributed to the Pliocene.

According to Ring et al. [1999b], the tectono-metamorphic units of Samos have recorded five successive deformation stages. D_1 and D_2 stages are associated with the HP-LT metamorphic event and show a roughly consistent E-W orientation with bivergent sense of shear. They correspond to the thrusting of the Ampelos nappe onto the Kerketeas marbles in the western part of the island. D_3 event corresponds to the greenschist-facies metamorphism associated with crustal extension. This event is mainly associated with ESE-WSW transport direction, except in the core of the Ampelos nappe where D_3 stretching lineation displays a N-S orientation with top-to-the-N and top-to-the-S kinematic indicators. Ring et al. [1999b] therefore conclude to a large component of coaxial strain during the exhumation of these units. Finally, D_4 corresponds to a short contractional brittle event between 8.6 and 9 Ma whereas D_5 is extensional, corresponding to the formation of N-S trending high-angle normal faults.

2.2.2. Fourni and Thymaena islands

Whereas Thymaena Island benefited from a map coverage by the study of Papanikolaou [1980], there is no geological map available of Fourni Island (Figs. 2b and 2c). In Thymaena, the non-metamorphic succession from the middle to upper Triassic consists in sandstones and red

ACCEPTED MANUSCRIPT

nodular limestones with mafic igneous rocks, and white dolomites and neritic limestones with megalodon. A series of north-directed thrusts affected this sequence (Fig. 2b). According to Papanikolaou [1980], thrusting may be related to the middle-upper Miocene period.

2.2.3. Dodecanese islands

Dodecanese islands (Figs. 1 and 3) were mapped by Desio [1931] and then by the Greek Geological Survey (IGME) (e.g. Leros geological map from Stavropoulos & Gerolymatos [1999]). However, the tectono-metamorphic evolution of Kalymnos, Leros, Lipsi and Arki remains fragmentary. The metamorphic succession consists in the tectonic superimposition of two tectono-metamorphic units, i.e. the Marina and Temenia units from the top to the base, respectively [Franz et al., 2005; Roche et al., 2018a]. Furthermore, a thin Neogene to recent sedimentary cover is also present on Leros and Lipsi (Fig. 3).

Outcrops of Marina unit are well exposed in Kalimnos and Leros and locally in the southeastern part of Lipsi (Figs. 3c and 3d). The first-order architecture of this unit is defined by crystalline rocks that are transgressively overlain by weakly metamorphosed, violet schists, conglomerates and sandstones, which grade upwards into upper Triassic to Liassic dolomites and limestones. On Leros Island, this contact juxtaposes low-grade metamorphism schists with amphibolites and kyanite-staurolite-garnet micaschist yielding ages between 320 and 230 (amphibole and white micas [Franz et al., 2005]). According to Papanikolaou [2013], these formations are similar to the volcano-sedimentary-type Tyros Beds at the base of the Tripolis unit in the Hellenides. Conversely, Dürr et al. [1978] suggest that the sedimentary formation of

ACCEPTED MANUSCRIPT

Marina unit correspond to units of the Lycian Nappes in SW Turkey, which consists, from base to top, of (i) a parautochthonous unit, mainly composed of shallow-water and pelagic limestones from Late Cretaceous to Early Miocene age; (2) an intermediate complex consisting of thrust sheets comprising shallow-water limestones, dolomites, pelagic and turbiditic cherty limestones and flysch from Middle Triassic to Cenomanian, topped by an assemblage of basaltic pillow lavas and (3) a large peridotite nappe with serpentinites and fragments of doleritic dykes [Bernoulli et al., 1974]. It is followed by well-bedded upper Jurassic to lower Cretaceous (?) limestone with cherty replacement [Dürr, 1975; Dürr et al., 1978; Franz et al., 2005]. Crystalline rocks are represented by the Panormos and Emporios units [Franz et al., 2005]. The first consists mostly in a succession of marbles, plagioclase gneisses and kyanite-staurolite-garnet micaschists with intercalations of banded epidote and garnet amphibolites. The base of this unit is formed of fine-grained schist and minor coarse-grained massive amphibolite with a thickness of about 100 m. The overlying Emporios unit is made of albite gneisses and chloritoid-biotite schists [Franz et al., 2005]. K-Ar dating of the basement rocks of the Dodecanese islands shows Variscan ages partially reset by a very low-grade Alpine overprint, suggesting a polyphased deformation [Franz et al., 2005].

The underlying Temenia unit is mainly exposed in Arki, Lipsi and Leros (Fig. 3) and consists of late Paleozoic to Mesozoic sediments affected by an Alpine HP-LT metamorphism [Franz & Okrusch, 1992]. It consists of interlayered phyllites, micaschists, quarzites and marbles with rare occurrences of metabasites. The presence of Mg-riebeckite, glaucophane and aragonite in Leros and Arki islands [Katagas & Sapountzis, 1977; Katagas, 1980; Franz & Okrusch, 1992; Roche et al., 2018a], implies a subduction-related metamorphism with a

ACCEPTED MANUSCRIPT

minimum pressure of ~ 8 kbar. Roche et al. [2018a] show that glaucophane/Mg-riebeckite is locally preserved and may destabilize into winchite, suggesting a greenschist-facies overprint. Dürr [1975] considers this unit as an equivalent of the Kara Dag unit in the Lycian Nappes of western Turkey (Fig. 1). However, Roche et al. [2018a] challenged this hypothesis, suggesting that this unit belongs to the Lower Cycladic Blueschist Nappe (LCB) as attested by the similar P-T conditions as on Folegandros and Milos islands [Augier et al., 2015; Grasemann et al., 2018]. For more information about this sub-unit which belonging to the CBU, it is possible to refer to the studies of Grasemann et al. [2018] and Roche et al. [2018a].

Crustal-scale tectonic evolution of Dodecanse islands is still poorly known. Nonethess, a recent study of Roche et al. [2018a] on Leros reveals that Temenia unit has been exhumed under Marina unit through a top-to-the-NE ductile shearing. Deformation is thus preferentially localized along the main tectonic contact (i.e. Temenia shear zone), although second-order ductile shear zones with similar kinematics are also evidenced, especially along lithological contacts such as marble - schist lithologies (e.g. Xirokampos shear zone, Fig. 3d). In addition, top-to-the-SW ductile-brittle deformation is also recognized at different places (see Fig. 6 in Roche et al. [2018a]), suggesting a significant component of coaxial flow in the latest increment of deformation.

3. New field data

We carried out several field surveys in the eastern Aegean region, including field mapping in order to complement the existing IGME geological maps or to realize new geological maps

ACCEPTED MANUSCRIPT

(e.g. Fourni Island). Geological mapping was complemented by a detailed study of metamorphic evidences in all islands. Large-scale analysis of the distribution of metamorphic markers thus leads to roughly constrained P-T conditions for several deformation events. Results also include maps of finite strain markers, foliation trajectories, kinematic indicators and field measurements on stereographic plots.

3.1. Samos

3.1.1. Distribution of metamorphic record

On Samos, our study provides additional data for the distribution of HP-LT assemblages, notably well expressed in metabasite boudins of the Ampelos and Vourliotes nappes (Fig. 4a). There, glaucophane, epidote ± chloritoid and white mica are common and well preserved (Fig. 4b). Depending on the areas, epidote-chlorite-albite assemblage is evidenced and indicate retrogression to greenschist-facies conditions (Fig. 4c). Although Okrusch et al. [1984] described the paragenesis carpholite-kyanite in a pebble collected on Psili Amos beach (Fig. 4a), we were not able to recognize any *in-situ* Fe-Mg-carpholite occurrence in the field. In old metabauxites mines along the eastern coast of Samos, we however observed the chloritoid-diaspore assemblage and the diaspore-quartz association (Figs. 4d and 4e). The latter has only been found in Sulawesi (New Caledonia), Amorgos (Cyclades) and Vanoise Massif (Western Alps) [Theye et al., 1997]. It leads to a minimum pressure of 13 kbar and maximum temperatures of 430 °C, i.e. about 100 °C colder than previously published P-T estimates (Fig. 4a) [Ring et al., 1999b]. Such cold HP-

ACCEPTED MANUSCRIPT

LT conditions are compatible with the Fe-Mg-carpholite reported by Okrusch et al. [1984], but are not common in the Cyclades.

3.1.2. Structural geology

At first glance, our observations on Samos confirm the conclusions of Ring et al. [1999b] for the main trends of stretching lineation and shearing associated with blueschist- to greenschist-facies assemblages (Fig. 5a). The best examples of shear sense observed in the field are located near the Pythagoras Thrust in the Ampelos nappe (Fig. 5a). There, blueschist parageneses are associated with E-W or WNW-ESE stretching lineations and top-to-the-W-WNW shear bands (Fig. 5b). These observations suggest that the fabric formed together with the Pythagoras Thrust (probably Eocene) has been preserved here and not severely reworked by the subsequent extension, except for the recent normal fault controlling the topography. This localized shearing along this thrust confirms that it is the major tectonic contact in the island as proposed by Ring et al. [1999b]. Nonetheless, our study show some N-S stretching lineations and rather clear top-to-the-N shear sense associated with greenschist-facies parageneses near Kumarradei and Marathokambos in the Ampelos nappe (Figs. 5c and 5d). The same kinematics is also observed in the southwestern part of Samos in the Vourliotes nappe (Fig. 5a). However, these criteria are very local and do not allow any definite conclusion. If these observations were confirmed, it would mean that the kinematic direction during the HP-LT event and the retrogression were almost perpendicular to each other, at least locally, in contrast to the interpretation of Ring et al. [1999b] that suggest a continuum of ENE-WSW-directed transport during exhumation.

ACCEPTED MANUSCRIPT

Furthermore, although the contact between the Kallithea nappe and the Kerketeas unit does not crop out continuously, it is characterized in the field by thin dark-grey marble ultramylonites (approximately 10 cm high) at the top of dolomites (Fig. 5e). This thin layer carries a NE-trending stretching lineation with locally some normal-sense shear bands spaced a few centimeters apart, and sigmoidal foliation indicating top-to-the-NE shearing (Fig. 5f). This ductile deformation is then overprinted by brittle deformation as suggested by the presence of ultracataclasites and brittle low-angle faults. Locally, centimetric antithetic high-angle normal fault also affected the penetrative foliation. Below this contact, the dolomite is not affected by this deformation indicating a strongly localized deformation.

3.2. Fourni and Thymaena islands

We present in Figure 2b the first geological map of Fourni and Thymaena islands. The geology of the two islands is characterized by a metamorphic sequence comprising three main units (Fig. 2b). (i) The Korakas unit crops out in the eastern part of the island and mainly consists of dolomitic marbles with local schists on top. (ii) The overlying Chrisomilia unit, is mainly made of metabasites with minor occurrences of marbles in the upper part. The lower part of this unit is exposed in southeastern, and consists in thin marble layers. (iii) The uppermost Fourni unit mostly crops out in the central part of the island. It includes mainly schists, marbles, quartzites and minor occurrences of metabasites. Finally, above these tectono-metamorphic units, a non-metamorphic nappe (i.e. the Thymaena unit) is observed [Papanikolaou, 1980].

We distinguish three main contacts between these units: (i) Chrisomilia thrust cropping out in the north of Fourni Island and separating Chrisomilia unit from Korakas unit, (ii) Plagia thrust

ACCEPTED MANUSCRIPT

separating Fourni unit from Chrisomilia unit, and (iii) Thymaena Detachment between Thymaena and Fourni units, cropping out only on Thymaena Island and possibly in the central part of Fourni (Fig. 2b).

3.2.1. Distribution of metamorphic record

We report here preliminary results on metamorphic conditions recorded on Fourni and Thymaena islands. Observed metamorphic parageneses from metabasites in the Chrisomilia unit mainly consist of porphyroblasts of albite - quartz - white mica - chlorite - kyanite, indicating a greenschist-facies metamorphic event (Fig. 6a). Locally, some chloritoid pods are also observed in quartzitic levels (Fig. 6b) that may suggest a former higher-pressure event. The Fourni unit seems to have also recorded the greenschist-facies event. Foliation within schist layers is marked by quartz - white mica - chlorite with locally stretched albite surrounded by chlorite pressure shadows (Fig. 6c). It is noteworthy that both units (i.e. Chrisomilia and Fourni units) seem to have recorded lower peak-metamorphic conditions than the nearby Cyclades and Samos islands.

3.2.2. Structural geology

On Fourni and Thymaena islands, foliation trajectories are given in Figure 2b. The main foliation strikes E-W with moderate dips towards north or south in the central and western parts of the island. In the south, the foliation in both Fourni and Chrisomilia units turns with an average strike around N45°E, whereas it appears more variable in the north, and particularly within Chrisomilia unit. In addition, the foliation is locally deflected in the vicinity of late steep faults

ACCEPTED MANUSCRIPT

associated with strike-slip kinematic indicators. The original lithological contacts are generally transposed into the main penetrative foliation, as shown by isoclinal folds locally observed within dolomitic marble layers (Fig. 6d). A later folding event is also observed in the landscape with the main foliation that is affected by a series of large-scale open folds with E-W axes (Fig. 2b). In addition, kink structures are well developed in both Fourni and Chrisomilia units, showing a N50°E strike (Fig. 6e). Locally, dykes crosscut the main foliation of the Fourni unit which strikes NE-SW (Fig. 6f).

Stretching lineation is mainly underlined by stretched calcite in marbles layers and by elongated aggregates of albite and white micas in metapelites and metabasites. Its orientation is centered on a value of N150°E with a dominant southwestward plunge in the lower structural level, whereas the orientation of stretching is around N0°E to N10°E in the upper levels (Fourni unit, Fig. 7). Lineation and foliation are, however, bent by the main brittle faults, especially strike-slip faults, resulting in a slight scattering of the stretching direction. For instance, in the eastern part of the island, the orientation of stretching lineation is around N90°E with a dominant eastward plunge (Fig. 7) whereas it trends NW-SE in other areas.

Fourni unit is affected by two shearing events, top-to-the-SE and top-to-the-NNE with kinematic indicators often unambiguous at all scales (Fig. 8). As shown in Figure 7, top-to-the-NNE pervasive shearing deformation affected the upper part of this unit, below the Thymaena Detachment, whereas top-to-the-SE kinematic indicators are well preserved in deeper structural levels. In the top of this unit, top-to-the-NNE shear bands are particularly abundant in metapelites and calcschists (Fig. 8a; see stereographic projection in Fig. 7). Depending on areas, their spacing ranges from a few millimeters in the weakest lithologies in the vicinity of the main contacts (e.g.

ACCEPTED MANUSCRIPT

close to the Thymeana Detachment) to decimeters in more competent levels. Locally, the angle between shear bands and the main foliation varies, from high-angle in the upper levels of Fourni unit, suggesting an increasingly brittle behavior, to 20 – 35° at the base of this unit. Non-coaxial deformation is also accommodated by sheared quartz veins (Fig. 8a) and asymmetric boudinage of competent levels (e.g. marbles, metabasites) into a weaker, generally metapelitic matrix. Controversy, top-to-the-SE kinematic indicators are well preserved in deeper structural levels of this unit with common kinematic criteria including quartz- and white mica-bearing pressure shadows on pyrites (Fig. 8b), shear bands and asymmetric quartz veins. In addition, top-to-the-SE more localized brittle-ductile deformation is locally observed (Fig. 8c). Chrisomilia unit is only affected by top-to-the-SE ductile deformation. For instance, metric shear bands affecting foliation are abundant (Figs. 8d and 8e). The relative timing of these two episodes of shearing appears clearly in the field. In the whole island of Fourni, below the Thymaena Detachment, shallow or steep north-dipping shear bands deform the main regional foliation associated with ductile top-to-the-SE shearing, showing that the-top-to-the-NNE shearing event overprints the-top-to-the-SE deformation.

On Fourni and Thymaena islands, the main contact between Fourni unit and the upper non-metamorphic Thymaena unit is marked by breccia and cataclasites (Fig. 9a) over a thickness of approximately 20 meters. Yellowish foliated cataclasites associated with fluid circulations are folded asymetricaly, and locally show sigmoidal foliation compatible with the top-to-the-NNE shearing (Fig. 9b). Below this contact, top-to-the-NNE deformation gradually decreases, while the-top-to-the-SE deformation is totally erased. In addition, in the vicinity of strike-slip faults, top-to-the-E ductile deformation is also recorded in the Chrisomilia unit (Fig. 7) and overprinted

ACCEPTED MANUSCRIPT

by a clear top-to-the-N brittle deformation (Fig. 9c). A new set of major SE-NW to E-W striking faults with a strike-slip component offset the contacts between the main units (e.g. Chrisomilia and Korakas units, Fig. 7; Chrisomilia and Fourni units, Fig. 9d). Shallow-dipping striae along the main fault planes (Fig. 9e) and on smaller-scale faults in the breccia in the north are consistent with a NW-SE extension (see stereogram on Figs. 7 and 9g). This set of faults is crosscut by steeply N-S striking high-angle normal faults (Fig. 7). According to Ring et al. [2017], this set of faults represents the youngest increment, related to the late Miocene to recent extension (for complementary informations, see detailed study of Ring et al. [2017]).

3.3. Dodecanese islands

3.3.1. Distribution of metamorphic record

We propose here new maps of Arki and Lipsi islands (Fig. 3) where the metamorphic record was investigated by studing parageneses from metabasites belonging to Temenia and Marina units (Fig. 10). The geology of Leros and the associated metamorphic record are detailed in Roche et al. [2018a] and also summarized in this study.

Near the lighthouse of Arki harbor, an outcrop of Temenia unit shows several bands of blueschists bearing porphyroblastic blue amphibole, interlayered with micaschists, quartz - micaschists and marbles. In other parts of the island, microscopic observations have revealed blue amphiboles (Fig. 10b). Greenschist-facies intercalations are also observed and chloritoids mark a stretching lineation around N60°E (Fig. 10c). On Lipsi Island, metamorphic assemblages present in metabasites and schists of Temenia unit show chlorite - phengite ± epidote ± quartz ± sphene

ACCEPTED MANUSCRIPT

(e.g. Fig. 10d). The absence of blue amphiboles on Lipsi does not allow ascribing these rocks to the blueschists-facies. Nonetheless, the lithologies are very similar as those found in Leros and Arki islands where HP-LT parageneses have been recorded [e.g. Franz & Okrush, 1992; Roche et al., 2018a; this study]. This suggests that the Temenia unit outcropping on Lipsi was probably not far from the blueschists-facies conditions. The whole Temenia unit would then have been affected by an HP-LT alpine event followed by a retrogression stage in greenschist-facies conditions where chlorite - albite - winchite - epidote - phengite are generally observed. Conversely, Marina unit shows mainly chloritized garnet-bearing rocks and well-preserved amphibolites showing hornblende and plagioclase parageneses (Figs. 10e and 10f). This unit crops out in Leros and Lipsi islands (Figs. 4 and 10a). These rocks are consistent with the Barrovian medium-temperature and medium-pressure (MT-MP) conditions described by Franz et al. [2005].

3.3.2. Structural geology

In Temenia unit of Dodecanese islands, foliation trajectories and lineations are given in Figures 4 and 11. The main foliation strikes N90°E to N135°E with variable dips. It is affected by a series of large-scale upright open folds with N45°E plunging axes in the deepest part of Temenia unit (see foliation data on Leros, Figs. 4d and 12a). There, metabasites are located in the core of schist and marble antiforms (Fig. 4d). Foliation in Marina unit is also characterized by a N90°E to N135°E strike, and is gently to steeply dipping. Furthermore, the main foliation tends to increase in intensity toward the Marina - Temenia contact in both units, while the strike and

ACCEPTED MANUSCRIPT

dip of this foliation do not change significantly across it. There, folded foliation develops a new crenulation with fold axes almost parallel to the main stretching lineation (see stereogram on Fig. 12b). Depending on localities, isoclinal folds with axes perpendicular to stretching lineation (trending ENE-WSW to E-W, see stereogram on Fig. 12c) are also observed. Both folding events are located close to the main contact (i.e. the Temenia shear zone) and thus probably contemporaneous with the mylonitic foliation localized between the Temenia and Marina units. These events are thus apparently related to layer-normal thinning during shear deformation. This overall strain gradient is complicated by strain localization over a limited number of ductile shear zones developed along lithological contacts (e.g. Arki and Gatis shear zones, Figs. 3b and 3c), including a well-developed mylonitic foliation at the contact between marbles and schists in Arki or in Lipsi (e.g. Fig. 12d). In the following, we focus mainly on the study of the deformation within the Temenia unit, which recorded HP-LT Alpine parageneses on Arki and Leros islands, and problably on Lipsi Island even if HP-LT evidences were not found.

Stretching lineation is marked by various types of indicators, depending upon lithology, deformation and P-T conditions. Lineation is outlined by stretched quartz and elongated phyllosilicates aggregates such as chlorites and white micas in metapelites, epidote and rare blue amphiboles in metabasites and chloritoids in quartzite levels (e.g. Fig. 10b). On Arki, the direction of stretching appears more scattered than on Lipsi, with an average trend around N-S (Fig. 11). On Lipsi, the orientation of stretching lineation is centered on a value of N45°E with a dominant northeastward plunge, whereas on Leros it shows a larger dispersion between N0° and N90°E with an average around NE-SW and a variable plunge depending on the area (Fig. 11).

ACCEPTED MANUSCRIPT

At first glance, the whole Temenia unit is affected by a pervasive top-to-the-NE ductile shearing attested by numerous kinematic indicators in the three islands (Figs. 11 and 12, see also Roche et al. [2018a] for Leros field pictures). Shear bands are well developed at all scales (Figs. 10d, 12e and 12f) and are associated with large-scale asymmetric boudinage in alternating lithologies and cm-scale top-to-the-NE kinematic indicators well preserved in metaconglomerate levels (Fig. 12g). At the scale of the outcrop, the rarity of HP-LT rocks occurrences in the field makes difficult any discussion about the kinematics of deformation active during the HP event. Conversely, greenschist-facies parageneses appear conspicuously associated with top-to-the-NE shearing deformation (e.g. Fig. 10d). Indeed, the regional foliation is made of greenschist-facies minerals such as epidote and chlorite concentrates in pressure shadows or in folded layers in both metapelites and metabasites.

Althoug predominant top-to-the-NE ductile kinematics are present in all Dodecanese islands, the distribution of ductile-brittle criteria appears more complex in all units. On Lipsi, Neogene sediments are often in fault contact with the metamorphic rocks. There, the contact is characterized by a low-angle normal fault parallel to the regional foliation (Fig. 13a). Locally, striae along the main fault plane are compatible with the same NE-SW direction of extension (Fig. 13b). This major contact may therefore be interpreted as a low-angle detachment, which we name the Ghialos Detachment. Hence, the observed Alpine structures within metamorphic rocks (Fig. 12g) and at their contact with Neogene sediments (Fig. 13b) suggests a continuum of stretching from ductile to brittle conditions with top-to-the-NE shearing. Similar ductile-brittle deformation is recorded within the main contact (i.e. Temenia shear zone) on Leros, but with a top-to-the-SW sense of shear. In the area of Agios Isidoros (Fig. 3d), ductile deformation within

ACCEPTED MANUSCRIPT

Temenia is intense as attested by numerous low-angle shear zones spaced of a few meters. Top-to-the-WSW shear bands become more brittle approaching the base of Marina unit (Figs. 13c and 13d). The coexistence of opposite kinematic indicators is thus ascribed to the coaxial component of deformation, as also illustrated by large-scale boudinage on Leros [Roche et al. 2018a].

Brittle deformation is fairly consistent through all Dodecanese islands showing N-S to NE-SW direction of extension (see stereographic projection on Fig. 11). On Lipsi, brittle deformation is well-developed, overprinting ductile deformation and controlling relationships between the different units (i.e. Neogene sediments, Temenia and Marina units). For instance, although the tectonic contact between Neogene sediments and Temenia unit is well exposed (strikes N80°E dipping gently toward the north), it is transected by NW-SE striking high-angle normal faults with a strike-slip component (Fig. 13e). Displacement on faults ranges typically between a few meters to decameters. The stress tensor analysis shows a subvertical orientation for the maximum principal stress axis ($\sigma 1$) whereas the minimum principal stress axis ($\sigma 3$) is horizontal striking approximately NE-SW (see stereographic plot #4 in Fig. 13g). Similar faults are also observed in the southern part of Lipsi where a thick damage zone affects marbles and schists of Temenia unit (Fig. 13f). There, foliation strikes N-S and dips deeply toward the north (~ 60°), and turns close to the fault, suggesting a dextral component (Fig. 13f). On Leros, low-angle brittle normal faults, dipping 20 – 30°, may also control the deposition of Neogene sediments (the Lakki detachment, see Roche et al. [2018a]). Here, brittle indicators are again compatible with a NE-SW to N-S extension (see stereographic projections on Figs. 11 and 13g, #6a and #6b).

ACCEPTED MANUSCRIPT

4. Discussion

4.1. Correlations between western Anatolia and the Aegean region

The location of the eastern Aegean islands and the Dodecanese at the transition between the Aegean and western Anatolian regions allows discussing the correlations between these two domains based on our new field observations. Two main criteria can be used for these correlations. (i) One can correlate units with similar stratigraphic successions, and thus pre-orogenic paleogeographic domains, but these domains may have very large areal extents and be involved in different parts of the same belt (Fig. 14). (ii) One may alternatively correlate units with approximately similar stratigraphic succession and similar P-T-time evolution or, rather, similar peak pressure-temperature conditions (Fig. 15). In this case, the emphasis is put on the position of these units within the subduction channel or accretionary wedge, thus on a syn-orogenic situation. Although the complex evolution before the Eocene is not in the scope of the present paper, it might have had some consequences in differentiating two domains with two different lithospheres. Therefore, some general comparisons have to be recalled about the ophiolite emplacement and the nature of the continental basement.

4.1.1. General correlations

According to the literature [e.g. Papanikolaou & Demirtasli, 1987; Papanikolaou, 2009; 2013], the following lateral correlations can be made: 1) The Late Triassic-Early Jurassic event (i.e. closure basin stage & subduction) known as the Cimmerides orogeny occurs only in the

ACCEPTED MANUSCRIPT

eastern Aegean islands of Lesvos and Chios and possibly also in the Circum Rhodope belt. 2) The late Jurassic - early Cretaceous event, corresponding to the obduction of the Axios/Vardar oceanic basin, is widespread in the so-called internal Hellenides of Brunn [1960] in continental Greece with sparse outcrops in the Aegean, especially in Crete below the Asteroussia nappe [e.g. Bonneau, 1972] (see Appendix). 3) The late Cretaceous second obduction event can be followed through the Anatolides-Taurides [e.g. Okay et al., 2001] (e.g. Tavşanlı Zones, Afyon and Ören units, the Kurudere-Nebiler units, see Appendix for more information) to the Aegean and from the internal Hellenides in the Vardar region [e.g. Bonneau, 1984]. In the Cyclades, the Upper Cycladic Nappe shows large units of ophiolite with associated amphibolites yielding Late Cretaceous ages [e.g. Patzak et al., 1994; Bröcker & Franz, 1998].

Furthermore, a crucial point is the correlation of the Variscan basement below the Southern Cyclades (Paros, Naxos, Ios) with the "Menderes core" nappes in Turkey. Indeed, the limited outcropping surfaces of basement rocks in the Cyclades and the Hellenides shows that most of the basement has been subducted [Jolivet et al., 2004a], while the widely outcropping continental basement in the Menderes Massif shows that the crustal wedge is made of basement units to a large extent (see Appendix). Although this continental basement has a similar structural position as the Variscan basement seen in Ios or Naxos [e.g. Henjes-Kunst & Kreuzer, 1982; Andriessen et al., 1987], it is mostly of Panafrican age and no trace of a Panafrican event has been detected in the Aegean domain [e.g. Bonneau & Kienast, 1982; Candan et al., 2011]. However, occurrence of Triassic intrusions and the presence of a common Mesozoic sedimentary cover affinity in both regions suggest a common evolution since this period [Jolivet et al., 2004a]. In addition, according to Dürr et al. [1978], the sedimentary formations of the Marina

ACCEPTED MANUSCRIPT

unit resemble the SW Lycian Nappes. In this framework, a solution is to see the presence of the large amount of basement on Leros and Kalymnos as a lateral equivalent of Lycian Nappes (without HP-LT evidences), but with a preserved Paleozoic basement that would have overthrust the Menderes Massif and its cover, a basement that is so far unknown in western Turkey. Nonetheless, Franz et al. [2005] suggest that the pre-Alpidic basement rocks in the Dodecanese islands reveals similarities with the basement in Eastern Crete (i.e. similar lithologies and pre-Alpidic metamorphic evolution). In all cases, while the Cycladic Basement was clearly involved in the Hellenic orogenic wedge, associated with an HP-LT Alpine metamorphic overprint, this event was less severe in the Dodecanese islands (300 – 370 °C at 1 – 3 kbar [Franz & Okrush, 1992]), and in Eastern Crete (250 – 330 °C at 4.5 – 8 kbar [Franz et al., 2005]). In addition, this HP-LT Alpine event is not recognized within the basement of the Menderes Massif.

4.1.2. Fourni, Samos, western Anatolia and the Cyclades

The nappe stack of Fourni and Samos offers possible correlations with the nearby Menderes Massif and the Lycian Nappes. From top to bottom, the Kallithea nappe can be correlated with the upper Cycladic Nappe and its Pelagonian basement when looking west, and with the Lycian ophiolite or Lycian ophiolitic mélange that root in the Izmir-Ankara suture zone, when looking east in western Turkey (Fig. 14). The presence of a late Cretaceous HT-LP metamorphism associated with an ophiolite on several Cycladic islands (e.g. Anafi [Reinecke et al., 1982]) shows that the Vardar Ocean ophiolite was once distributed over a large part of the Aegean domain. In addition, the non-metamorphic Thymaena unit on Fourni [Papanikolaou,

ACCEPTED MANUSCRIPT

1980] and Kefala-Fanari units on Ikaria, may also belong to this Upper Cycladic Nappe/Pelagonian domain (Fig. 14) (see Appendix).

The underlying Fourni unit on Fourni Island and Agios-Kirikos unit on Ikaria present similar lithostratigraphic successions and an apparent lack of a significant HP-LT imprint [Papanikolaou, 1978], excluding correlation with the CBU. Indeed, Agios-Kirikos unit is made of marbles and metapelites intercalations, and Raman spectroscopy on carbonaceous material (RSCM) results displayed lower temperature ranging between 390 and 450 °C [Beaudoin et al., 2015]. These two units could thus be lateral equivalents of the Menderes cover series, having escaped deep burial and stacked together with the Cycladic Blueschists nappes in a late stage of accretion of the orogenic wedge. In this frame, the Ikaria unit which is tectonically located under the Agios-Kirikos unit, may also correlate with the Menderes cover series (Fig. 14) [Kumerics et al., 2005].

In the eastern part of Samos Island, the preservation of HP-LT parageneses in Vourliotes nappe with the paragenesis diaspore - quartz suggests that this unit was equilibrated along a very low-temperature and high-pressure gradient (Fig. 15a), similar to the gradient observed on Amorgos (i.e. Amorgos unit), in the cover of the Menderes Massif, or in the Ören unit, three areas where Fe-Mg carpholite has been observed [Minoux et al, 1981; Rimmelé et al., 2003a; 2003b; Jolivet et al., 2004a] (Fig. 15a). However, this cold HP unit overlies on Samos the Upper Cycladic Blueschist Nappe (UCB), which has recorded eclogite-facies parageneses. Hence, this structural position differs from the classic structural position of the CBU described first by Grasemann et al. [2018] where the LCB nappe overlies the UCB Nappe (see also Roche et al. [2018a]). Therefore the correlation in this area is difficult. It could be an equivalent of the Afyon

ACCEPTED MANUSCRIPT

and Ören units where HP-LT parageneses have been found (Fig. 14) [e.g. Okay, 1984; Rimmelé et al., 2003a; Pourteau et al., 2014]. An alternative solution is that this unit is an equivalent of the LCB Nappe, overthrusted in a late stage of formation of the accretionary wedge on top of the UCB Nappe.

The underlying Ampelos nappe and Selçuk nappe on Samos are similar to the metasediments and ophiolitic mélange of the CBU of the Dilek Peninsula (see Appendix for more information), resting on top of the Menderes Massif [Candan et al., 1997; Oberhänsli et al., 1998; Ring et al., 1999a]. It may therefore be correlated with the UCB Nappe that crops out mainly on Syros, Sifnos and Tinos (Fig. 14). Even though Chrisomilia unit of Fourni shows a strong retrogression in greenschist-facies conditions, it can be either correlated with the Ampelos nappe (and hence with the UCB Nappe) because of the significant amount of metabasite or it would be a part of the LCB Nappe that crops out in more external zones of the CBU (e.g. Folegandros, Leros) (Figs. 14 and 15b).

Finally, a thick marble sequence is recognized in both the lowermost Kerketeas (Samos) and Korakas (Fourni) units. We can correlate these units with the Basal Unit (Fig. 14), which can be observed in the Olympos, Ossa and Almyropotamos tectonic windows [Godfriaux 1962; 1965; Godfriaux & Pichon, 1980] and also possibly the Panormos marbles on Tinos [Avigad & Garfunkel, 1989], all lateral equivalents of the Gavrovo-Tripolitza nappe.

4.1.3. Dodecaneses islands, Menderes cover and Amorgos Island

Before discussing all possible correlations, it has to be recalled that no consensus exists on the belonging of the HP-LT sequences of the Kurudere-Nebiler units (south Menderes, see

ACCEPTED MANUSCRIPT

Appendix). This unit has indeed recorded peak conditions of ~ 440 – 570 °C and 10 – 12 kbar [e.g. Rimmelé et al., 2003b; 2005; Whitney et al., 2008] while the UCB Nappe were buried at deeper depths of 530 ± 30 °C and 22 ± 2 kbar (Fig. 15a) [e.g. Laurent et al., 2018]. In Pourteau et al. [2010; 2013], the Kurudere unit is correlated with the CBU as a whole, but the lithologies and P-T conditions are not equivalent to the typical occurrence of the CBU (Fig. 15) that should show a large amount of metabasites and well-preserved eclogites. It seems more reasonable to consider the cover of the Menderes Massif as an equivalent of the LCB Nappe (Figs. 14 and 15a).

The ubiquitous presence of blueschist-facies parageneses in Temenia unit in Leros and Arki islands consolidates the hypothesis of Franz et al. [2005] suggesting that the whole Temenia unit was affected by an HP-LT alpine event, although it was not clearly evidenced in Lipsi Island. The preservation of aragonite, the absence of garnet together with RSCM results (T_{max} conditions around 368 to 487 °C) [Roche et al., 2018a] however show that Temenia unit has recorded lower peak-metamorphic conditions than the nearby Cyclades islands where the UCB Nappe is cropping out (Fig. 15a). In this framework, Temenia unit could be either an equivalent of (i) the metamorphic Ören unit (and hence the lower part of the Lycian Nappes) where HP-LT parageneses with Fe-Mg carpholite have been reported or (ii) the LCB Nappe (Figs. 14 and 15b). Because of similar lithologies and metamorphic conditions between the Temenia unit and the LCB Nappe, we are on the same line as Roche et al. [2018a], suggesting that this unit can be compared with the LCB Nappe, which could in turn be correlated with the cover of the Menderes Massif.

Amorgos exposes a sequence of HP-LT rocks that have undergone two different blueschist-facies metamorphic events (Fig. 15a). A first event is estimated at < 13 kbar and 500 – 600 °C

ACCEPTED MANUSCRIPT

[Rosenbaum et al., 2007] and may correspond to the eclogite-blueschists-facies observed in the UCB Nappe. The second event is associated with Fe-Mg-carpholite and saliotite found in metabauxites and is estimated at 8 – 12 kbar and 300 – 350 °C [Theye et al., 1997]. This unit (i.e. named Amorgos unit) consists of a thick Mesozoic marble sequence capped by an early Tertiary metaflysch, and may be correlated with the cover of the Menderes Massif in terms of lithology and metamorphism (Figs. 14 and 15a).

This discussion emphasizes the difficulty of correlating the different nappes of the Hellenides once they have been dispersed by the Oligo-Miocene Aegean extension. The complexity of the situation in the Eastern Aegean region is also due to a lack of metamorphic age constraints on a number of these islands. Further works should thus focus on enlarging the radiochronological data set there. Although all these units have followed different P-T evolutions, a similar structural position is recognized through the entire region. From bottom to top, one then finds (i) the colder units such as the Amorgos unit and the Menderes and its cover before the Main Menderes Metamorphism overprint [Sengör et al., 1984], the LCB Nappe (i.e. Folegandros, the lower unit of Milos, the western Cyclades, a part of the Dodecanese islands, and probably Fourni unit), (ii) the eclogitic rocks observed mainly in the central part of the Cyclades, in Samos and on Dilek peninsula (i.e. the UCB Nappe), and (iii) the Lycian units and Vourliotes nappe in Samos (?) that were buried and exhumed earlier (Figs. 14 and 15). This overall vertical succession can be locally modified suggesting late out-of-sequence thrusting.

4.2. Tectonic evolution of the Aegean-Anatolia region

ACCEPTED MANUSCRIPT

Figure 16 is a map of kinematic indicators covering the Aegean Sea and the Menderes Massif, based on previous works [Jolivet et al., 2013 and references therein] and enriched with our new observations made in the eastern Aegean islands, the Dodecanese and the Menderes Massif. It is worthwhile noting that the main shearing directions and the main sense of shear are not significantly affected by Miocene to recent paleomagnetic rotations, especially in the central and eastern regions [Walcott & White, 1998, van Hinsbergen et al., 2010b; Uzel et al., 2015].

4.2.1. Kinematics of deformation from the Cretaceous to the Oligocene

4.2.1.1. Prograde deformation

The first stage of deformation corresponds to the stacking of units by thrusting, probably during prograde evolution or at peak pressure. Most kinematic indicators related to this episode of nappe stacking have been erased during subsequent exhumation and further extension, but a limited number of outcrops evidence this kinematics in the Cyclades and in the Olympos-Ossa region. On Syros, Philippon et al. [2011] suggest that the sense of shear was toward the south during the prograde episode (Fig. 16a). Syn-orogenic top-to-the-SW shear sense criteria have also been preserved in the Olympos-Ossa region [Schermer et al., 1990; Ricou et al., 1998; Jolivet et al., 2004a; Lacassin et al., 2007]. In addition, our study shows that top-to-the-SE kinematic indicators associated with thrusts are also well preserved on Fourni Island, in the lower part of Fourni unit (Figs. 7 and 16a). Although no clear P-T conditions are established on Fourni, we suggest that these kinematic indicators were recorded during the prograde compressional event.

ACCEPTED MANUSCRIPT

The overall architecture of the Menderes Massif and Lycian Nappes also calls for a top-to-the-S emplacement of nappes. The Lycian Nappes, including the lowermost Ören metamorphic unit, was tectonically transported from the northern margin of the Menderes, as the thrusting front was propagating southward [Collins & Robertson, 1998; Rimmelé et al., 2003a; 2005; Pourteau et al., 2013]. Similarly, large-scale top-to-the-S shear zone are described within the Menderes Massif (i.e. Selimiye Shear Zone (SSZ); Fig. 16a), between the basement and the cover [e.g. Bozkurt & Park, 1994; Hetzel & Reischmann, 1996], which may be ascribed to this prograpde phase, although their significance, whether they are thrusts or detachments or both, is still debated [e.g. Bozkurt & Park, 1994; Whitney & Bozkurt, 2002; Ring et al., 1999a; 2003].

4.2.1.2. Syn-orogenic deformation

The exhumation process encompassed the syn-orogenic stage through different extensional and compressional structures. Extensional structures are observed in the Cyclades domain within the CBU and in southern Turkey. On Samos Island, a continuum from ductile blueschist- to greenschist-facies deformation is preserved across the contact between the Kerketeas and the Ampelos units with a top-to-the-W-NW shearing (Fig. 16a) [Ring et al., 1999b], suggesting that the Pythagoras shear zone has accommodated a part of the syn-orogenic exhumation during the HP-LT metamorphic event. Top-to-the-E shearing deformation along the Vari Detachment (in Syros Island) also allowed the exhumation of the CBU sequence within the subduction channel (Fig. 16a) [e.g. Jolivet et al., 2003; 2010; Huet et al., 2009; Laurent et al., 2016]. However, the apparent inconsistency between N-S and E-W lineation at the base and to the top of the CBU, respectively, is difficult to explain. One may assume that the original trend of the lineation is not

ACCEPTED MANUSCRIPT

known in the absence of paleomagnetic data and it could be envisaged that is was more NE (or N?)-trending, according to HP lineations recorded on the neighboring Sifnos Island [e.g. Roche et al., 2016]. In the HP-LT Lycian Nappes in Western Turkey, contrasted P-T conditions indicate the existence of numerous shear zones accommodating their exhumation [Rimmelé et al., 2003a]. Top-to-the-E shear senses are recorded within the entire HP-LT sequence, and deformation appears more localized close to the contact between the Lycian and Menderes Massif [Rimmelé et al., 2005]. Hence, this deformation post-dated the early southward translation of the Lycian Nappes and corresponds to the exhumation of HP-LT rocks that was aided by the reactivation of major thrusts with a new top-to-the-NE to -E shearing.

Compressional structures are mainly recorded in the southern Cyclades. For instance, top-to-the-S thrusting in Ios Island is also coeval with the extensional shear zone of Vari (Fig. 16a) [Huet et al., 2009]. According to this study, an extrusion structure is proposed to explain exhumation of the CBU [see also Ring et al., 2007; Huet et al., 2009]. However, recent studies [e.g. Grasemann et al., 2018; Roche et al., 2018a] show the existence of a LCB Nappe outcropping in the southern Cycaldes (Fig. 16a), as a consequence this basal thrust cannot explain the entire exhumation of CBU.

This short discussion emphasizes the 3-D complexity of the wedge, where HP-LT syn-orogenic exhumation shearing may be approximately E-W in some places (i.e. parallel to the trench; e.g. Syros, Samos, Ören unit) whereas it is for instance N-S in other areas (e.g. Ios Island) (Fig. 16a). In any case, the accretionary complex is particularly wide and made of different tectonic slices such as continental basement (e.g. Menderes Massif, Cycladic Basement), oceanic (e.g. the CBU) and cover units (e.g. Kurudere-Nebiler units, Ören unit).

ACCEPTED MANUSCRIPT

4.2.2. An overall NNE-SSW gradient of extension from Oligo-Miocene to Present

The overall picture of the extensional kinematics of the Aegean Sea and western Anatolia shows that the direction and sense of displacement along the main detachments during slab retreat is consistent over the entire eastern and central Cyclades. This area presents a pervasive network of large-scale to small-scale ductile-brittle shear zones in all metamorphic units and ductile and brittle criteria show an overall consistent top-to-the-NNE kinematics from the Central Aegean (Paros-Naxos) to the Dodecanese and Eastern Aegean islands with rare top-to-the-SW (e.g. locally on Leros) and top-to-the-WNW kinematics (e.g. locally on Samos) (Fig. 16b). Because the top-NNE kinematics of the eastern and central Cyclades is associated with HT-LP metamorphic overprint (with local anatexy) at many places (e.g. in Ikaria, Mykonos and Naxos from ~ 20 Ma to the Late Miocene) (e.g. a-type domes [Jolivet et al., 2004b], and with the emplacement of the Aegean granitoids [e.g. Altherr & Siebel, 2002; Rabillard et al., 2018], we suggest that most of post-orogenic exention is accommodated by top-to-the-NNE shearing in this large area. However, this is not the case further west (western Cyclades), south (southern Cyclades) and east (Menderes Massif). There, deformation appears more symmetrical, characterized by several detachment systems exhibiting opposing kinematics (e.g. the WCDS and NCDS in the Cyclades [e.g. Jolivet et al., 2010; Grasemann et al., 2012], the Santorini detachment [Schneider et al., 2018], the Büyük Menderes and the Gediz detachments [e.g. Hetzel et al., 1995a; Gessner et al., 2001]; Fig. 16b). However, the bivergent pattern in the Menderes Massif is mostly due to the most recent part of extension, from ~ 20 Ma to the present [e.g. Hetzel et al., 1995b; Gessner et al., 2001]. Before this event, the main detachment exhuming the

ACCEPTED MANUSCRIPT

Menderes Massif was active in the north (Simav Detachment) with a top-to-the-N kinematics [e.g. Işık & Tekeli, 2001], exhuming partially molten crust (Fig. 16b). Characterized by episodic activities, this detachment fault started in the late Oligocene and have continued until 8 Ma [e.g. Ring et al., 2003; Seyítoğlu et al., 2004; Bozkurt et al., 2011; Cenki-tok et al., 2016].

Furthermore, according to Ring et al. [1999b], NNE extension was interrupted by a short-lived phase of E-W shortening between 9 and 8.6 Ma, essentially recorded in the brittle crust. This compressional event, which may also be associated with some strike-slip component [Papanikolaou, 1979], is ascertained in Samos by the presence a several reverse faults that affect both the margins of the Miocene basin and the basin itself. Folds formed in the Miocene deposits before the deposition of the Mytilini formation are also compatible with this event. This Miocene compressional event has also been recognized on Mykonos during the late stages of cooling of the intrusion some 9 Ma ago [Menant et al., 2013]. Following Menant et al. [2013], we suggest that the extrusion of Anatolia may be responsible for this regional compressional event in the brittle crust of the central Cyclades, before strike-slip deformation localized on the edge of the Aegean domain when the NAF reached the north Aegean Sea in the Late Miocene [Armijo et al., 1999; Koukouvelas & Aydin, 2002]. Armijo et al. [2004] proposed that propagation of the NAF and its satellites would produce a compressional stress regime, just south of the western tip of the faults, while an extensional regime would be active north of the fault. The short compressional event could then be due to the propagation of such a strike-slip system, just north of Samos. However, this would make the NAF propagate earlier than usually postulated (~ 5 Ma) as the age of the compression is estimated ~ 9 Ma. It is thus important to obtain more data to precise this point.

ACCEPTED MANUSCRIPT

Finally, the late stage of brittle deformation is compatible with a N-S to NNE-SSW extension over large areas [e.g. Brun et al., 2016; Ring et al., 2017]. For instance, in the Menderes massif, E-W striking high-angle normal faults control the structure of Neogene basins. These set of faults, seismically active, started to operate around ~ 5 Ma ago [Ring et al., 2003], and are co-directional with the extension direction of earlier low-angle normal faults. In addition, inversion of GPS data that estimates the present-day strain field [Pérouse et al., 2012; Aktug et al., 2009], and fault mechanism from the earthquake on Lesbos (data from the USGS Earthquake Hazards Program) showing a normal component, are both consistent with a N-S extension.

4.3. Slab tearing: which consequences in the overriding plate?

Before discussing tectonic and thermal consequences of slab tearing, we need to clarify the timing of the tear formation below western Turkey. Paleomagnetic measurements show that the main differential rotation between the Hellenides and western Anatolia took place between 15 and 8 Ma [e.g. Morris & Anderson, 1996; van Hinsbergen et al., 2010b; van Hinsbergen & Schmid, 2012]. This timing also corresponds to the exhumation of high-temperature metamorphic domes below top-NE detachments in the central and eastern Aegean Sea and emplacement of the Aegean granitoids. Accordingly, Jolivet al. [2015] suggested a ~ 15 Ma age for the main slab tearing event, which is consistent with the timing of a K-rich magmatic pulse in western Turkey [e.g. Dilek & Altunkaynak, 2009; Ersoy & Palmer, 2013]. Alternatively, Govers and Fichtner [2016] suggested that the slab tear started to forms earlier (i.e. ~ 35 Ma) following the arrival of

ACCEPTED MANUSCRIPT

the Central Anatolian Crystalline Complex in the accretionary complex. Therefore, we cannot rule out that slab tearing might start earlier, but at a slower pace.

Within the transition zone from the Menderes Massif to the Cyclades, we showed that the direction of extension is consistently NNE-SSW with no major change in trend, and the sense of shear is predominantly top-to-the-NNE (Fig. 16b). Most of the observed deformation relates to low-angle normal faults and ductile shear zones, without any clear large-scale strike-slip fault systems that could have been expected above a slab tear. This confirms the ideas put forward by Gessner et al. [2013] and Jolivet et al. [2015] of a wide zone of gradient of extension accommodating the left-lateral displacement imposed by the faster retreat south of the Aegean Sea than of the Menderes Massif. Most of the related deformation in the lower crust is then accommodated by low-angle shear zones, which is compatible with the idea that the deformation in this region is largely controlled by the flow of asthenospheric mantle underneath [Jolivet al., 2009; 2015; Menant et al., 2016b]. Seismic anisotropy data [Endrun et al., 2011] are also compatible with this hypothesis, suggesting a strong coupling between SW-NE mantle fabrics and the frozen-in fabric in the lower crust. We therefore challenge the hypothesis of Ring et al. [2017] which suggest an important change in strain pattern in this region. Nonetheless, it is noteworthy that different fission-track age patterns have been recorded in both regions (i.e. Cyclades and Menderes Massif) (see the compilation of Ring et al. [2017]), suggesting a difference of exhumation and erosion rates. Alternatively, to reconcile complex deformation pattern recorded in the brittle crust and in sedimentary basins during the Miocene [Ring et al., 1999b; 2017] to the consistent NE-SW ductile flow in the metamorphic crust (Fig. 16b), one may suggest a possible decoupling between the brittle upper and the ductile lower crust at some

ACCEPTED MANUSCRIPT

periods. This hypothesis have to be further investigated but it would imply that the overall geometry and kinematics revealed by this study mainly results from basal drag due to the underlying asthenospheric flow.

The thermal effects induced by slab dynamics (i.e. mantle flows and shear heating) appear clearly since the Miocene (e.g. numerous K-rich magmatic pulses [Dilek & Altunkaynak, 2009; Ersoy & Palmer, 2013]) and are essential in the eastern Aegean domain [e.g. see Roche et al., 2018b]. Slab dynamics controls the bulk of heat source at the base of the crust and therefore explains (i) the different pattern of deformation, asymmetrical in the central and eastern Aegean Sea versus symmetrical in the western Cyclades and in the Menderes Massif, which may be related to the activity of asthenospheric flow underneath [Jolivet et al., 2015], (ii) the retrogression in greenschist-facies or amphibolite-facies conditions within the metamorphic domes in the Aegean domain, (ii) the current localization of geothermal resources in the Menderes Massif [Gessener et al., 2018; Roche et al., 2018c].

5. Conclusion

Based on a field study in the eastern part of the Cyclades (Eastern Aegean islands and Dodecanese), we (i) produce new geological maps and describe the tectonic evolution of this region, (ii) clarify the correlations and differences between the Aegean Sea and the Menderes Massif in terms of lithological and tectonic units and metamorphic evolution and we (iii) complete the description of extensional shearing direction and sense over the entire back-arc region. We highlight the structure of the accretionary complex that may be defined by three main

ACCEPTED MANUSCRIPT

metamorphic units: (i) the LCB Nappe and its Turkish equivalent with the Menderes cover (i.e. Kurudere-Nebiler units) and Amorgos unit, (ii) the UCB Nappe, and (iii) the HP-LT Lycian Nappes (possibly including the Vourliotes nappe of Samos). We further show that, in the transition zone between the Aegean domain and the Menderes massif, extension related to slab retreat and tearing keeps a constant NNE-SSW direction accommodating the difference in finite extension rates, with a simple ductile crustal flow that probably reflects the asthenospheric mantle flowing underneath. Neither localized first-order strike-slip fault nor significant rotation of blocks about a vertical axis, at least in the middle-lower crust are observed, but upper crustal deformation may be partly decoupled and thus have recorded a different stress regime.

Acknowledgement:

This work has received funding from the Labex Voltaire (ANR-10-LABX-100-01) homed at Orléans University and BRGM, from the European Research Council (ERC) under the seventh Framework Programme of the European Union (ERC Advanced Grant, grant agreement No 290864, RHEOLITH), and from the Institut Universitaire de France. The authors are grateful to S. Janiec and J.G. Badin (ISTO) for the preparation of thin sections and to Clément Conand for fieldwork together in Leros. We are gratefull to Bernhard Grasemann and an anonymous reviewer for their relevant suggestions.

ACCEPTED MANUSCRIPT

References

Aktug, B., Nocquet, J.M., Cingöz, A., Parsons, B., Erkan, Y., England, P., Lenk, O., Gürdal, M.A., Kilicoglu, A., Akdeniz, H., 2009. Deformation of western Turkey from a combination of permanent and campaign GPS data: Limits to block-like behavior. Journal of Geophysical Research: Solid Earth 114. https://doi.org/10.1029/2008JB006000.

Altherr, R., Siebel, W., 2002. I-type plutonism in a continental back-arc setting: Miocene granitoids and monzonites from the central Aegean Sea, Greece. Contributions to Mineralogy and Petrology, 143(4), 397-415. https://doi.org/10.1007/s00410-002-0352-y

Andriessen, P.A.M., Banga, G., Hebeda, E.H., 1987. Isotopic age study of pre-Alpine rocks in the basal units on Naxos, Sikinos and Ios, Greek Cyclades. Geologie en Mijnbouw 66, 3–14.

Armijo, R., Meyer, B., Hubert, A., Barka, A., 1999. Westward propagation of the North Anatolian fault into the northern Aegean: Timing and kinematics. Geology 27, 267–270. https://doi.org/10.1130/0091-7613(1999)027<0267:WPOTNA>2.3.CO;2

Armijo, R., Flerit, F., King, G., Meyer, B., 2004. Linear elastic fracture mechanics explains the past and present evolution of the Aegean. Earth and Planetary Science Letters, 217(1-2), 85-95. https://doi.org/10.1016/S0012-821X(03)00590-9

Aubouin, J., 1959. Contribution à l'étude géologique de la Grèce septentrionale: les confins de l'Epire et de la Thessalie; Place des Hellénides parmi les édifices structuraux de la Méditerranée orientale. Laboratoire de géologie de l'Université.

Augier, R., Jolivet, L., Gadenne, L., Lahfid, A., Driussi, O., 2015. Exhumation kinematics of the Cycladic Blueschists unit and back-arc extension, insight from the Southern Cyclades (Sikinos and Folegandros Islands, Greece). Tectonics 34, 152–185. https://doi.org/10.1002/2014TC003664

Avigad, D., Garfunkel, Z., 1989. Low-angle faults above and below a blueschist belt—Tinos Island, Cyclades, Greece. Terra Nova 1, 182–187. https://doi.org/10.1111/j.1365-3121.1989.tb00350.x

Avigad, D., Garfunkel, Z., 1991. Uplift and exhumation of high-pressure metamorphic terrains: the example of the Cycladic blueschist belt (Aegean Sea). Tectonophysics 188, 357–372. https://doi.org/10.1016/0040-1951(91)90464-4

Avigad, D., Baer, G., Heimann, A., 1998. Block rotations and continental extension in the central Aegean Sea: palaeomagnetic and structural evidence from Tinos and Mykonos (Cyclades, Greece). Earth and Planetary Science Letters 157, 23–40. https://doi.org/10.1016/S0012-821X(98)00024-7

ACCEPTED MANUSCRIPT

Barka, A.A., 1992. The north Anatolian fault zone, in: Annales Tectonicae. pp. 164–195.

Beaudoin, A., Augier, R., Laurent, V., Jolivet, L., Lahfid, A., Bosse, V., Arbaret, L., Rabillard, A., Menant, A., 2015. The ikaria high-temperature metamorphic core complex (Cyclades, Greece): geometry, kinematics and thermal structure. Journal of Geodynamics 92, 18–41. https://doi.org/10.1016/j.jog.2015.09.004

Beccaletto, L., Steiner, C., 2005. Evidence of two-stage extensional tectonics from the northern edge of the Edremit Graben, NW Turkey. Geodinamica Acta, 18(3-4), 283-297. https://doi.org/10.3166/ga.18.283-297

Berk Biryol, C., Beck, S.L., Zandt, G., Özacar, A.A., 2011. Segmented African lithosphere beneath the Anatolian region inferred from teleseismic P-wave tomography. Geophysical Journal International 184, 1037–1057. https://doi.org/10.1111/j.1365-246X.2010.04910.x

Bernoulli, D., De Graciansky, P. C., Monod, O., 1974. The extension of the Lycian Nappes (SW Turkey) into the southeastern Aegean Islands. Eclogae Geologicae Helvetiae, 67(1), 39-90.

Bijwaard, H., Spakman, W., Engdahl, E.R., 1998. Closing the gap between regional and global travel time tomography. Journal of Geophysical Research: Solid Earth 103, 30055–30078. https://doi.org/10.1029/98JB02467

Blake, M.C., Bonneau, M., Geyssant, J., Kienast, J.R., Lepvrier, C., Maluski, H., Papanikolaou, D., 1981. A geological reconnaissance of the Cyclacic blueschist belt, Greece. Bull Geol Soc Am 92:247–254

Bonneau, M., 1972. La nappe métamorphique de l'Asteroussia, lambeau d'affinités pélagoniennes charrié jusque sur la zone de Tripolitza de la Crète moyenne (Grèce). Cr Séances Acad. Sci. Paris 275, 2303–2306.

Bonneau, M., 1982. Evolution géodynamique de l'arc égéen depuis le Jurassique Supérieur jusqu'au Miocène. Bulletin de la Societé géologique de France 7, 229–242. https://doi.org/10.2113/gssgfbull.S7-XXIV.2.229

Bonneau, M., 1984. Correlation of the Hellenide nappes in the south-east Aegean and their tectonic reconstruction. Geological Society, London, Special Publications 17, 517–527. https://doi.org/10.1144/GSL.SP.1984.017.01.38

Bonneau, M., Kienast, J.R., 1982. Subduction, collision et schistes bleus; l'exemple de l'Egee (Grece). Bulletin de la Société geologique de France 7, 785–791. https://doi.org/10.2113/gssgfbull.S7-XXIV.4.785

ACCEPTED MANUSCRIPT

Bozkurt, E., Park, L.R., 1994. Southern Menderes Massif: an incipient metamorphic core complex in western Anatolia, Turkey. Journal of the Geological Society 151, 213–216. https://doi.org/10.1144/gsjgs.151.2.0213

Bozkurt, E., Satır, M., Buğdaycıoğlu, Ç., 2011. Surprisingly young Rb/Sr ages from the Simav extensional detachment fault zone, northern Menderes Massif, Turkey. Journal of geodynamics, 52(5), 406-431. https://doi.org/10.1016/j.jog.2011.06.002

Bröcker, M., Franz, L., 1998. Rb–Sr isotope studies on Tinos Island (Cyclades, Greece): additional time constraints for metamorphism, extent of infiltration-controlled overprinting and deformational activity. Geological Magazine, 135(3), 369-382.

Brun, J. P., Faccenna, C., 2008. Exhumation of high-pressure rocks driven by slab rollback. Earth and Planetary Science Letters, 272(1-2), 1-7. https://doi.org/10.1016/j.epsl.2008.02.038

Brun, J.P., Faccenna, C., Gueydan, F., Sokoutis, D., Philippon, M., Kydonakis, K., Gorini., C., 2016. The two-stage Aegean extension, from localized to distributed, a result of slab rollback acceleration. Can. J. Earth Sci. 53, 1142-1157; https://doi.org/1110.1139/cjes-2015-0203.

Brunn, J.H., 1956. Contribution a l'etude geologique du Pinde Septenrional et d'une partie de la Macedoine occidentale. Laboratoire de geologie de l'Universite.

Brunn, J.H., 1960. Les zones helléniques internes et leur extension. Réflexions sur l'orogénèse alpine. Bulletin de la Societe Geologique de France II, 470–486.

Brunn, J.H., Argyriadis, I., Ricou, L.E., Poisson, A., Marcoux, J., de Graciansky, P.-C., 1976. Eléments majeurs de liaison entre Taurides et Hellénides. Bulletin de la Société géologique de France 7, 481–497. https://doi.org/10.2113/gssgfbull.S7-XVIII.2.481

Brunn, J.H., Graciansky, P.-C. de, Gutnic, M., Juteau, T., Lefevre, R., Marcoux, J., Monod, O., Poisson, A., 1970. Structures majeures et corrélations stratigraphiques dans les Taurides occidentales. Bulletin de la Societe geologique de France 7, 515–556. https://doi.org/10.2113/gssgfbull.S7-XII.3.515

Buick, I.S., 1991. The late Alpine evolution of an extensional shear zone, Naxos, Greece. Journal of the Geological Society 148, 93–103. https://doi.org/10.1144/gsjgs.148.1.0093

Candan, O., Dora, O., Oberhänsli, R., Oelsner, F., Dürr, S., 1997. Blueschist relics in the Mesozoic series of the Menderes Massif and correlation with Samos Island, Cyclades. Schweiz Mineralogische und Petrographische Mitteilungen 77, 95–99.

Candan, O., Çetinkaplan, M., Oberhänsli, R., Rimmelé, G., Akal, C., 2005. Alpine high-P/low-T metamorphism of the Afyon Zone and implications for the metamorphic evolution of

ACCEPTED MANUSCRIPT

Western Anatolia, Turkey. Lithos, 84(1-2), 102-124. https://doi.org/10.1016/j.lithos.2005.02.005

Candan, O., Koralay, O.E., Akal, C., Kaya, O., Oberhänsli, R., Dora, O., Konak, N., Chen, F., 2011. Supra-Pan-African unconformity between core and cover series of the Menderes Massif/Turkey and its geological implications. Precambrian Research 184, 1–23. https://doi.org/10.1016/j.precamres.2010.09.010

Cenki-Tok, B., Expert, M., Işık, V., Candan, O., Monie, P., Bruguier, O., 2016. Complete Alpine reworking of the northern Menderes Massif, western Turkey. International Journal of Earth Sciences 105, 1507–1524. https://doi.org/10.1007/s00531-015-1271-2

Chatzaras, V., Xypolias, P., Kokkalas, S., Koukouvelas, I., 2011. Oligocene–Miocene thrusting in central Aegean: insights from the Cycladic island of Amorgos. Geological Journal 46, 619–636.

Chen, G., 1995. Evolution of the high-and medium-pressure metamorphic rocks on the island of Samos, Greece (PhD Thesis, University of Wurzburg). Annales Geologiques des Pays Helleniques, 36, 801-915.

Chen, G., Okrusch, M., Sauerschell, W., 1995. Polymetamorphic evolution of high-pressure rocks on Samos, Greece, in: International Earth Sciences Colloquium on the Aegean Region, Proceedings, Izmir, Turkey. pp. 359–365.

Collins, A. S., Robertson, A. H., 1998. Processes of Late Cretaceous to Late Miocene episodic thrust-sheet translation in the Lycian Taurides, SW Turkey. Journal of the Geological Society, 155(5), 759-772. https://doi.org/10.1144/gsjgs.155.5.0759

De Boorder, H., Spakman, W., White, S.H., Wortel, M.J.R., 1998. Late Cenozoic mineralization, orogenic collapse and slab detachment in the European Alpine Belt. Earth and Planetary Science Letters 164, 569–575. https://doi.org/10.1016/S0012-821X(98)00247-7

Delph, J.R., Biryol, C.B., Beck, S.L., Zandt, G., Ward, K.M., 2015. Shear wave velocity structure of the Anatolian Plate: anomalously slow crust in southwestern Turkey. Geophysical Journal International 202, 261–276. https://doi.org/10.1093/gji/ggv141

Delvaux, D., Sperner, B., 2003. New aspects of tectonic stress inversion with reference to the TENSOR program. Geological Society, London, Special Publications 212, 75–100. https://doi.org/10.1144/GSL.SP.2003.212.01.06

Desio, A., 1931. Le isole italiane dell'Egeo: studi geologici e geografico-fisici. Provveditorato generale dello stato libreria.

ACCEPTED MANUSCRIPT

Dewey, J. F. (1988). Extensional collapse of orogens. Tectonics, 7(6), 1123-1139. https://doi.org/10.1029/TC007i006p01123

Dilek, Y., Altunkaynak, Ş., 2009. Geochemical and temporal evolution of Cenozoic magmatism in western Turkey: mantle response to collision, slab break-off, and lithospheric tearing in an orogenic belt. Geological Society, London, Special Publications 311, 213–233. https://doi.org/10.1144/SP311.8

Dürr, S.H., 1975. Über Alter und geotektonische Stellung des Menderes Kristallins/SW Anatolien und seine Äquivalente in der Mittleren Aegean. University of Marburg.

Dürr, S., Altherr, R., Keller, J., Okrusch, M., Seidel, E., 1978. The median Aegean crystalline belt: stratigraphy, structure, metamorphism, magmatism. Alps, Apennines, Hellenides 38, 455–476.

Endrun, B., Lebedev, S., Meier, T., Tirel, C., Friederich, W., 2011. Complex layered deformation within the Aegean crust and mantle revealed by seismic anisotropy. Nature Geoscience 4, 203. https://doi.org/10.1038/ngeo1065

Ersoy, E. Y., Palmer, M. R., 2013. Eocene-Quaternary magmatic activity in the Aegean: implications for mantle metasomatism and magma genesis in an evolving orogeny. Lithos, 180, 5-24. https://doi.org/10.1016/j.lithos.2013.06.007

Faccenna, C., Jolivet, L., Piromallo, C., Morelli, A., 2003. Subduction and the depth of convection in the Mediterranean mantle. Journal of Geophysical Research: Solid Earth 108. https://doi.org/10.1029/2001JB001690

Faccenna, C., Bellier, O., Martinod, J., Piromallo, C., Regard, V., 2006. Slab detachment beneath eastern Anatolia: A possible cause for the formation of the North Anatolian fault. Earth and Planetary Science Letters 242, 85–97. https://doi.org/10.1016/j.epsl.2005.11.046

Franz, L., Okrusch, M., 1992. Aragonite-bearing blueschists on Arki island, Dodecanese, Greece. European Journal of Mineralogy 527–538. https://doi.org/10.1127/ejm/4/3/0527

Franz, L., Okrusch, M., Seidel, E., Kreuzer, H., 2005. Polymetamorphic evolution of pre-Alpidic basement relics in the external Hellenides, Greece. Neues Jahrbuch für Mineralogie-Abhandlungen: Journal of Mineralogy and Geochemistry 181, 147–172. https://doi.org/10.1127/0077-7757/2005/0013

Godfriaux, Y., 1962. L'Olympe, une fenêtre tectonique dans les Hellénides internes, CR Acad. Sc. Paris 255, 1761–1763.

Godfriaux, Y., 1965. Etude géologique de la région de l'Olympe. thèse d'Etat thesis, Université de Lille.

ACCEPTED MANUSCRIPT

Godfriaux, Y., Pichon, J.F., 1980. Sur l'importance des événements tectoniques et métamorphiques d'âge tertiaire en Thessalie septentrionale (L'Olympe, Ossa et Flamburon). Annales géol Soc Nord 99, 367–376.

Gautier, P., Brun, J.-P., 1994. Crustal-scale geometry and kinematics of late-orogenic extension in the central Aegean (Cyclades and Ewia Island). Tectonophysics 238, 399–424. https://doi.org/10.1016/0040-1951(94)90066-3

Gautier, P., Brun, J.-P., Jolivet, L., 1993. Structure and kinematics of Upper Cenozoic extensional detachment on Naxos and Paros (Cyclades Islands, Greece). Tectonics 12, 1180–1194. https://doi.org/10.1029/93TC01131

Gessner, K., Ring, U., Johnson, C., Hetzel, R., Passchier, C.W., Güngör, T., 2001. An active bivergent rolling-hinge detachment system: Central Menderes metamorphic core complex in western Turkey. Geology 29, 611–614. https://doi.org/10.1130/0091-7613(2001)029<0611:AABRHD>2.0.CO;2

Gessner, K., Gallardo, L.A., Markwitz, V., Ring, U., Thomson, S.N., 2013. What caused the denudation of the Menderes Massif: Review of crustal evolution, lithosphere structure, and dynamic topography in southwest Turkey. Gondwana Research 24, 243–274. https://doi.org/10.1016/j.gr.2013.01.005

Gessner, K., Markwitz, V., Güngör, T., 2018. Crustal fluid flow in hot continental extension: tectonic framework of geothermal areas and mineral deposits in western Anatolia. Geological Society, London, Special Publications 453, 289–311. https://doi.org/10.1144/SP453.7

Göncüoğlu, M.C., Dirik, K., Kozlu, H., 1997. General characteristics of pre-Alpine and Alpine Terranes in Turkey: Explanatory notes to the terrane map of Turkey, in: Annales Geologique de Pays Helleniques. pp. 515–536.

Govers, R., Wortel, M.J.R., 2005. Lithosphere tearing at STEP faults: Response to edges of subduction zones. Earth and Planetary Science Letters 236, 505–523. https://doi.org/10.1016/j.epsl.2005.03.022

Govers, R., Fichtner, A., 2016. Signature of slab fragmentation beneath Anatolia from full-waveform tomography. Earth and Planetary Science Letters 450, 10–19. https://doi.org/10.1016/j.epsl.2016.06.014

Grasemann, B., Schneider, D.A., Stöckli, D.F., Iglseder, C., 2012. Miocene bivergent crustal extension in the Aegean: Evidence from the western Cyclades (Greece). Lithosphere 4, 23–39. https://doi.org/10.1130/L164.1

ACCEPTED MANUSCRIPT

Grasemann, B., Huet, B., Schneider, D.A., Rice, A.H.N., Lemonnier, N., Tschegg, C., 2018. Miocene postorogenic extension of the Eocene synorogenic imbricated Hellenic subduction channel: New constraints from Milos (Cyclades, Greece). GSA Bulletin 130, 238–262. https://doi.org/10.1130/B31731.1

Henjes-Kunst, F., Kreuzer, H., 1982. Isotopic dating of pre-alpidic rocks from the island of Ios (Cyclades, Greece). Contributions to Mineralogy and Petrology 80, 245–253. https://doi.org/10.1007/BF00371354

Hetzel, R., Passchier, C.W., Ring, U., Dora, Ö.O., 1995a. Bivergent extension in orogenic belts: the Menderes Massif (southwestern Turkey). Geology 23, 455–458. https://doi.org/10.1130/0091-7613(1995)023<0455:BEIOBT>2.3.CO;2

Hetzel, R., Ring, U., Akal, C., Troesch, M., 1995b. Miocene NNE-directed extensional unroofing in the Menderes Massif, southwestern Turkey. Journal of the Geological Society 152, 639–654. https://doi.org/10.1144/gsjgs.152.4.0639

Hetzel, R., Reischmann, T., 1996. Intrusion age of Pan-African augen gneisses in the southern Menderes Massif and the age of cooling after Alpine ductile extensional deformation. Geological Magazine 133, 565–572. https://doi.org/10.1017/S0016756800007846

Huet, B., Labrousse, L., Jolivet, L., 2009. Thrust or detachment? Exhumation processes in the Aegean: Insight from a field study on Ios (Cyclades, Greece). Tectonics 28. https://doi.org/10.1029/2008TC002397

Işik, V., Tekeli, O., 2001. Late orogenic crustal extension in the northern Menderes Massif (western Turkey): evidence for metamorphic core complex formation. International Journal of Earth Sciences 89, 757–765. https://doi.org/10.1007/s005310000105

Jacobshagen, V., Dürr, S., Kockel, F., Kopp, K.O., Kowalczyk, G., Berckhemer, H., Büttner, D., 1978. Structure and geodynamic evolution of the Aegean region, in: Alps, Apennines, Hellenides. Schweizerbart Stuttgart, pp. 455–477.

Jolivet, L., 2001. A comparison of geodetic and finite strain pattern in the Aegean, geodynamic implications. Earth and Planetary Science Letters 187, 95–104. https://doi.org/10.1016/S0012-821X(01)00277-1

Jolivet, L., Faccenna, C., 2000. Mediterranean extension and the Africa-Eurasia collision. Tectonics 19, 1095–1106. https://doi.org/10.1029/2000TC900018

Jolivet, L., Brun, J.-P., 2010. Cenozoic geodynamic evolution of the Aegean. International Journal of Earth Sciences 99, 109–138. https://doi.org/10.1007/s00531-008-0366-4

ACCEPTED MANUSCRIPT

Jolivet, L., Faccenna, C., Goffé, B., Burov, E., Agard, P., 2003. Subduction tectonics and exhumation of high-pressure metamorphic rocks in the Mediterranean orogens. American Journal of Science 303, 353–409. https://doi.org/10.2475/ajs.303.5.353

Jolivet, L., Rimmelé, G., Oberhänsli, R., Goffé, B., Candan, O., 2004a. Correlation of syn-orogenic tectonic and metamorphic events in the Cyclades, the Lycian nappes and the Menderes massif. Geodynamic implications. Bulletin de la Société Géologique de France 175, 217–238. https://doi.org/10.2113/175.3.217

Jolivet, L., Famin, V., Mehl, C., Parra, T., Aubourg, C., Hébert, R., Philippot, P., 2004b. Progressive strain localisation, boudinage and extensional metamorphic complexes, the Aegean Sea Case, in Whitney DL, Teyssier C. and Siddoway CS, Gneiss domes in orogeny: Boulder, Colorado. Geological Society of America Special Paper 380, 185–210.

Jolivet, L., Faccenna, C., Piromallo, C., 2009. From mantle to crust: Stretching the Mediterranean. Earth and Planetary Science Letters, 285(1-2), 198-209. https://doi.org/10.1016/j.epsl.2009.06.017

Jolivet, L., Lecomte, E., Huet, B., Denèle, Y., Lacombe, O., Labrousse, L., Le Pourhiet, L., Mehl, C., 2010. The north cycladic detachment system. Earth and Planetary Science Letters 289, 87–104. https://doi.org/10.1016/j.epsl.2009.10.032

Jolivet, L., Faccenna, C., Huet, B., Labrousse, L., Le Pourhiet, L., Lacombe, O., Lecomte, E., Burov, E., Denèle, Y., Brun, J.-P., 2013. Aegean tectonics: Strain localisation, slab tearing and trench retreat. Tectonophysics 597, 1–33. https://doi.org/10.1016/j.tecto.2012.06.011

Jolivet, L., Faccenna, C., Agard, P., Frizon de Lamotte, D., Menant, A., Sternai, P., Guillocheau, F., 2015. Neo-Tethys geodynamics and mantle convection: from extension to compression in Africa and a conceptual model for obduction. Canadian journal of earth sciences 53, 1190–1204. https://doi.org/10.1139/cjes-2015-0118

Katagas, C.G., 1980. Metamorphic zones and physical conditions of metamorphism in Leros Island, Greece. Contr. Mineral. and Petrol. 73, 389–402. https://doi.org/10.1007/BF00376631

Katagas, C., Sapountzis, E., 1977. Petrochemistry of low and medium grade mafic metamorphic rocks from Leros island, Greece. TMPM Tschermaks Petr. Mitt. 24, 39–55. https://doi.org/10.1007/BF01081744

Kornprobst, J., Kienast, J. R., Vilminot, J. C., 1979. The high-pressure assemblages at Milos, Greece. Contributions to Mineralogy and Petrology, 69(1), 49-63. https://doi.org/10.1007/BF00375193.

ACCEPTED MANUSCRIPT

Koukouvelas, I.K., Aydin, A., 2002. Fault structure and related basins of the North Aegean Sea and its surroundings. Tectonics 21, 10–1. https://doi.org/10.1029/2001TC901037

Kumerics, C., Ring, U., Brichau, S., Glodny, J., Monié, P., 2005. The extensional Messaria shear zone and associated brittle detachment faults, Aegean Sea, Greece. Journal of the Geological Society, 162(4), 701-721. https://doi.org/10.1144/0016-764904-041

Lacassin, R., Arnaud, N., Leloup, P. H., Armijo, R., Meyer, B., 2007. Syn-and post-orogenic exhumation of metamorphic rocks in North Aegean. Eearth, 2, 51-63.

Laurent, V., Jolivet, L., Roche, V., Augier, R., Scaillet, S., Cardello, G.L., 2016. Strain localization in a fossilized subduction channel: Insights from the Cycladic Blueschist Unit (Syros, Greece). Tectonophysics 672–673, 150–169. https://doi.org/10.1016/j.tecto.2016.01.036

Laurent, V., Lanari, P., Naïr, I., Augier, R., Lahfid, A., Jolivet, L., 2018. Exhumation of eclogite and blueschist (Cyclades, Greece): Pressure–temperature evolution determined by thermobarometry and garnet equilibrium modelling. Journal of Metamorphic Geology 36, 769–798. https://doi.org/10.1111/jmg.12309

Le Pichon, X., Angelier, J., 1979. The hellenic arc and trench system: A key to the neotectonic evolution of the eastern mediterranean area. Tectonophysics 60, 1–42. https://doi.org/10.1016/0040-1951(79)90131-8

Le Pichon, X., Angelier, J., 1981. The Aegean Sea. Phil. Trans. R. Soc. Lond. A 300, 357–372. https://doi.org/10.1098/rsta.1981.0069

Le Pichon, X., Chamot-Rooke, N., Lallemant, S., Noomen, R., Veis, G., 1995. Geodetic determination of the kinematics of central Greece with respect to Europe: Implications for eastern Mediterranean tectonics. Journal of Geophysical Research: Solid Earth 100, 12675–12690. https://doi.org/10.1029/95JB00317

Li, C., van der Hilst, R.D., Meltzer, A.S., Engdahl, E.R., 2008. Subduction of the Indian lithosphere beneath the Tibetan Plateau and Burma. Earth and Planetary Science Letters 274, 157–168. https://doi.org/10.1016/j.epsl.2008.07.016

Lips, A.L.W., Cassard, D., Sözbilir, H., Yilmaz, H., Wijbrans, J.R., 2001. Multistage exhumation of the Menderes Massif, western Anatolia (Turkey). Int J Earth Sci 89, 781–792. https://doi.org/10.1007/s005310000101

Lister, G.S., Banga, G., Feenstra, A., 1984. Metamorphic core complexes of Cordilleran type in the Cyclades, Aegean Sea, Greece. Geology 12, 221–225. https://doi.org/10.1130/0091-7613(1984)12<221:MCCOCT>2.0.CO;2

ACCEPTED MANUSCRIPT

McClusky, S., Balassanian, S., Barka, A., Demir, C., Ergintav, S., Georgiev, I., Gurkan, O., Hamburger, M., Hurst, K., Kahle, H., Kastens, K., Kekelidze, G., King, R., Kotzev, V., Lenk, O., Mahmoud, S., Mishin, A., Nadariya, M., Ouzounis, A., Paradissis, D., Peter, Y., Prilepin, M., Reilinger, R., Sanli, I., Seeger, H., Tealeb, A., Toksöz, M.N., Veis, G., 2000. Global Positioning System constraints on plate kinematics and dynamics in the eastern Mediterranean and Caucasus. Journal of Geophysical Research: Solid Earth 105, 5695–5719. https://doi.org/10.1029/1999JB900351

McKenzie, D., 1972. Active Tectonics of the Mediterranean Region. Geophysical Journal of the Royal Astronomical Society 30, 109–185. https://doi.org/10.1111/j.1365-246X.1972.tb02351.x

Menant, A., Jolivet, L., Augier, R., Skarpelis, N., 2013. The North Cycladic Detachment System and associated mineralization, Mykonos, Greece: Insights on the evolution of the Aegean domain. Tectonics 32, 433–452. https://doi.org/10.1002/tect.20037

Menant, A., Jolivet, L., Vrielynck, B., 2016a. Kinematic reconstructions and magmatic evolution illuminating crustal and mantle dynamics of the eastern Mediterranean region since the late Cretaceous. Tectonophysics 675, 103–140. https://doi.org/10.1016/j.tecto.2016.03.007

Menant, A., Sternai, P., Jolivet, L., Guillou-Frottier, L., Gerya, T., 2016b. 3D numerical modeling of mantle flow, crustal dynamics and magma genesis associated with slab roll-back and tearing: The eastern Mediterranean case. Earth and Planetary Science Letters 442, 93–107. https://doi.org/10.1016/j.epsl.2016.03.002

Mercier, J.L., Sorel, D., Vergely, P., Simeakis, K., 1989. Extensional tectonic regimes in the Aegean basins during the Cenozoic. Basin Research 2, 49–71.

Mezger, K., Okrusch, M., 1985. Metamorphism of the variegated sequence at Kallithea, Samos, Greece. TMPM Tschermaks Petr. Mitt. 34, 67–82. https://doi.org/10.1007/BF01082458

Minoux, L., Bonneau, M., & Kienast, J. R., 1980. L'île d'Amorgos, une fenêtre des zones externes au coeur de l'Egée (Grèce), métamorphisée dans le faciès schistes bleus. Comptes Rendu de l'Academie des Sciences de Paris, 291, 745-8.

Morris, A., Anderson, M., 1996. First palaeomagnetic results from the Cycladic Massif, Greece, and their implications for Miocene extension directions and tectonic models in the Aegean. Earth and Planetary Science Letters 142, 397–408. https://doi.org/10.1016/0012-821X(96)00114-8

Mposkos, E., 1978. Diasporit-und Smirgelvorkommen der Insel Samos (Griechenland). Presented at the Fourth International Congress for the Study of Bauxites, pp. 614–631.

ACCEPTED MANUSCRIPT

Mposkos, E., Perdikatsis, V., 1984. Petrology of glaucophane metagabbros and related rocks from Samos, Aegean-Island (Greece). Neues Jahrbuch Mineralogische Abhandlung 43–63.

Oberhänsli, R., Monié, P., Candan, O., Warkus, F., Partzsch, J., Dora, O., 1998. The age of blueschist metamorphism in the Mesozoic cover series of the Menderes massif. Schweiz Mineral Petrogr Mitt 309–316.

Oberhänsli, R., Partzsch, J., Candan, O., Cetinkaplan, M., 2001. First occurrence of Fe-Mg-carpholite documenting a high-pressure metamorphism in metasediments of the Lycian Nappes, SW Turkey. Int J Earth Sci 89, 867–873. https://doi.org/10.1007/s005310000103

Okay, A.I., 1984. Distribution and characteristics of the northwest Turkish blueschists. Geol Soc Lond Spec Publ 17:455. https://doi.org/10.1144/GSL.SP.1984.017.01.33

Okay AI (2002) Jadeite-chloritoid-glaucophane-lawsonite blueschists in northwest Turkey: unusually high P/T ratios in continental crust. J Metamorph Geol 20:757–768. https://doi.org/10.1046/j.1525-1314.2002.00402.x

Okay, A. I., Tansel, I., & Tüysüz, O., 2001. Obduction, subduction and collision as reflected in the Upper Cretaceous–Lower Eocene sedimentary record of western Turkey. Geological Magazine, 138(2), 117-142.

Okrusch, M., Bröcker, M., 1990. Eclogites associated with high-grade blueschists in the Cyclades archipelago, Greece: a review. European Journal of Mineralogy, 451-478. https://doi.org/10.1127/ejm/2/4/0451

Okrusch, M., Richter, P., Katsikatsos, G., 1984. High-pressure rocks of Samos, Greece. Geological Society, London, Special Publications 17, 529–536. https://doi.org/10.1144/GSL.SP.1984.017.01.39

Papanikolaou, D., 1978. Contribution to the geology of Ikaria Island, Aegean Sea. Annales Geologiques des Pays Helleniques, 29, 1-28.

Papanikolaou, D., 1979. Unites tectoniques et phases de deformation dans l'ile de Samos, Mer Egee, Grece. Bulletin de la Société Géologique de France S7-XXI, 745–752. https://doi.org/10.2113/gssgfbull.S7-XXI.6.745

Papanikolaou, D., 1980. Thrust sheets of the island of Thymaena-indication of northward displacements in the Aegean during miocene. Comptes rendus hebdomadaires des seances de l academie des sciences, serie d, 290(4), 307-310.

Papanikolaou, D.J., 1987. Tectonic Evolution of the Cycladic Blueschist Belt (Aegean Sea, Greece), in: Helgeson, H.C. (Ed.), Chemical Transport in Metasomatic Processes, NATO

ACCEPTED MANUSCRIPT

ASI Series. Springer Netherlands, Dordrecht, pp. 429–450. https://doi.org/10.1007/978-94-009-4013-0_16

Papanikolaou, D., 1997. The tectonostratigraphic terranes of the Hellenides. Annales Geologiques des Pays Helleniques, 37, 495-514.

Papanikolaou, D., 2009. Timing of tectonic emplacement of the ophiolites and terrane paleogeography in the Hellenides. Lithos, Ophiolites and related geology of the Balkan region 108, 262–280. https://doi.org/10.1016/j.lithos.2008.08.003

Papanikolaou, D., 2013. Tectonostratigraphic models of the Alpine terranes and subduction history of the Hellenides. Tectonophysics, The Aegean : A natural laboratory for tectonics - Tectonometamorphics 595–596, 1–24. https://doi.org/10.1016/j.tecto.2012.08.008

Papanikolaou, D., Demirtasli, E., 1987. Geological correlations between the alpine segments of the Hellenides-Balkanides and Taurides-Pontides.In: Flugel H.W., Sassi, F.P. & Grecula, P. editors, Pre-Variscan and Variscan events in the alpine Mediterranean mountain belts, Mineralia Slovaca, Monography, Bratislava, 387-396.

Patzak, M., Okrusch, M., Kreuzer, H., 1994. The Akrotiri Unit on the island of Tinos, Cyclades, Greece: Witness to a lost terrane of Late Cretaceous age.(with 18 figures and 8 tables in the text). Neues Jahrbuch fur Geologie und Palaontologie-Abhandlungen, 194(2), 211-252.

Pérouse, E., Chamot-Rooke, N., Rabaute, A., Briole, P., Jouanne, F., Georgiev, I., Dimitrov, D., 2012. Bridging onshore and offshore present-day kinematics of central and eastern Mediterranean: Implications for crustal dynamics and mantle flow. Geochemistry, Geophysics, Geosystems 13. https://doi.org/10.1029/2012GC004289

Philippon, M., Brun, J.-P., Gueydan, F., 2011. Tectonics of the Syros blueschists (Cyclades, Greece): From subduction to Aegean extension. Tectonics 30. https://doi.org/10.1029/2010TC002810

Plunder, A., Agard, P., Chopin, C., Okay, A. I., 2013. Geodynamics of the Tavşanlı zone, western Turkey: Insights into subduction/obduction processes. Tectonophysics, 608, 884-903. https://doi.org/10.1016/j.tecto.2013.07.028

Piromallo, C., Morelli, A., 2003. P wave tomography of the mantle under the Alpine-Mediterranean area. Journal of Geophysical Research: Solid Earth 108. https://doi.org/10.1029/2002JB001757

Pourteau, A., Candan, O., Oberhänsli, R., 2010. High-pressure metasediments in central Turkey: Constraints on the Neotethyan closure history. Tectonics 29. https://doi.org/10.1029/2009TC002650

ACCEPTED MANUSCRIPT

Pourteau, A., Sudo, M., Candan, O., Lanari, P., Vidal, O., Oberhänsli, R., 2013. Neotethys closure history of Anatolia: insights from 40Ar–39Ar geochronology and P–T estimation in high-pressure metasedimentary rocks. Journal of Metamorphic Geology 31, 585–606. https://doi.org/10.1111/jmg.12034

Pourteau, A., Bousquet, R., Vidal, O., Plunder, A., Duesterhoeft, E., Candan, O., Oberhänsli, R., 2014. Multistage growth of Fe–Mg–carpholite and Fe–Mg–chloritoid, from field evidence to thermodynamic modelling. Contrib Mineral Petrol 168, 1090. https://doi.org/10.1007/s00410-014-1090-7

Rabillard, A., Jolivet, L., Arbaret, L., Bessière, E., Laurent, V., Menant, A., ... Beaudoin, A., 2018. Synextensional Granitoids and Detachment Systems Within Cycladic Metamorphic Core Complexes (Aegean Sea, Greece): Toward a Regional Tectonomagmatic Model. Tectonics, 37(8), 2328-2362. https://doi.org/10.1029/2017TC004697

Régnier, J.L., Ring, U., Passchier, C.W., Gessner, K., Güngör, T., 2003. Contrasting metamorphic evolution of metasedimentary rocks from the Çine and Selimiye nappes in the Anatolide belt, western Turkey. Journal of Metamorphic Geology 21, 699–721. https://doi.org/10.1046/j.1525-1314.2003.00473.x

Reilinger, R., McClusky, S., Vernant, P., Lawrence, S., Ergintav, S., Cakmak, R., Ozener, H., Kadirov, F., Guliev, I., Stepanyan, R., Nadariya, M., Hahubia, G., Mahmoud, S., Sakr, K., ArRajehi, A., Paradissis, D., Al-Aydrus, A., Prilepin, M., Guseva, T., Evren, E., Dmitrotsa, A., Filikov, S.V., Gomez, F., Al-Ghazzi, R., Karam, G., 2006. GPS constraints on continental deformation in the Africa-Arabia-Eurasia continental collision zone and implications for the dynamics of plate interactions. Journal of Geophysical Research: Solid Earth 111. https://doi.org/10.1029/2005JB004051

Reilinger, R., McClusky, S., Paradissis, D., Ergintav, S., Vernant, P., 2010. Geodetic constraints on the tectonic evolution of the Aegean region and strain accumulation along the Hellenic subduction zone. Tectonophysics, Extensional Tectonics in the Basin and Range, the Aegean, and Western Anatolia 488, 22–30. https://doi.org/10.1016/j.tecto.2009.05.027

Reinecke, T., Altherr, R., Hartung, B., Hatzipanagiotou, K., Kreuzer, H., Harre, W. et al., 1982. Remnants of a late Cretaceous high temperature bet on the island of Anafi (Cyclades, Greece). N Jb Min Abh 145:157–182

Ricou, L.-E., Burg, J.-P., Godfriaux, I., Ivanov, Z., 1998. Rhodope and Vardar: the metamorphic and the olistostromic paired belts related to the Cretaceous subduction under Europe. Geodinamica Acta 11, 285–309. https://doi.org/10.1080/09853111.1998.11105326

ACCEPTED MANUSCRIPT

Rimmelé, G., Jolivet, L., Oberhänsli, R., Goffé, B., 2003a. Deformation history of the high-pressure Lycian Nappes and implications for tectonic evolution of SW Turkey. Tectonics 22. https://doi.org/10.1029/2001TC901041

Rimmelé, G., Oberhänsli, R., Goffé, B., Jolivet, L., Candan, O., Çetinkaplan, M., 2003b. First evidence of high-pressure metamorphism in the "Cover Series" of the southern Menderes Massif. Tectonic and metamorphic implications for the evolution of SW Turkey. Lithos 71, 19–46. https://doi.org/10.1016/S0024-4937(03)00089-6

Rimmelé, G., Parra, T., Goffé, B., Oberhänsli, R., Jolivet, L., Candan, O., 2005. Exhumation Paths of High-Pressure–Low-Temperature Metamorphic Rocks from the Lycian Nappes and the Menderes Massif (SW Turkey): a Multi-Equilibrium Approach. J Petrology 46, 641–669. https://doi.org/10.1093/petrology/egh092

Ring, U., Gessner, K., Güngör, T., Passchier, C.W., 1999a. The Menderes Massif of western Turkey and the Cycladic Massif in the Aegean—do they really correlate? Journal of the Geological Society 156, 3–6. https://doi.org/10.1144/gsjgs.156.1.0003

Ring, Uwe, Laws, S., Bernet, M., 1999b. Structural analysis of a complex nappe sequence and late-orogenic basins from the Aegean Island of Samos, Greece. Journal of Structural Geology 21, 1575–1601. https://doi.org/10.1016/S0191-8141(99)00108-X

Ring, U., Layer, P.W., Reischmann, T., 2001. Miocene high-pressure metamorphism in the Cyclades and Crete, Aegean Sea, Greece: Evidence for large-magnitude displacement on the Cretan detachment. Geology 29, 395–398. https://doi.org/10.1130/0091-7613(2001)029<0395:MHPMIT>2.0.CO;2

Ring, U., Johnson, C., Hetzel, R., Gessner, K., 2003. Tectonic denudation of a Late Cretaceous–Tertiary collisional belt: regionally symmetric cooling patterns and their relation to extensional faults in the Anatolide belt of western Turkey. Geol. Mag. 140, 421–441. https://doi.org/10.1017/S0016756803007878

Ring, U., Will, T., Glodny, J., Kumerics, C., Gessner, K., Thomson, S., Güngör, T., Monié, P., Okrusch, M., Drüppel, K., 2007. Early exhumation of high-pressure rocks in extrusion wedges: Cycladic blueschist unit in the eastern Aegean, Greece, and Turkey. Tectonics 26. https://doi.org/10.1029/2005TC001872

Ring, U., Glodny, J., Will, T., Thomson, S., 2010. The Hellenic Subduction System: High-Pressure Metamorphism, Exhumation, Normal Faulting, and Large-Scale Extension. Annual Review of Earth and Planetary Sciences 38, 45–76. https://doi.org/10.1146/annurev.earth.050708.170910

ACCEPTED MANUSCRIPT

Ring, U., Gessner, K., Thomson, S.N., 2017. South Menderes Monocline: Low-temperature thermochronology constrains role of crustal extension in structural evolution of southwest Turkey. Tectonophysics 712–713, 455–463. https://doi.org/10.1016/j.tecto.2017.06.019

Robertson, A.H.F., Clift, P.D., Degnan, P.J., Jones, G., 1991. Palaeogeographic and palaeotectonic evolution of the Eastern Mediterranean Neotethys. Palaeogeography, Palaeoclimatology, Palaeoecology, Palaeogeography and Paleoceanography of Tethys 87, 289–343. https://doi.org/10.1016/0031-0182(91)90140-M

Roche, V., Laurent, V., Cardello, G.L., Jolivet, L., Scaillet, S., 2016. Anatomy of the Cycladic Blueschist Unit on Sifnos Island (Cyclades, Greece). Journal of Geodynamics 97, 62–87. https://doi.org/10.1016/j.jog.2016.03.008

Roche, V., Conand, C., Jolivet, L., Augier, R., 2018a. Tectonic evolution of Leros Island (Dodecanese, Greece) and correlations between the Aegean Domain and the Menderes Massif. Journal of the Geological Society jgs2018-028. https://doi.org/10.1144/jgs2018-028

Roche, V., Sternai, P., Guillou-Frottier, L., Menant, A., Jolivet, L., Bouchot, V., Gerya, T., 2018b. Emplacement of metamorphic core complexes and associated geothermal systems controlled by slab dynamics. Earth and Planetary Science Letters 498, 322–333. https://doi.org/10.1016/j.epsl.2018.06.043

Roche, V., Bouchot, V., Beccaletto, L., Jolivet, L., Guillou-Frottier, L., Tuduri, J., Bozkurt, E., Oguz, K., Tokay, B., 2018c. Structural, lithological, and geodynamic controls on geothermal activity in the Menderes geothermal Province (Western Anatolia, Turkey). Int J Earth Sci (Geol Rundsch). https://doi.org/10.1007/s00531-018-1655-1

Rosenbaum, G., Ring, U., Kühn, A., 2007. Tectonometamorphic evolution of high-pressure rocks from the island of Amorgos (Central Aegean, Greece). Journal of the Geological Society 164, 425–438. https://doi.org/10.1144/0016-76492006-005

Royden, L.H., 1993. Evolution of retreating subduction boundaries formed during continental collision. Tectonics 12, 629–638. https://doi.org/10.1029/92TC02641

Salaün, G., Pedersen, H.A., Paul, A., Farra, V., Karabulut, H., Hatzfeld, D., Papazachos, C., Childs, D.M., Pequegnat, C., 2012. High-resolution surface wave tomography beneath the Aegean-Anatolia region: constraints on upper-mantle structure. Geophys J Int 190, 406–420. https://doi.org/10.1111/j.1365-246X.2012.05483.x

Schermer, E.R., Lux, D.R., Burchfiel, B.C., 1990. Temperature-time history of subducted continental crust, Mount Olympos Region, Greece. Tectonics 9, 1165–1195. https://doi.org/10.1029/TC009i005p01165

ACCEPTED MANUSCRIPT

Schneider, D.A., Senkowski, C., Vogel, H., Grasemann, B., Iglseder, C., Schmitt, A.K., 2011. Eocene tectonometamorphism on Serifos (western Cyclades) deduced from zircon depth-profiling geochronology and mica thermochronology. Lithos 125, 151–172. https://doi.org/10.1016/j.lithos.2011.02.005

Seaton, N.C.A., Whitney, D.L., Teyssier, C., Toraman, E., Heizler, M.T., 2009. Recrystallization of high-pressure marble (Sivrihisar, Turkey). Tectonophysics 479:241–253. https://doi.org/10.1016/j.tecto.2009.08.015

Sengör, A.M.C., Satir, M., Akkök, R., 1984. Timing of tectonic events in the Menderes Massif, western Turkey: Implications for tectonic evolution and evidence for pan-African basement in Turkey. Tectonics 3, 693–707. https://doi.org/10.1029/TC003i007p00693

Seyítoğlu, G., Scott, B.C., Rundle, C.C., 1992. Timing of Cenozoic extensional tectonics in west Turkey. Journal of the Geological Society 149, 533–538. https://doi.org/10.1144/gsjgs.149.4.0533

Seyítoğlu, G., Scott, B.C., 1996. The cause of N-S extensional tectonics in western Turkey: Tectonic escape vs back-arc spreading vs orogenic collapse. Journal of Geodynamics 22, 145–153. https://doi.org/10.1016/0264-3707(96)00004-X

Seyitoğlu, G., Işık, V., Cemen, I., 2004. Complete Tertiary exhumation history of the Menderes massif, western Turkey: an alternative working hypothesis. Terra Nova, 16(6), 358-364. https://doi.org/10.1111/j.1365-3121.2004.00574.x

Spakman, W., Wortel, M.J.R., Vlaar, N.J., 1988. The Hellenic Subduction Zone: A tomographic image and its geodynamic implications. Geophysical Research Letters 15, 60–63. https://doi.org/10.1029/GL015i001p00060

Stavropoulos, A., Gerolymatos, I., 1999. Geological map of Leros. IGME, Madrid.

Sternai, P., Jolivet, L., Menant, A., Gerya, T., 2014. Driving the upper plate surface deformation by slab rollback and mantle flow. Earth and Planetary Science Letters 405, 110–118. https://doi.org/10.1016/j.epsl.2014.08.023

Theodoropoulos, D. (1979). Geological Map of Greece 1: 50000, Samos Island. NIGMR, Athens.

Theye, T., Chopin, C., Grevel, K.-D., Ockenga, E., 1997. The assemblage diaspore+quartz in metamorphic rocks: a petrological, experimental and thermodynamic study. Journal of Metamorphic Geology 15, 17–28. https://doi.org/10.1111/j.1525-1314.1997.1501050.x

Trotet, F., Vidal, O., Jolivet, L., 2001. Exhumation of Syros and Sifnos metamorphic rocks (Cyclades, Greece). New constraints on the P-T paths. European Journal of Mineralogy 13, 901–902. https://doi.org/10.1127/0935-1221/2001/0013-0901

ACCEPTED MANUSCRIPT

Urai, J.L., Schuiling, R.D., Jansen, J.B.H., 1990. Alpine deformation on Naxos (Greece). Geological Society, London, Special Publications 54, 509–522. https://doi.org/10.1144/GSL.SP.1990.054.01.47

Uzel, B., Langereis, C. G., Kaymakci, N., Sözbilir, H., Özkaymak, Ç., Özkaptan, M., 2015. Paleomagnetic evidence for an inverse rotation history of Western Anatolia during the exhumation of Menderes core complex. Earth and Planetary Science Letters, 414, 108-125. https://doi.org/10.1016/j.epsl.2015.01.008

van Hinsbergen, D.J.J., 2010. A key extensional metamorphic complex reviewed and restored: The Menderes Massif of western Turkey. Earth-Science Reviews 102, 60–76. https://doi.org/10.1016/j.earscirev.2010.05.005

van Hinsbergen, D.J.J., Schmid, S.M., 2012. Map view restoration of Aegean–West Anatolian accretion and extension since the Eocene. Tectonics 31. https://doi.org/10.1029/2012TC003132

van Hinsbergen, D.J.J. van, Hafkenscheid, E., Spakman, W., Meulenkamp, J.E., Wortel, R., 2005. Nappe stacking resulting from subduction of oceanic and continental lithosphere below Greece. Geology 33, 325–328. https://doi.org/10.1130/G20878.1

van Hinsbergen, D.J.J., Kaymakci, N., Spakman, W., Torsvik, T.H., 2010a. Reconciling the geological history of western Turkey with plate circuits and mantle tomography. Earth Planet Sci Lett 297:674–686. https://doi.org/10.1016/j.epsl.2010.07.024

van Hinsbergen, D.J.J., Dekkers, M.J., Bozkurt, E., Koopman, M., 2010b. Exhumation with a twist: Paleomagnetic constraints on the evolution of the Menderes metamorphic core complex, western Turkey. Tectonics 29. https://doi.org/10.1029/2009TC002596

Walcott, C.R., White, S.H., 1998. Constraints on the kinematics of post-orogenic extension imposed by stretching lineations in the Aegean region. Tectonophysics 298, 155–175. https://doi.org/10.1016/S0040-1951(98)00182-6

Weidmann, M., Solounias, N., Drake, R.E., Curtis, G.H., 1984. Neogene stratigraphy of the Eastern basin, Samos island, Greece. Geobios 17, 477–490. https://doi.org/10.1016/S0016-6995(84)80020-0

Whitney, D. L., Bozkurt, E., 2002. Metamorphic history of the southern Menderes massif, western Turkey. Geological Society of America Bulletin, 114(7), 829-838. https://doi.org/10.1130/0016-7606(2002)114<0829:MHOTSM>2.0.CO;2

Whitney, D.L., Evans, B.W., 2010. Abbreviations for names of rock-forming minerals. American mineralogist, 95(1), 185-187. https://doi.org/10.2138/am.2010.3371

ACCEPTED MANUSCRIPT

Whitney, D. L., Teyssier, C., Kruckenberg, S. C., Morgan, V. L., Iredale, L. J., 2008. High-pressure–low-temperature metamorphism of metasedimentary rocks, southern Menderes Massif, western Turkey. Lithos, 101(3-4), 218-232. https://doi.org/10.1016/j.lithos.2007.07.001

Will, T., Okrusch, M., Schmädicke, E., Chen, G., 1998. Phase relations in the greenschist-blueschist-amphibolite-eclogite facies in the system Na2O-CaO-FeO-MgO-Al2O3-SiO2-H2O (NCFMASH), with application to metamorphic rocks from Samos, Greece. Contrib Mineral Petrol 132, 85–102. https://doi.org/10.1007/s004100050406

Wortel, M.J.R., Spakman, W., 2000. Subduction and Slab Detachment in the Mediterranean-Carpathian Region. Science 290, 1910–1917. https://doi.org/10.1126/science.290.5498.1910

ACCEPTED MANUSCRIPT

ACCEPTED MANUSCRIPT

Abstract

Slab tearing below western Turkey had first-order tectonic and magmatic consequences by inducing a lateral gradient of extension in the upper plate and toroidal flow of asthenosphere that affected the typology and distribution of melts at the surface. But the coupling mechanisms between the 3D mantle flow at depth and deformation in the upper plate above a slab tear have received little attention so far. This paper is focused on the description of the distribution and kinematics of deformation in the eastern part of the Aegean Sea, within the transition zone between the Cyclades and the Menderes Massif, which have been little studied. By investigating the Dodecanese and Eastern Aegean islands, we thus complete the description of the extensional strain field in the overriding plate around the slab tear. There, extension related to slab retreat and tearing keeps a constant NNE-SSW direction accommodating the difference in finite rates of extension, without localized crustal-scale strike-slip faults and block rotations above the tear. In addition, despite the complexity involved in the Aegean-Anatolian orogenic wedge, a similar structural position is recognized through the entire region. From top to bottom, we found that (i) the Lycian units which were exhumed earlier, in the Late Cretaceous, (ii) the higher-pressure and higher-temperature units (i.e. the Upper Cycladic Blueschist Nappe), with exception of the Vourliotes nappe in Samos, and finally (iii) the colder units such as Amorgos unit, the Menderes and its cover before the Main Menderes Metamorphism overprint and the Lower Cycladic Blueschist Nappe (e.g. Milos, Folegandros, a part of the Dodecanese and Fourni islands).

ACCEPTED MANUSCRIPT

Key Points:

- Extension in Dodecanese and Fourni islands is accommodated by low-angle detachments
- Consistent NNE-SSW-directed flow in lower crust above slab tear in Aegean/Anatolian transition zone
- No localized strike-slip deformation in the lower crust above slab tearing
- Three “nappes” are distinguished in the orogenic wedge with different P-T conditions

ACCEPTED MANUSCRIPT

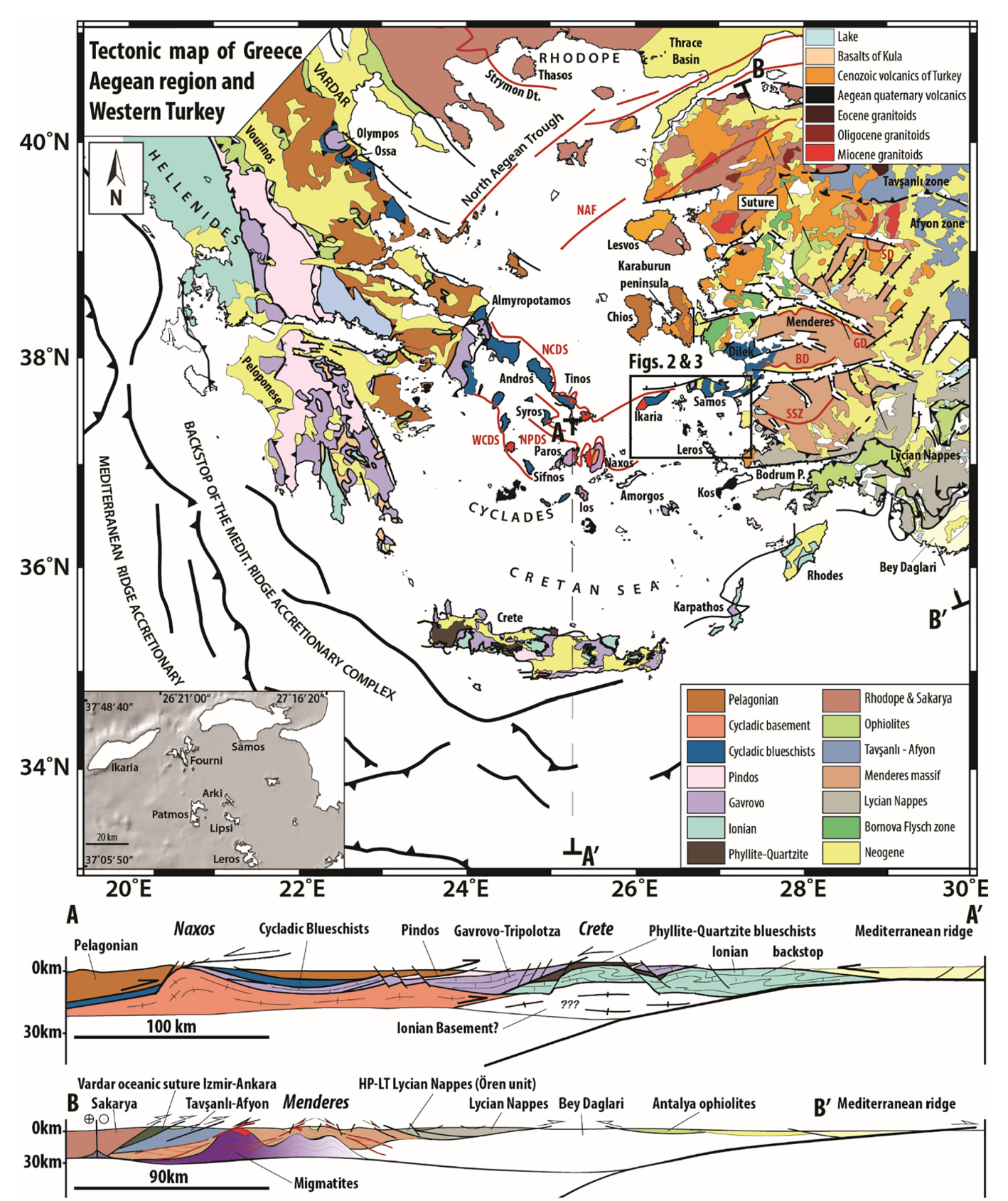
Tectonic map of Greece
Aegean region and
Western Turkey
Lake
Basalts of Kula
Cenozoic volcanics of Turkey
Aegean quaternary volcanics
Eocene granitoids
Oligocene granitoids
Miocene granitoids
RHODOPE
Thrace
Basin
Thasos
Strymon Dt.
VARDAR
Vourinos
Olympos
Ossa
North Aegean Trough
HELLENIDES
NAF
Suture
Tavşanlı zone
Afyon zone
SD
Lesvos
Karaburun
peninsula
Chios
Almyropotamos
Menderes
GD
BD
Dilek
NCDS
Figs. 2 & 3
Andros
Tinos
Syros
Samos
Ikaria
SSZ
WCDS
NPDS
Paros
Leros
Lycian Nappes
Naxos
Sifnos
Bodrum P.
Kos
Amorgos
Ios
CYCLADES
Peloponese
BACKSTOP OF THE MEDIT. RIDGE ACCRETIONARY COMPLEX
MEDITERRANEAN RIDGE ACCRETIONARY
CRETAN SEA
Rhodes
Bey Daglari
Karpathos
Crete
40°N
38°N
36°N
34°N
20°E
22°E
24°E
26°E
28°E
30°E
N
A
A′
B
B′
26°21′00″
27°16′20″
37°48′40″
37°05′50″
Samos
Fourni
Ikaria
Arki
Patmos
Lipsi
Leros
20 km
Pelagonian
Cycladic basement
Cycladic blueschists
Pindos
Gavrovo
Ionian
Phyllite-Quartzite
Rhodope & Sakarya
Ophiolites
Tavşanlı - Afyon
Menderes massif
Lycian Nappes
Bornova Flysch zone
Neogene
A
A′
Naxos
Cycladic Blueschists
Pindos
Gavrovo-Tripolotza
Crete
Phyllite-Quartzite blueschists
Mediterranean ridge
Pelagonian
Ionian
backstop
0km
30km
100 km
???
Ionian Basement?
B
B′
Vardar oceanic suture Izmir-Ankara
HP-LT Lycian Nappes (Ören unit)
Sakarya
Tavşanlı-Afyon
Menderes
Lycian Nappes
Bey Daglari
Antalya ophiolites
Mediterranean ridge
0km
30km
90km
Migmatites

Figure 1

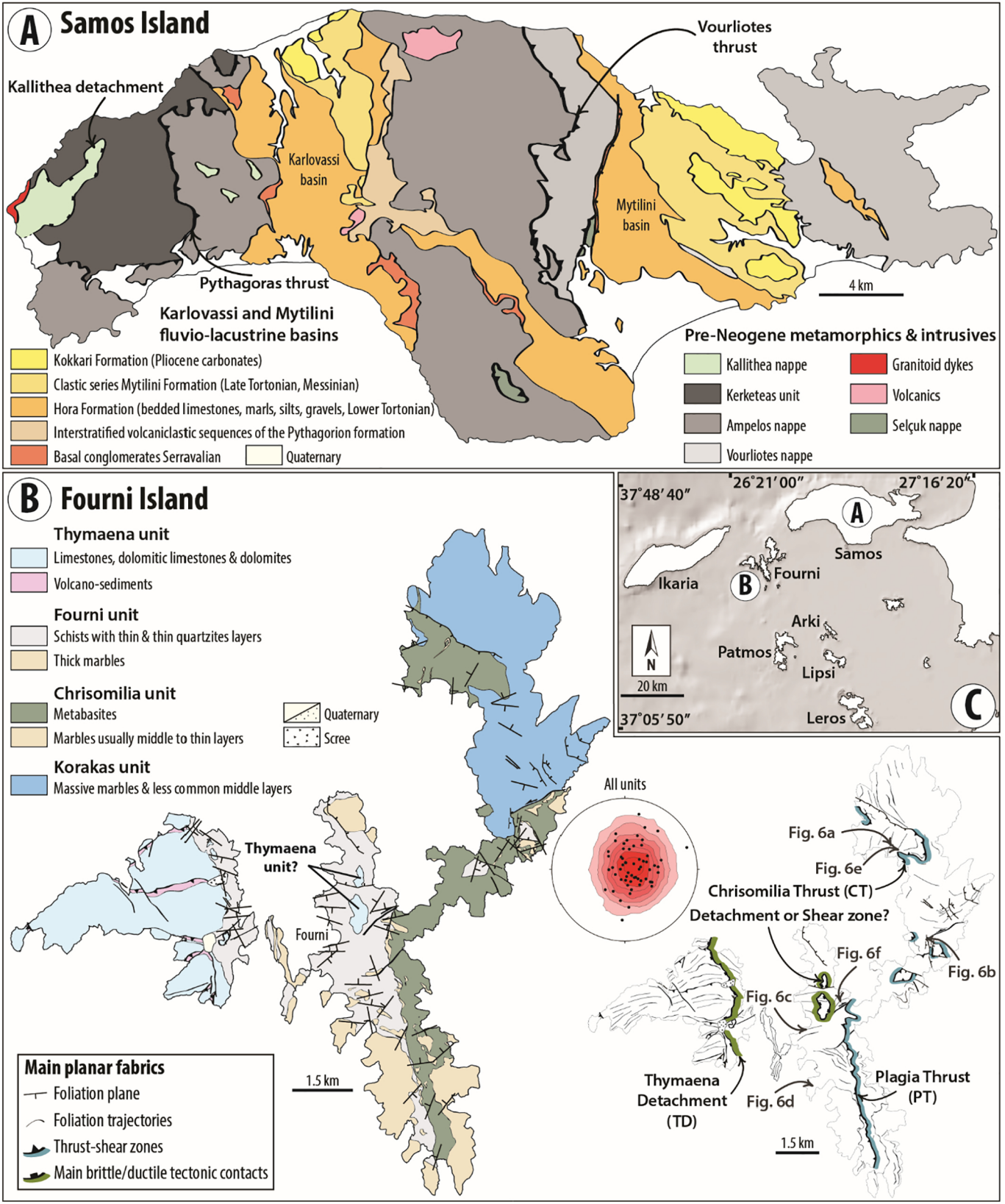
A Samos Island
Kallithea detachment
Vourliotes thrust
Karlovassi basin
Mytilini basin
Pythagoras thrust
4 km
Karlovassi and Mytilini fluvio-lacustrine basins
Kokkari Formation (Pliocene carbonates)
Clastic series Mytilini Formation (Late Tortonian, Messinian)
Hora Formation (bedded limestones, marls, silts, gravels, Lower Tortonian)
Interstratified volcaniclastic sequences of the Pythagorion formation
Basal conglomerates Serravalian
Quaternary
Pre-Neogene metamorphics & intrusives
Kallithea nappe
Kerketeas unit
Ampelos nappe
Vourliotes nappe
Granitoid dykes
Volcanics
Selçuk nappe
B Fourni Island
Thymaena unit
Limestones, dolomitic limestones & dolomites
Volcano-sediments
Fourni unit
Schists with thin & thin quartzites layers
Thick marbles
Chrisomilia unit
Metabasites
Marbles usually middle to thin layers
Korakas unit
Massive marbles & less common middle layers
Quaternary
Scree
Thymaena unit?
Fourni
1.5 km
All units
Main planar fabrics
Foliation plane
Foliation trajectories
Thrust-shear zones
Main brittle/ductile tectonic contacts
37°48′40″
26°21′00″
27°16′20″
37°05′50″
A
B
C
Samos
Ikaria
Fourni
Arki
Patmos
Lipsi
Leros
N
20 km
Fig. 6a
Fig. 6e
Chrisomilia Thrust (CT)
Detachment or Shear zone?
Fig. 6f
Fig. 6b
Fig. 6c
Thymaena Detachment (TD)
Fig. 6d
Plagia Thrust (PT)
1.5 km

Figure 2

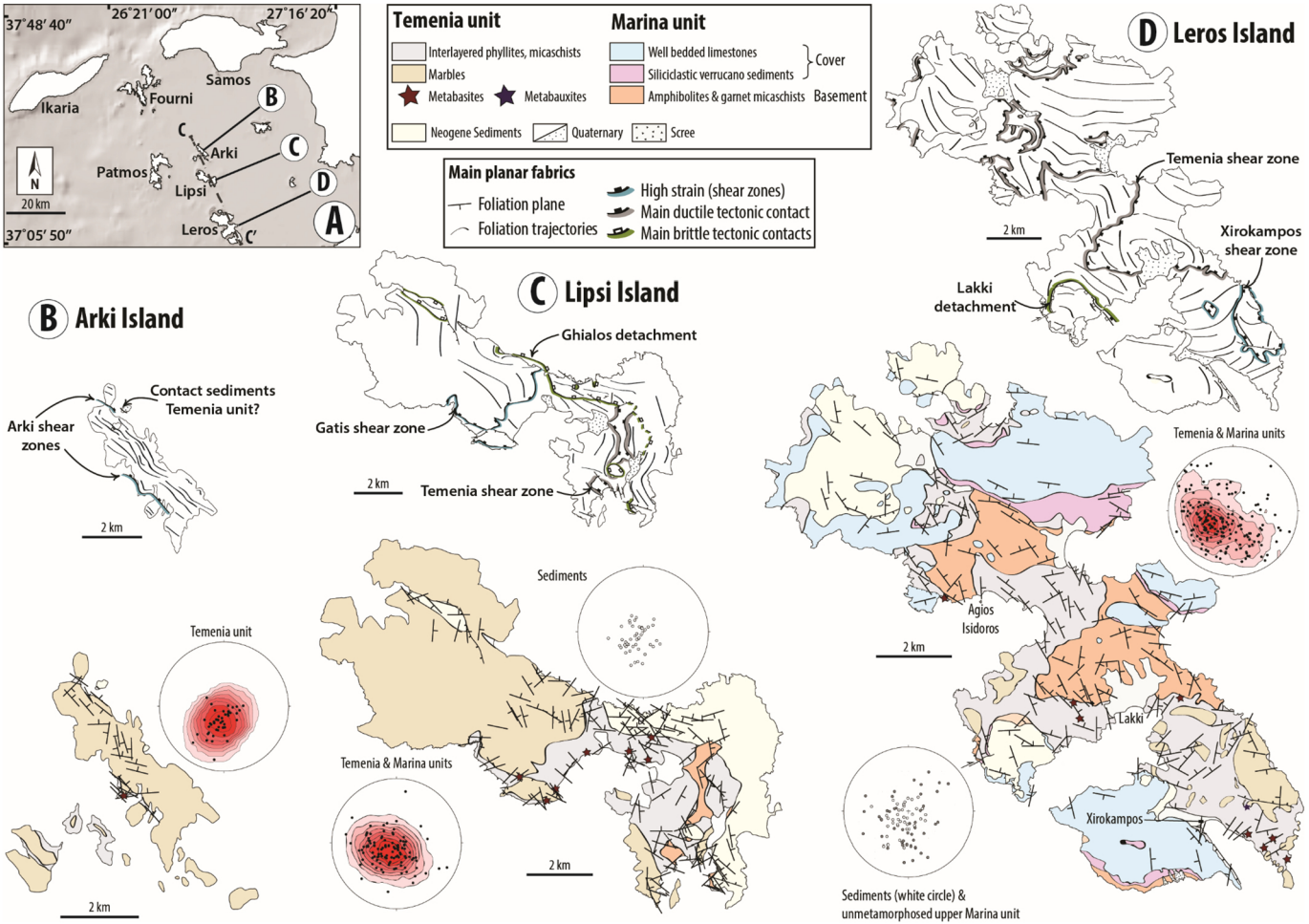
37°48′40″
26°21′00″
27°16′20″
37°05′50″
Samos
Fourni
Ikaria
Arki
Patmos
Lipsi
Leros
B
C
D
A
C′
N
20 km
Temenia unit
Interlayered phyllites, micaschists
Marbles
Metabasites
Metabauxites
Marina unit
Well bedded limestones
Siliciclastic verrucano sediments
Amphibolites & garnet micaschists
Cover
Basement
Neogene Sediments
Quaternary
Scree
Main planar fabrics
Foliation plane
Foliation trajectories
High strain (shear zones)
Main ductile tectonic contact
Main brittle tectonic contacts
B Arki Island
Contact sediments
Temenia unit?
Arki shear
zones
2 km
Temenia unit
2 km
C Lipsi Island
Ghialos detachment
Gatis shear zone
2 km
Temenia shear zone
Sediments
Temenia & Marina units
2 km
D Leros Island
Temenia shear zone
2 km
Xirokampos
shear zone
Lakki
detachment
Temenia & Marina units
Agios
Isidoros
2 km
Lakki
Xirokampos
Sediments (white circle) &
unmetamorphosed upper Marina unit

Figure 3

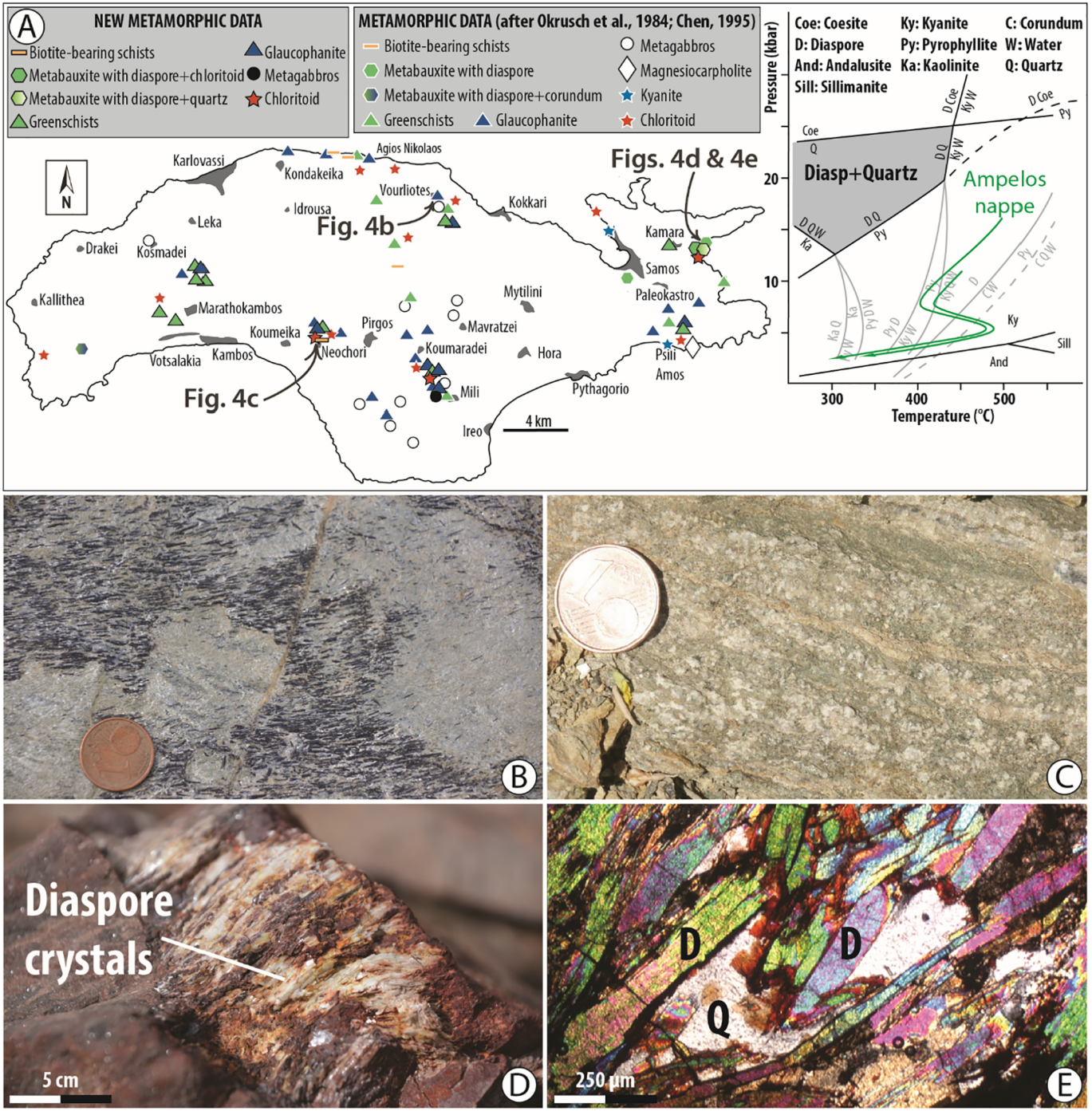
A
NEW METAMORPHIC DATA
Biotite-bearing schists
Glaucophanite
Metabauxite with diaspore+chloritoid
Metagabbros
Metabauxite with diaspore+quartz
Chloritoid
Greenschists
METAMORPHIC DATA (after Okrusch et al., 1984; Chen, 1995)
Biotite-bearing schists
Metagabbros
Metabauxite with diaspore
Magnesiocarpholite
Metabauxite with diaspore+corundum
Kyanite
Greenschists
Glaucophanite
Chloritoid
N
Karlovassi
Agios Nikolaos
Kondakeika
Vourliotes
Idrousa
Kokkari
Leka
Fig. 4b
Figs. 4d & 4e
Drakei
Kosmadei
Kamara
Samos
Kallithea
Marathokambos
Mytilini
Paleokastro
Koumeika
Pirgos
Mavratzei
Votsalakia
Kambos
Neochori
Koumaradei
Hora
Psili Amos
Fig. 4c
Mili
Pythagorio
Ireo
4 km
Coe: Coesite
Ky: Kyanite
C: Corundum
D: Diaspore
Py: Pyrophyllite
W: Water
And: Andalusite
Ka: Kaolinite
Q: Quartz
Sill: Sillimanite
Pressure (kbar)
Diasp+Quartz
Ampelos nappe
Ky
Sill
And
Temperature (°C)
300
400
500
B
C
Diaspore crystals
5 cm
D
D
D
Q
250 µm
E

Figure 4

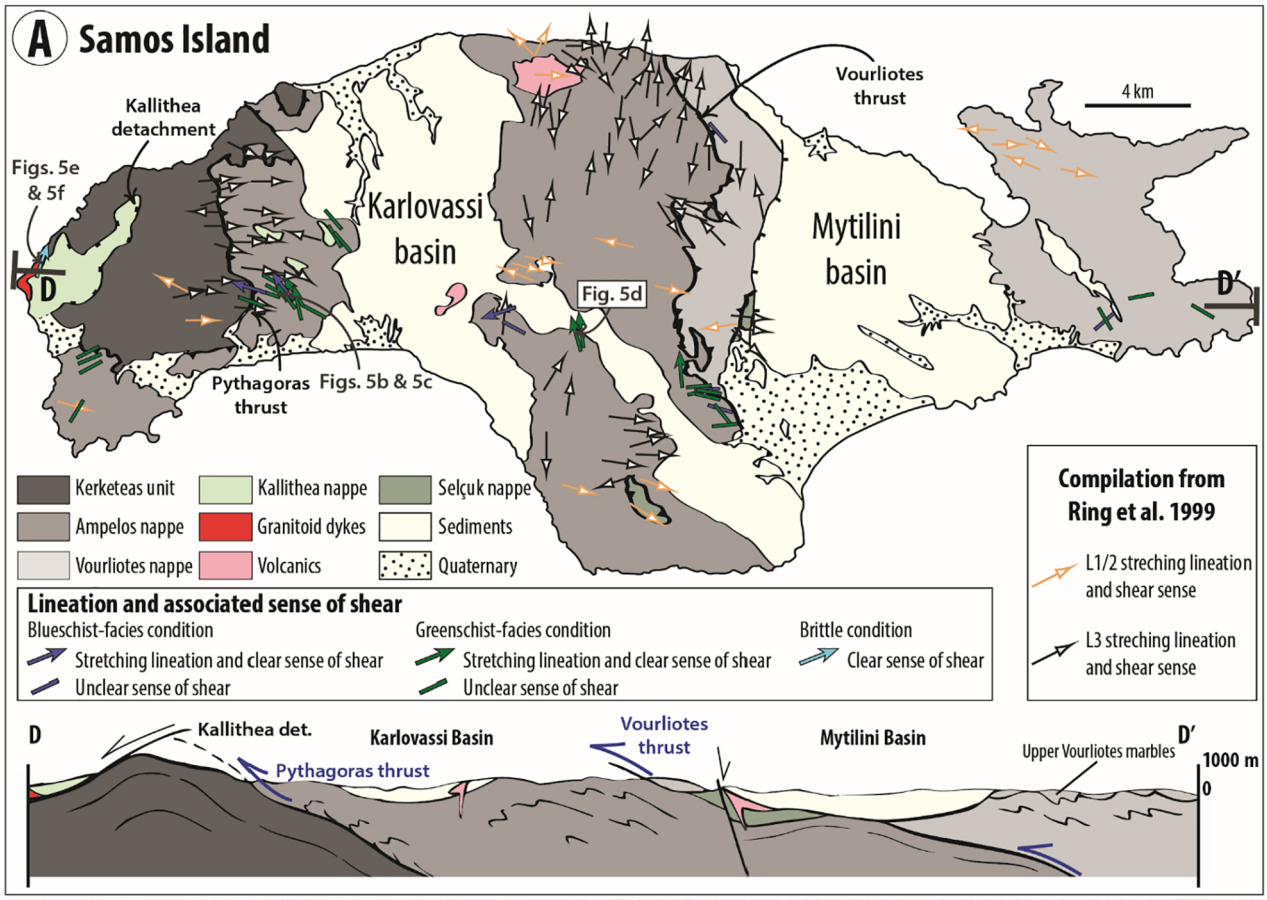
A Samos Island
Kallithea detachment
Figs. 5e & 5f
D
Karlovassi basin
Vourliotes thrust
4 km
Mytilini basin
D′
Fig. 5d
Pythagoras thrust
Figs. 5b & 5c
Kerketeas unit
Ampelos nappe
Vourliotes nappe
Kallithea nappe
Granitoid dykes
Volcanics
Selçuk nappe
Sediments
Quaternary
Compilation from Ring et al. 1999
L1/2 streching lineation and shear sense
L3 streching lineation and shear sense
Lineation and associated sense of shear
Blueschist-facies condition
Stretching lineation and clear sense of shear
Unclear sense of shear
Greenschist-facies condition
Stretching lineation and clear sense of shear
Unclear sense of shear
Brittle condition
Clear sense of shear
D
Kallithea det.
Karlovassi Basin
Pythagoras thrust
Vourliotes thrust
Mytilini Basin
D′
Upper Vourliotes marbles
1000 m
0

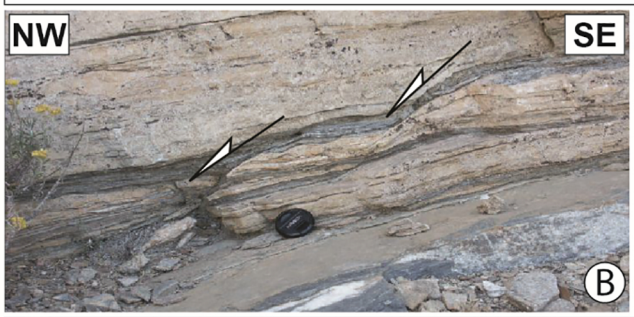
NW
SE
B

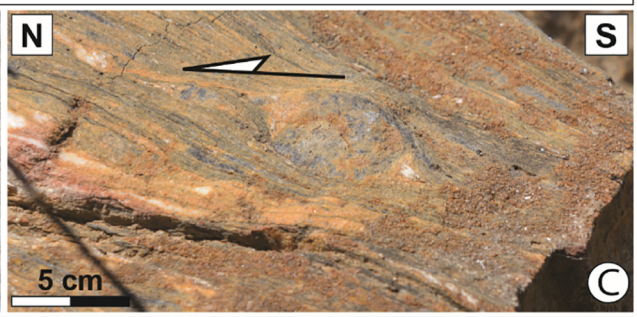
N
S
5 cm
C

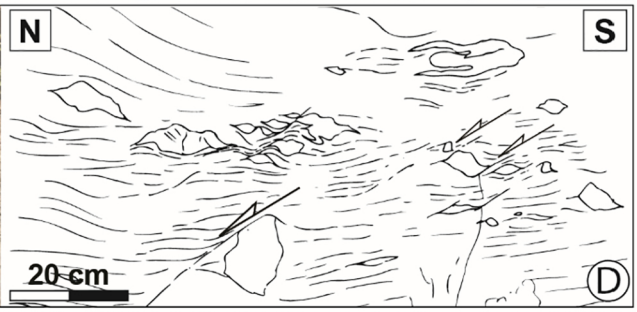
N
S
20 cm
D

E
W
2 m
E

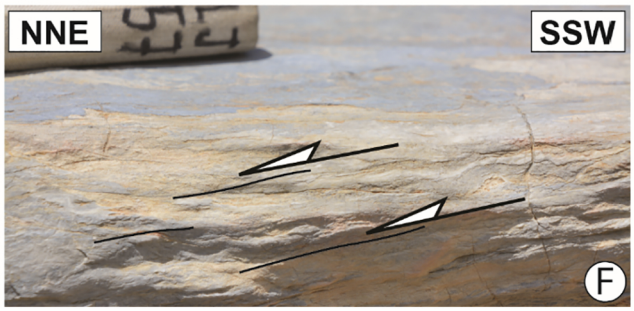
NNE
SSW
F

Figure 5

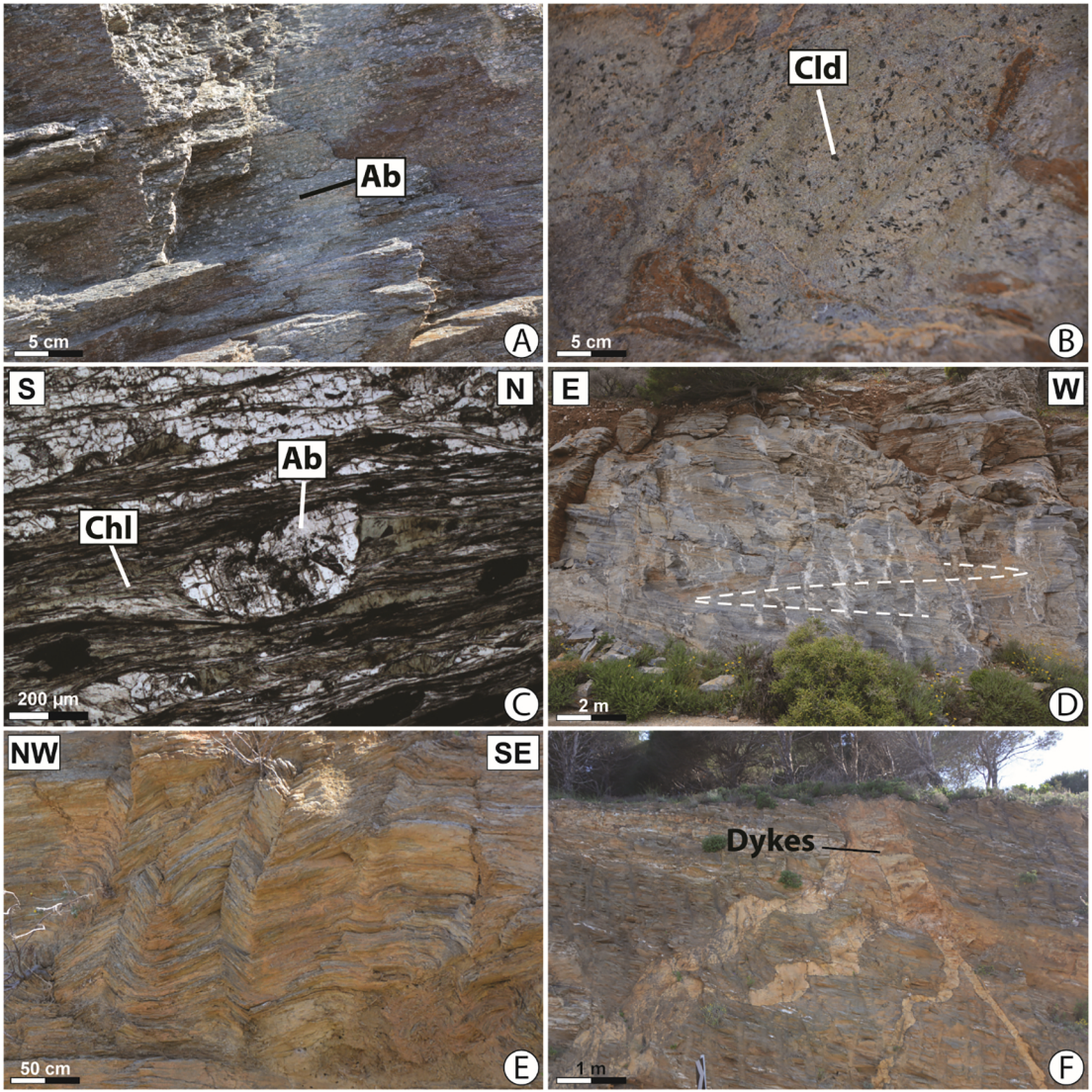

Figure 6

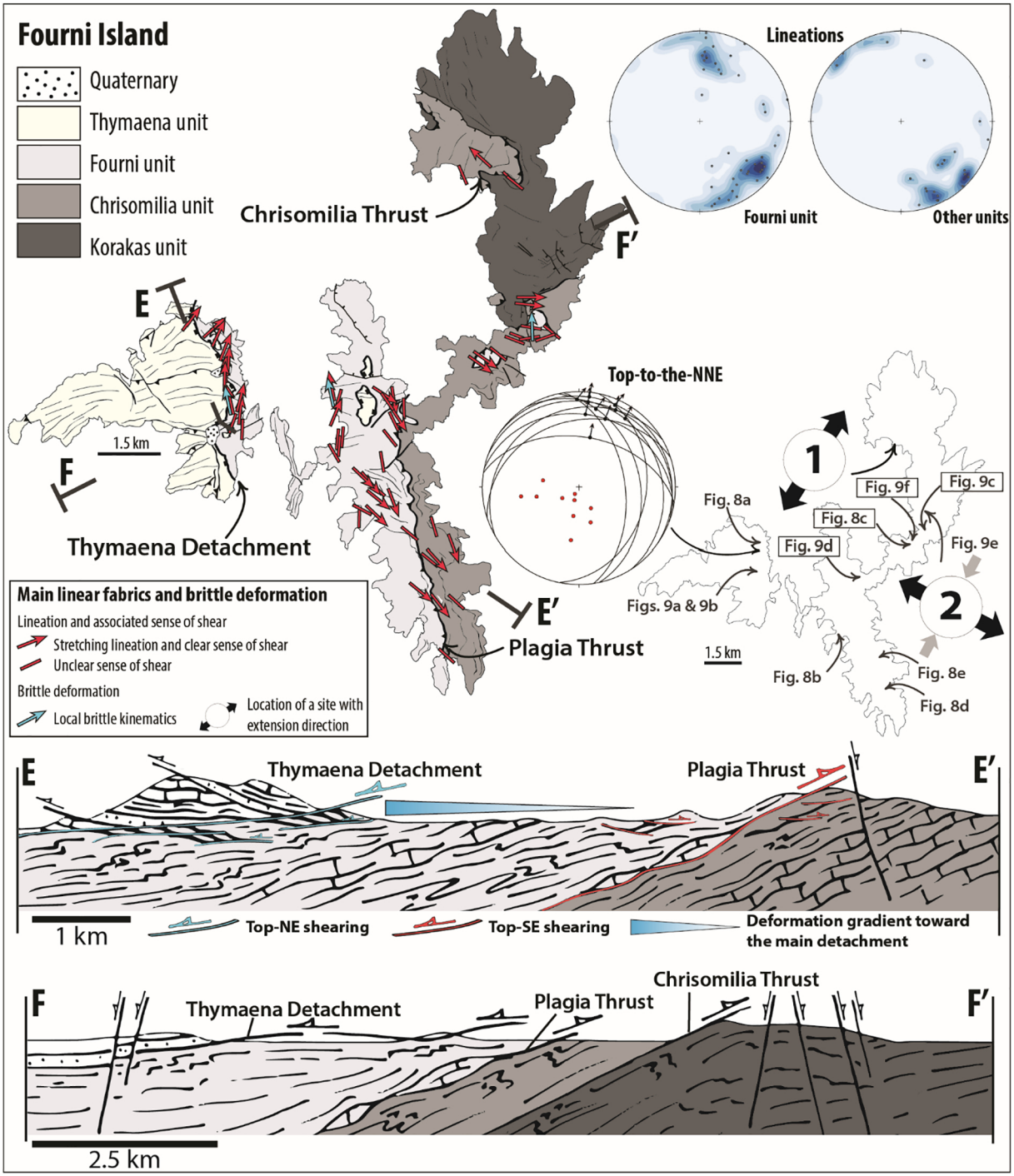
Fourni Island
Quaternary
Thymaena unit
Fourni unit
Chrisomilia unit
Korakas unit
Chrisomilia Thrust
F'
E
F
1.5 km
Thymaena Detachment
E'
Plagia Thrust
Lineations
Fourni unit
Other units
Top-to-the-NNE
Fig. 8a
Figs. 9a & 9b
Fig. 8b
Fig. 8c
Fig. 8d
Fig. 8e
Fig. 9c
Fig. 9d
Fig. 9e
Fig. 9f
1
2
1.5 km
Main linear fabrics and brittle deformation
Lineation and associated sense of shear
Stretching lineation and clear sense of shear
Unclear sense of shear
Brittle deformation
Local brittle kinematics
Location of a site with extension direction
E
Thymaena Detachment
Plagia Thrust
E'
1 km
Top-NE shearing
Top-SE shearing
Deformation gradient toward the main detachment
F
Thymaena Detachment
Plagia Thrust
Chrisomilia Thrust
F'
2.5 km

Figure 7

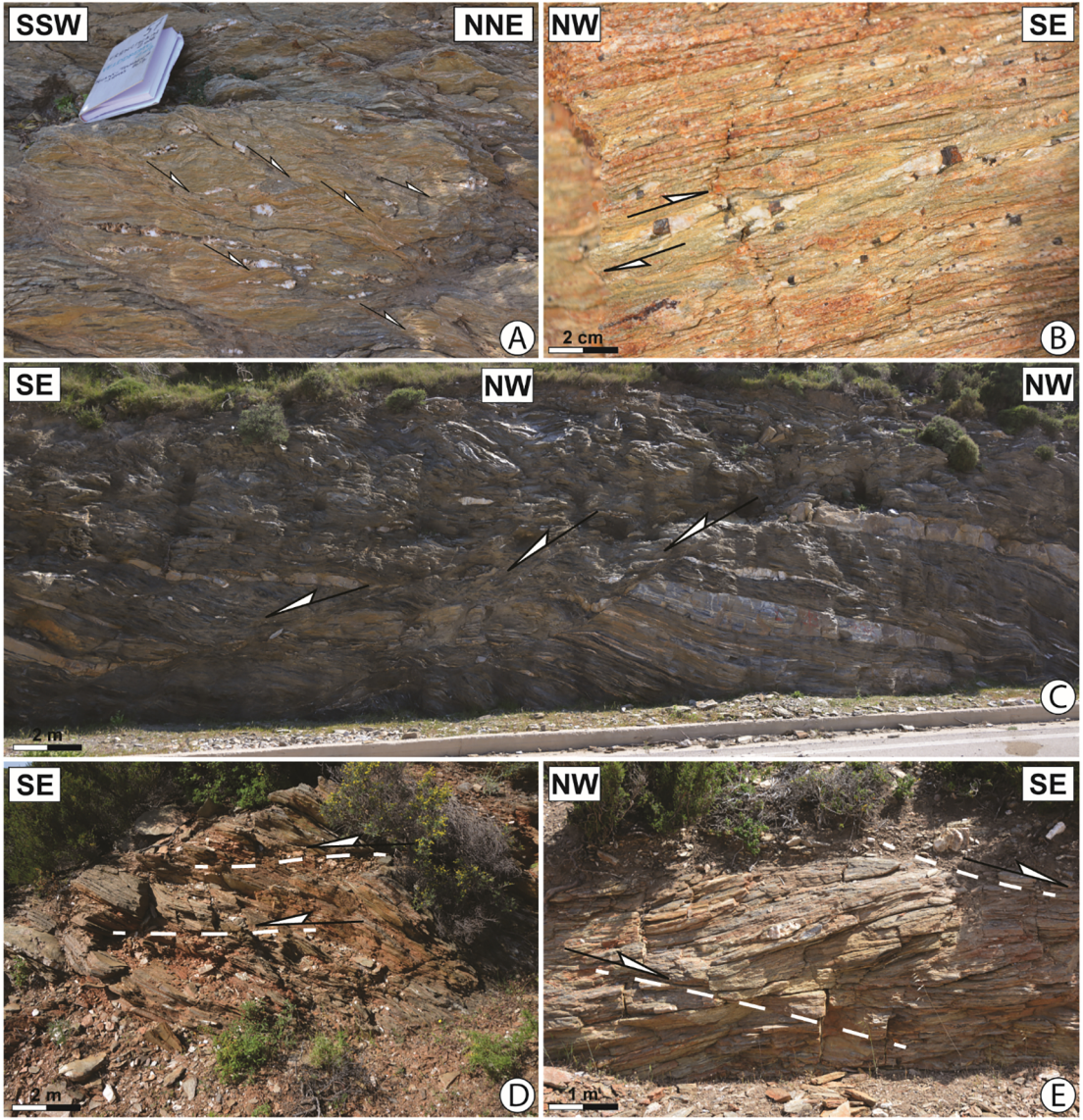

Figure 8

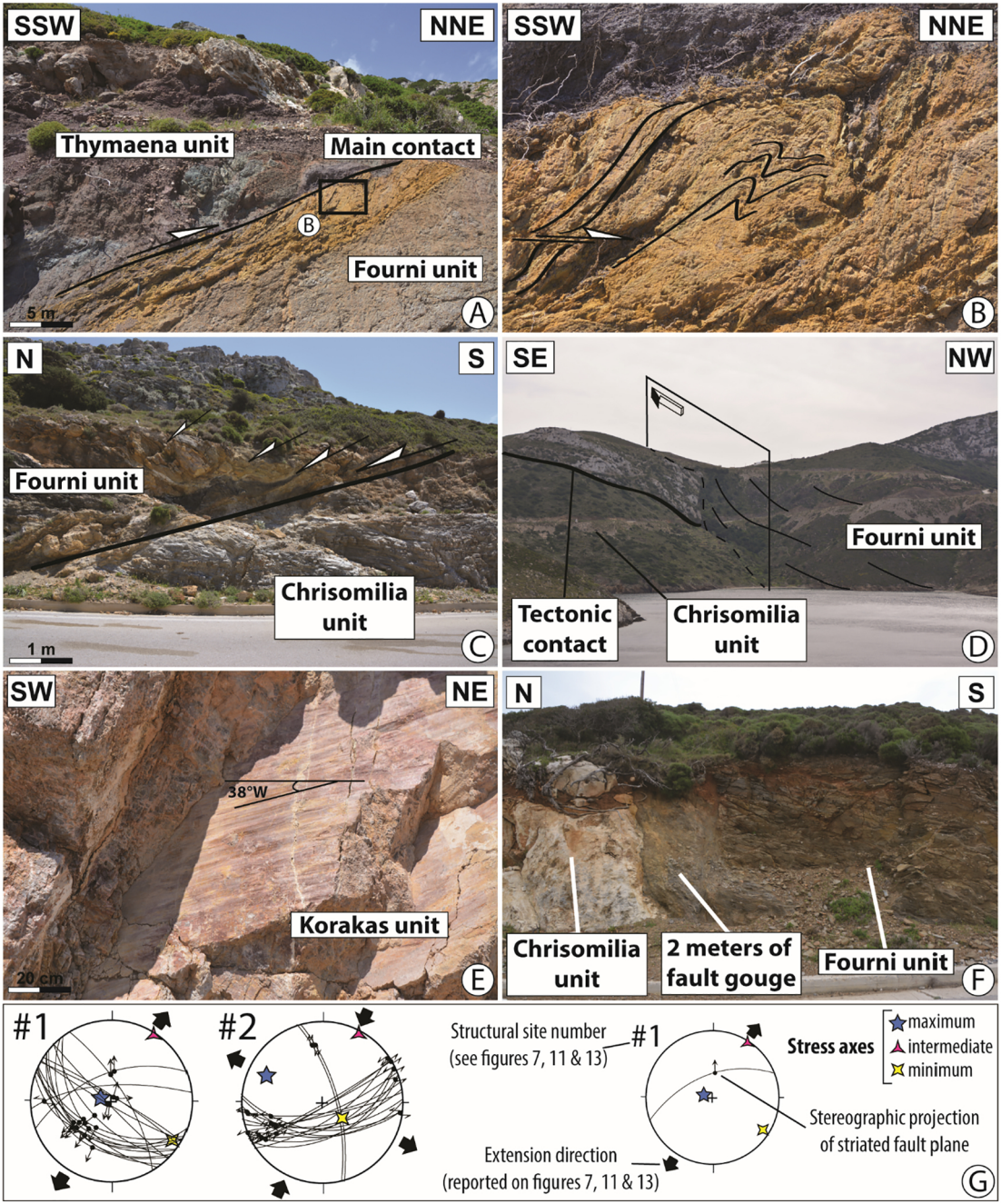
SSW
NNE
Thymaena unit
Main contact
B
Fourni unit
5 m
A
SSW
NNE
B
N
S
Fourni unit
Chrisomilia unit
1 m
C
SE
NW
Fourni unit
Tectonic contact
Chrisomilia unit
D
SW
NE
38°W
Korakas unit
20 cm
E
N
S
Chrisomilia unit
2 meters of fault gouge
Fourni unit
F
#1
#2
Structural site number (see figures 7, 11 & 13)
#1
Stress axes
maximum
intermediate
minimum
Stereographic projection of striated fault plane
Extension direction (reported on figures 7, 11 & 13)
G

Figure 9

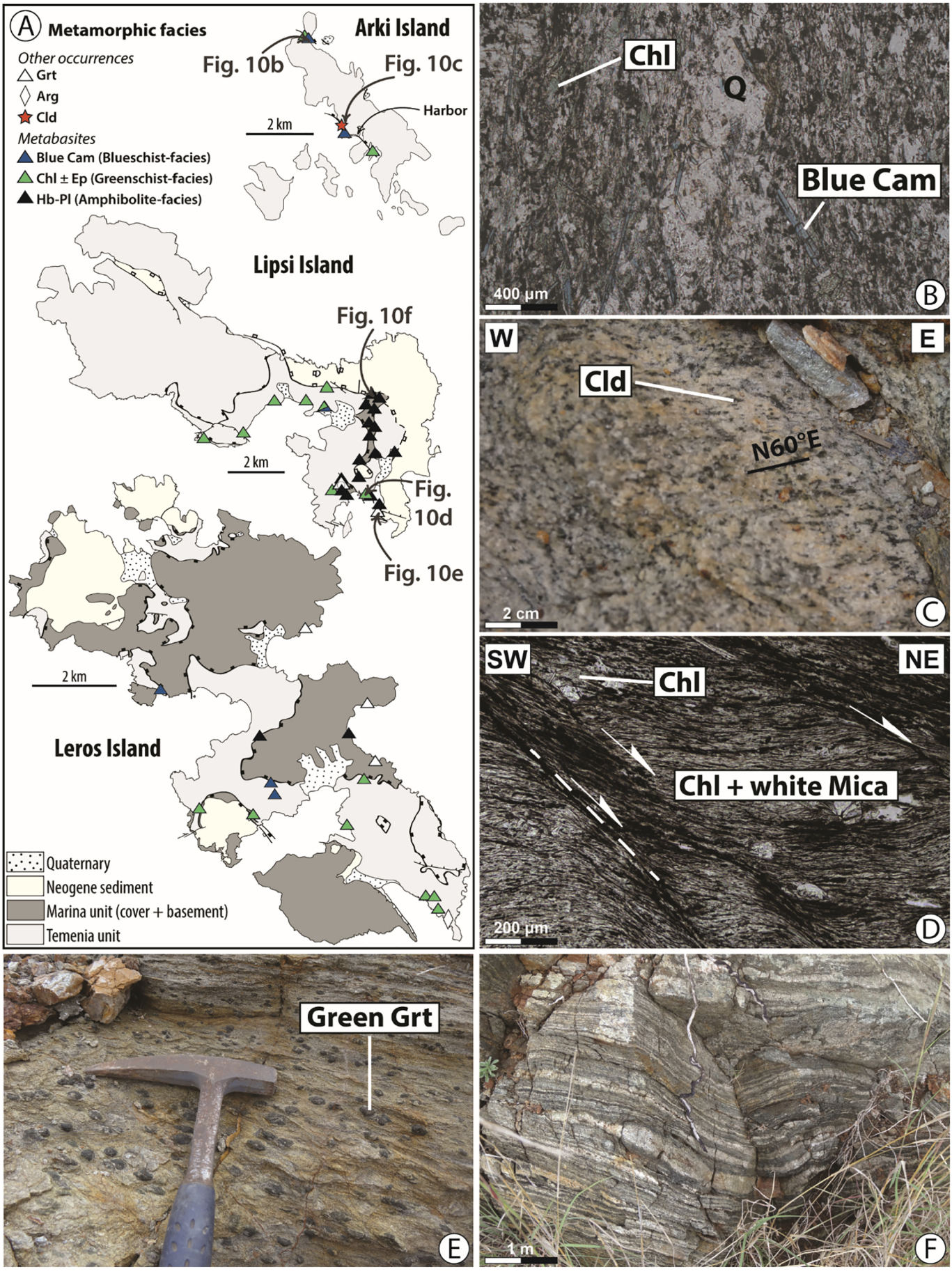
A
Metamorphic facies
Other occurrences
Grt
Arg
Cld
Metabasites
Blue Cam (Blueschist-facies)
Chl ± Ep (Greenschist-facies)
Hb-Pl (Amphibolite-facies)
Arki Island
Fig. 10b
Fig. 10c
Harbor
2 km
Lipsi Island
Fig. 10f
2 km
Fig. 10d
Fig. 10e
2 km
Leros Island
Quaternary
Neogene sediment
Marina unit (cover + basement)
Temenia unit
Chl
Q
Blue Cam
400 µm
B
W
E
Cld
N60°E
2 cm
C
SW
NE
Chl
Chl + white Mica
200 µm
D
Green Grt
E
1 m
F

Figure 10

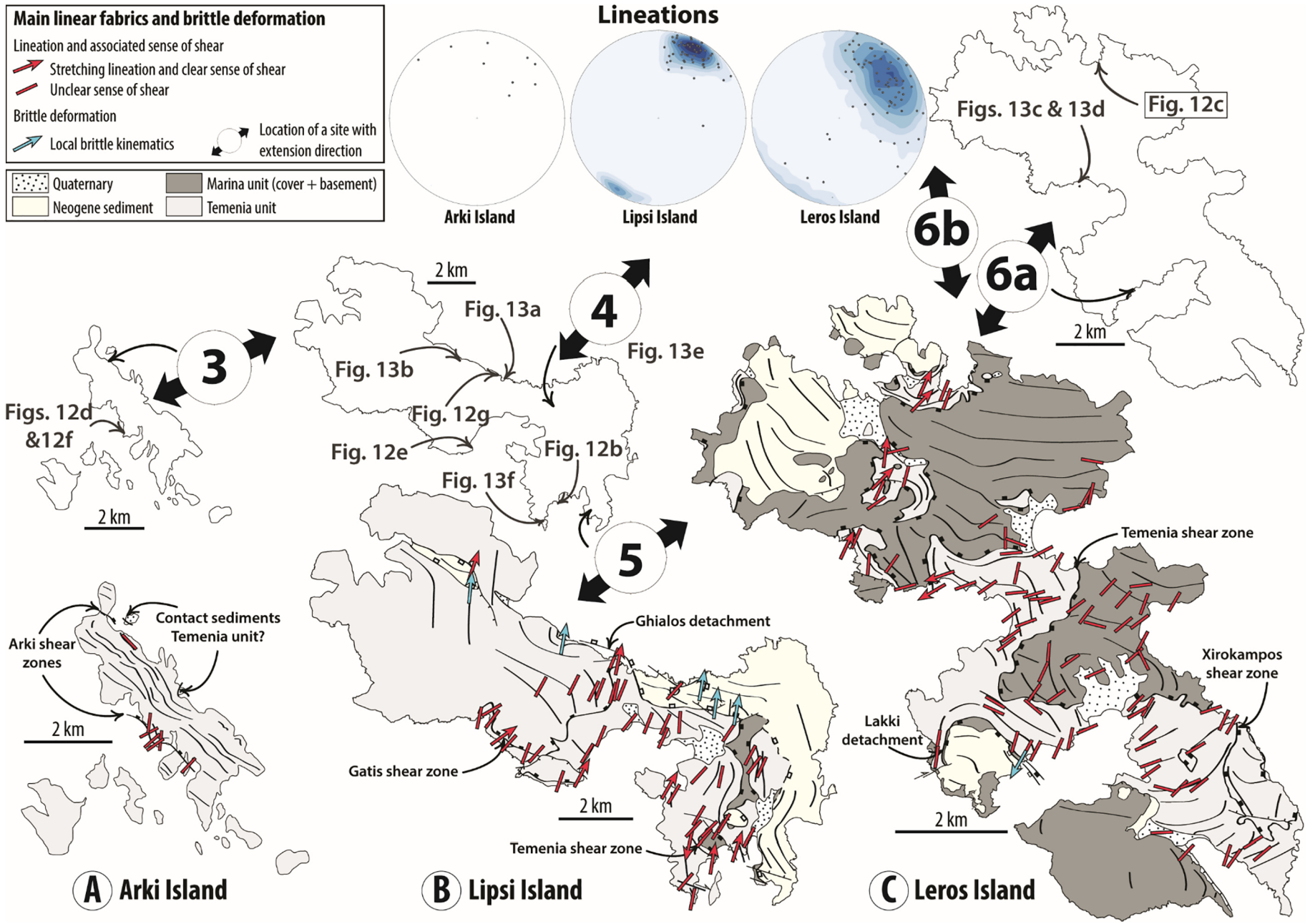
Main linear fabrics and brittle deformation
Lineation and associated sense of shear
Stretching lineation and clear sense of shear
Unclear sense of shear
Brittle deformation
Local brittle kinematics
Location of a site with extension direction
Quaternary
Neogene sediment
Marina unit (cover + basement)
Temenia unit
Lineations
Arki Island
Lipsi Island
Leros Island
Figs. 13c & 13d
Fig. 12c
6b
6a
2 km
3
4
5
Fig. 13a
Fig. 13b
Fig. 13e
Fig. 12g
Fig. 12e
Fig. 12b
Fig. 13f
Figs. 12d &12f
Contact sediments Temenia unit?
Arki shear zones
Ghialos detachment
Gatis shear zone
Temenia shear zone
Xirokampos shear zone
Lakki detachment
A Arki Island
B Lipsi Island
C Leros Island

Figure 11

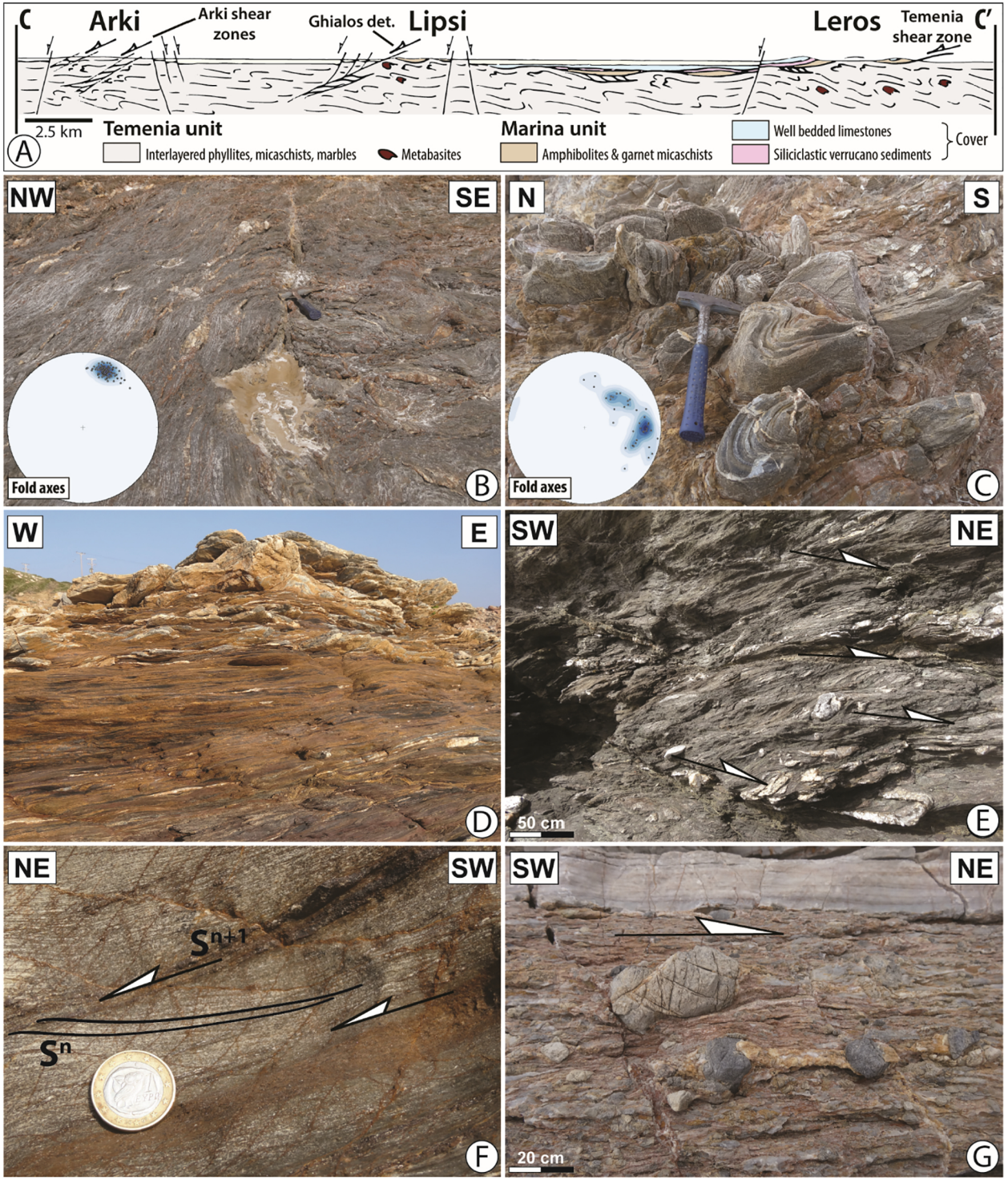
C
Arki
Arki shear zones
Ghialos det.
Lipsi
Leros
Temenia shear zone
C′
2.5 km
A
Temenia unit
Interlayered phyllites, micaschists, marbles
Metabasites
Marina unit
Amphibolites & garnet micaschists
Well bedded limestones
Siliciclastic verrucano sediments
Cover
NW
SE
Fold axes
B
N
S
Fold axes
C
W
E
D
SW
NE
50 cm
E
NE
SW
Sn+1
Sn
F
SW
NE
20 cm
G

Figure 12

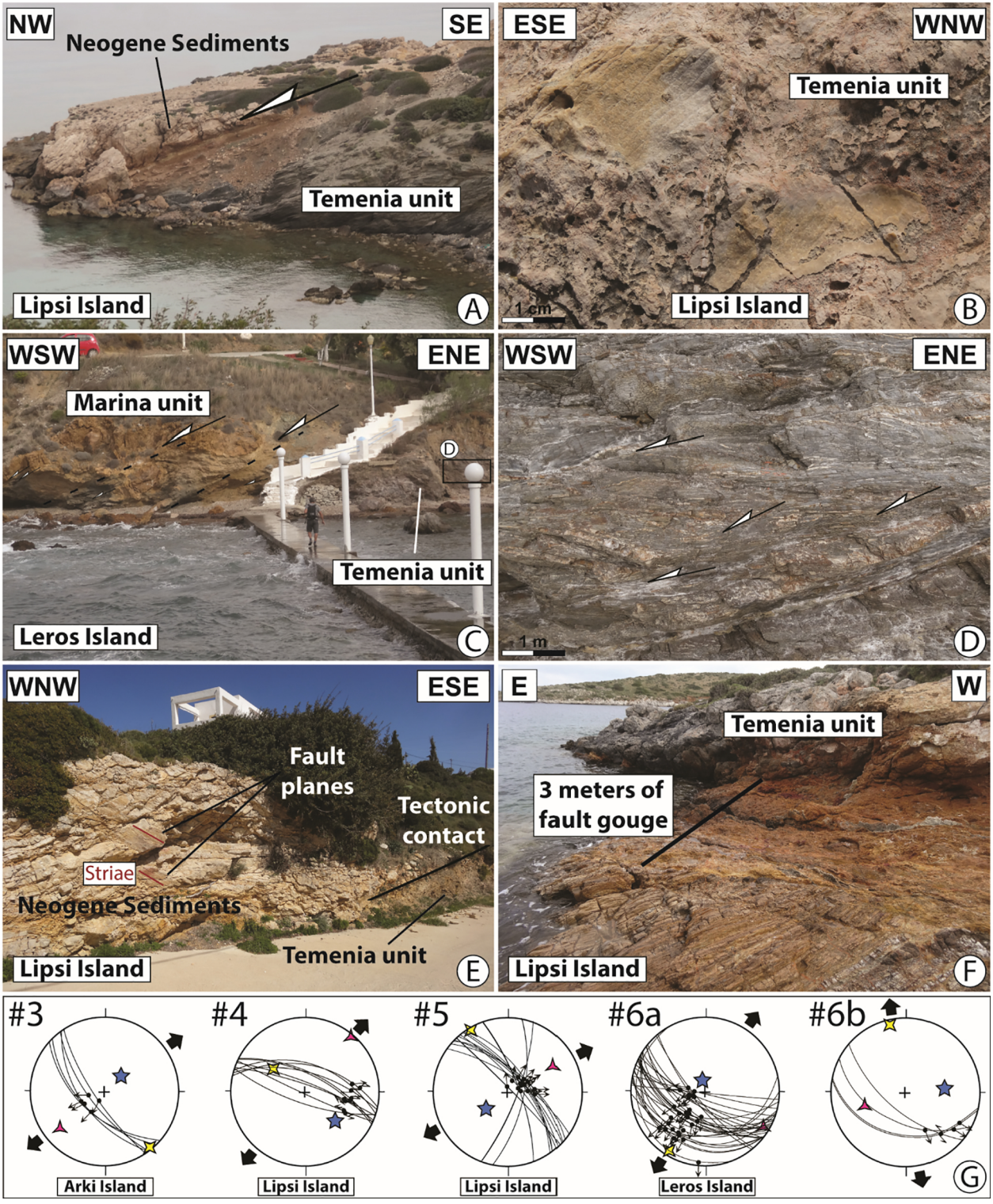
NW
SE
Neogene Sediments
Temenia unit
Lipsi Island
A
ESE
WNW
Temenia unit
1 cm
Lipsi Island
B
WSW
ENE
Marina unit
D
Temenia unit
Leros Island
C
WSW
ENE
1 m
D
WNW
ESE
Fault planes
Tectonic contact
Striae
Neogene Sediments
Temenia unit
Lipsi Island
E
E
W
Temenia unit
3 meters of fault gouge
Lipsi Island
F
#3
Arki Island
#4
Lipsi Island
#5
Lipsi Island
#6a
Leros Island
#6b
G

Figure 13

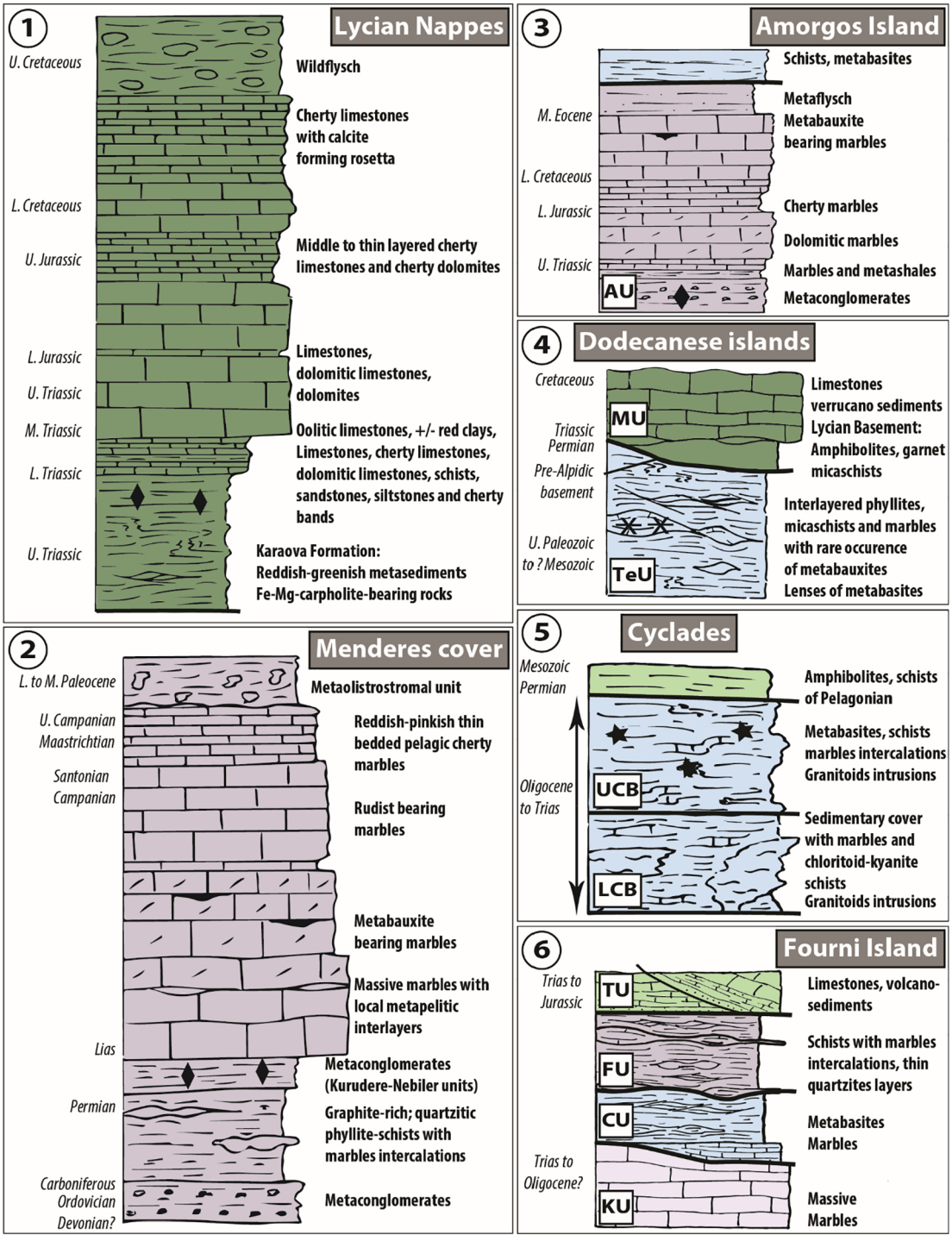
1
Lycian Nappes
U. Cretaceous
Wildflysch
Cherty limestones with calcite forming rosetta
L. Cretaceous
U. Jurassic
Middle to thin layered cherty limestones and cherty dolomites
L. Jurassic
U. Triassic
Limestones, dolomitic limestones, dolomites
M. Triassic
L. Triassic
Oolitic limestones, +/- red clays, Limestones, cherty limestones, dolomitic limestones, schists, sandstones, siltstones and cherty bands
U. Triassic
Karaova Formation: Reddish-greenish metasediments Fe-Mg-carpholite-bearing rocks
2
Menderes cover
L. to M. Paleocene
Metaolistrostromal unit
U. Campanian Maastrichtian
Reddish-pinkish thin bedded pelagic cherty marbles
Santonian Campanian
Rudist bearing marbles
Metabauxite bearing marbles
Massive marbles with local metapelitic interlayers
Lias
Metaconglomerates (Kurudere-Nebiler units)
Permian
Graphite-rich; quartzitic phyllite-schists with marbles intercalations
Carboniferous Ordovician Devonian?
Metaconglomerates
3
Amorgos Island
Schists, metabasites
M. Eocene
Metaflysch Metabauxite bearing marbles
L. Cretaceous
L. Jurassic
Cherty marbles
Dolomitic marbles
U. Triassic
Marbles and metashales
AU
Metaconglomerates
4
Dodecanese islands
Cretaceous
Limestones verrucano sediments
MU
Triassic Permian
Lycian Basement: Amphibolites, garnet micaschists
Pre-Alpidic basement
Interlayered phyllites, micaschists and marbles with rare occurence of metabauxites Lenses of metabasites
U. Paleozoic to ? Mesozoic
TeU
5
Cyclades
Mesozoic Permian
Amphibolites, schists of Pelagonian
Metabasites, schists marbles intercalations Granitoids intrusions
Oligocene to Trias
UCB
Sedimentary cover with marbles and chloritoid-kyanite schists Granitoids intrusions
LCB
6
Fourni Island
Trias to Jurassic
TU
Limestones, volcano-sediments
FU
Schists with marbles intercalations, thin quartzites layers
CU
Metabasites Marbles
Trias to Oligocene?
KU
Massive Marbles

Figure 14r1

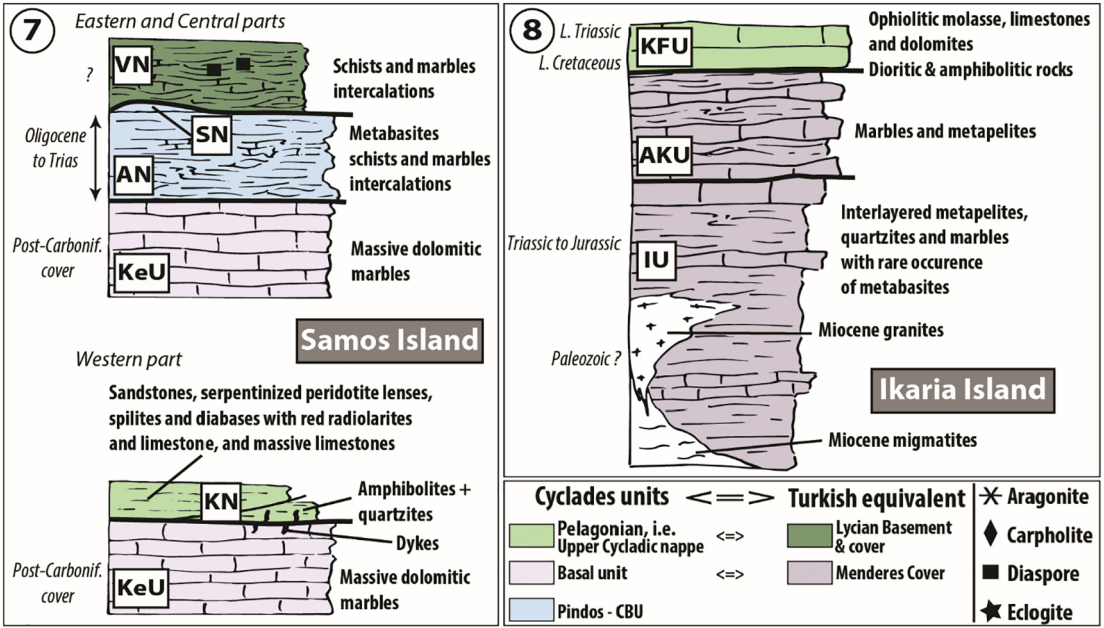
7
Eastern and Central parts
?
VN
Schists and marbles intercalations
Oligocene to Trias
SN
AN
Metabasites schists and marbles intercalations
Post-Carbonif. cover
KeU
Massive dolomitic marbles
Samos Island
Western part
Sandstones, serpentinized peridotite lenses, spilites and diabases with red radiolarites and limestone, and massive limestones
KN
Amphibolites + quartzites
Dykes
Post-Carbonif. cover
KeU
Massive dolomitic marbles
8
L. Triassic
L. Cretaceous
KFU
Ophiolitic molasse, limestones and dolomites
Dioritic & amphibolitic rocks
AKU
Marbles and metapelites
Triassic to Jurassic
IU
Interlayered metapelites, quartzites and marbles with rare occurence of metabasites
Miocene granites
Paleozoic ?
Ikaria Island
Miocene migmatites
Cyclades units <==> Turkish equivalent
Pelagonian, i.e. Upper Cycladic nappe
<=>
Lycian Basement & cover
Basal unit
<=>
Menderes Cover
Pindos - CBU
Aragonite
Carpholite
Diaspore
Eclogite

Figure 14r2

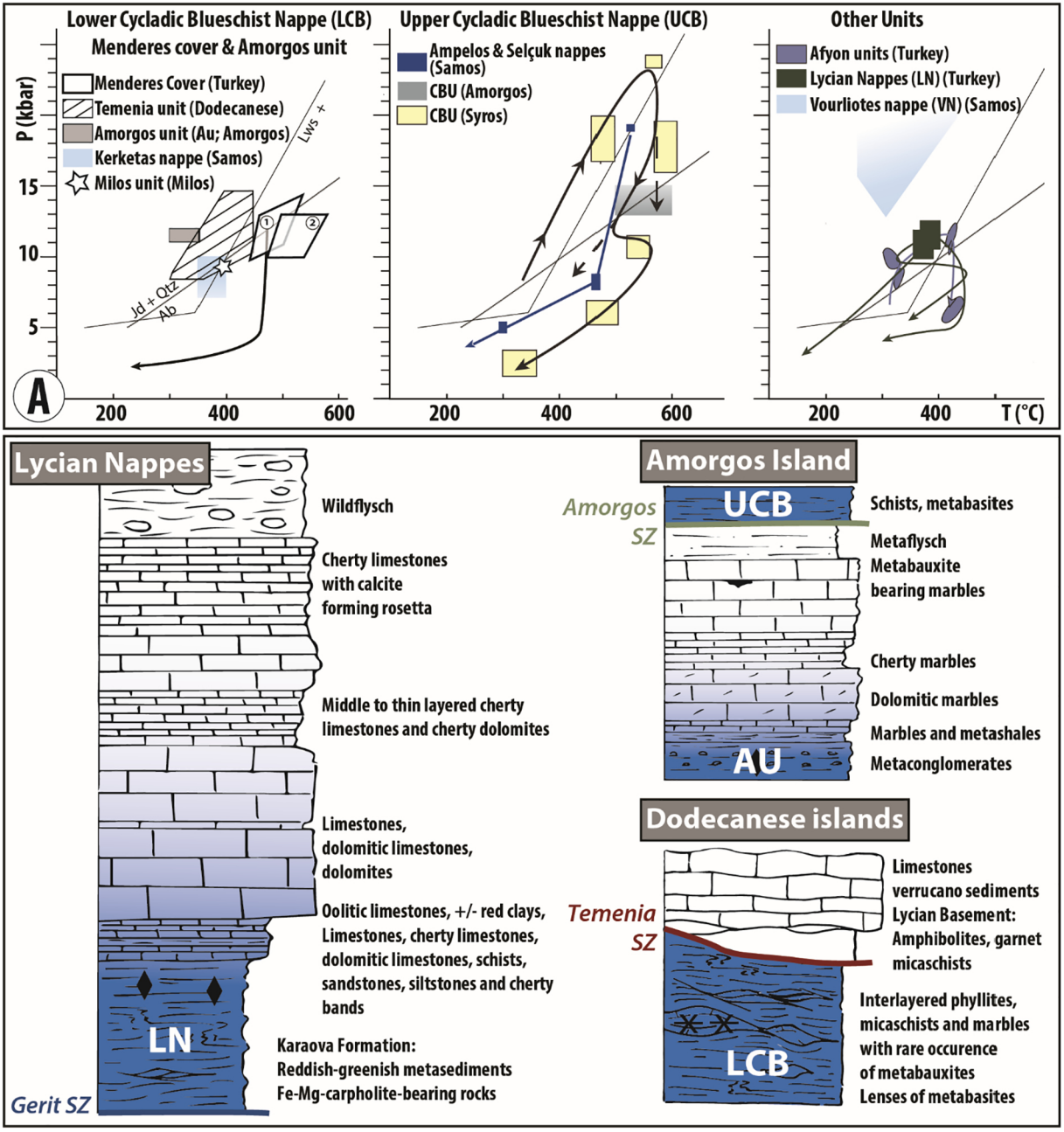
Lower Cycladic Blueschist Nappe (LCB)
Menderes cover & Amorgos unit
Menderes Cover (Turkey)
Temenia unit (Dodecanese)
Amorgos unit (Au; Amorgos)
Kerketas nappe (Samos)
Milos unit (Milos)
Lws +
Jd + Qtz
Ab
P (kbar)
15
10
5
A
200
400
600
Upper Cycladic Blueschist Nappe (UCB)
Ampelos & Selçuk nappes (Samos)
CBU (Amorgos)
CBU (Syros)
200
400
600
Other Units
Afyon units (Turkey)
Lycian Nappes (LN) (Turkey)
Vourliotes nappe (VN) (Samos)
200
400
T (°C)
Lycian Nappes
Wildflysch
Cherty limestones with calcite forming rosetta
Middle to thin layered cherty limestones and cherty dolomites
Limestones, dolomitic limestones, dolomites
Oolitic limestones, +/- red clays, Limestones, cherty limestones, dolomitic limestones, schists, sandstones, siltstones and cherty bands
LN
Karaova Formation:
Reddish-greenish metasediments
Fe-Mg-carpholite-bearing rocks
Gerit SZ
Amorgos Island
Amorgos SZ
UCB
Schists, metabasites
Metaflysch
Metabauxite bearing marbles
Cherty marbles
Dolomitic marbles
Marbles and metashales
Metaconglomerates
AU
Dodecanese islands
Temenia SZ
Limestones verrucano sediments
Lycian Basement:
Amphibolites, garnet micaschists
Interlayered phyllites, micaschists and marbles with rare occurence of metabauxites
Lenses of metabasites
LCB

Figure 15r1

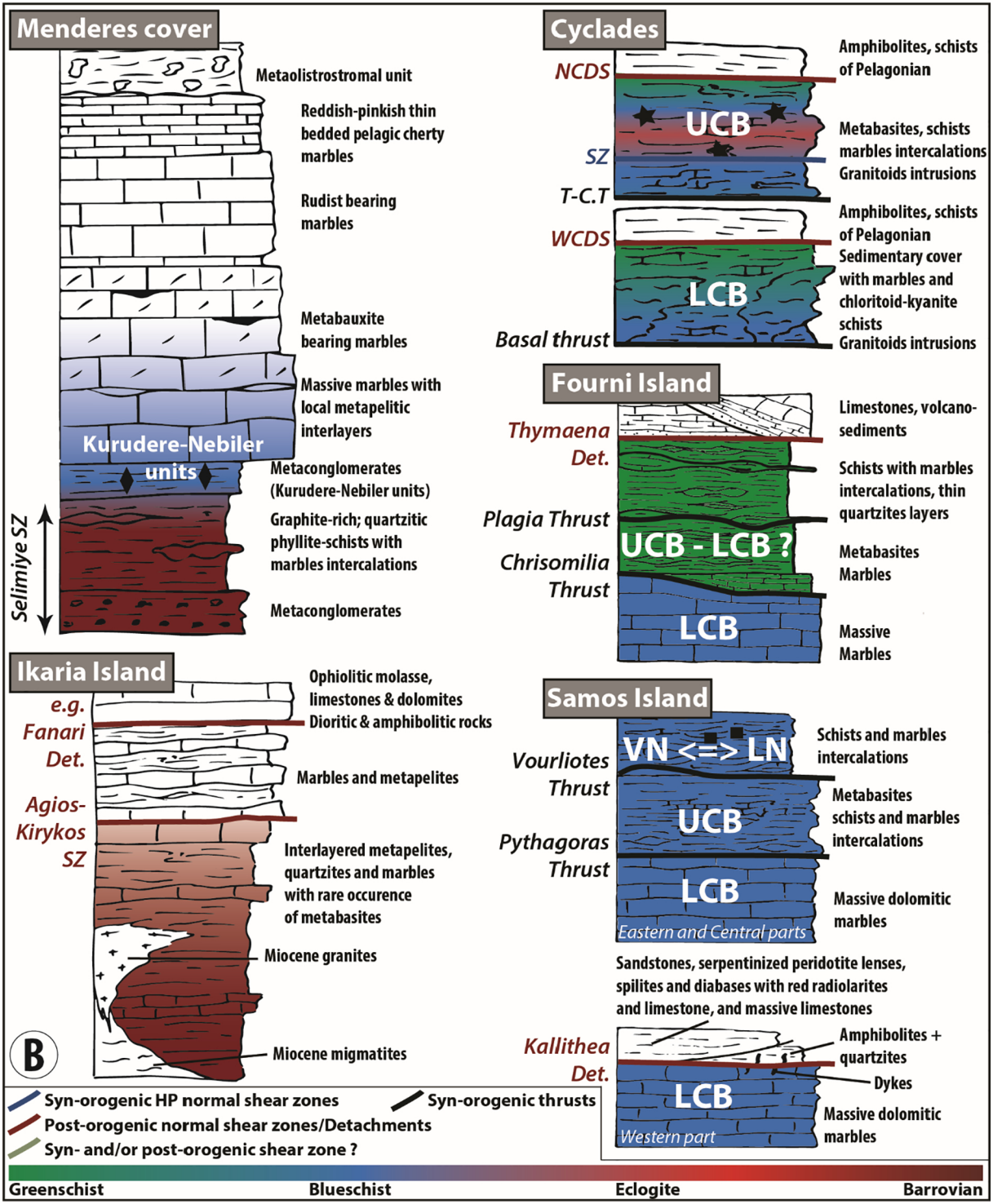
Menderes cover
Metaolistrostromal unit
Reddish-pinkish thin bedded pelagic cherty marbles
Rudist bearing marbles
Metabauxite bearing marbles
Massive marbles with local metapelitic interlayers
Kurudere-Nebiler units
Metaconglomerates (Kurudere-Nebiler units)
Graphite-rich; quartzitic phyllite-schists with marbles intercalations
Metaconglomerates
Selimiye SZ
Cyclades
NCDS
UCB
SZ
T-C.T
WCDS
LCB
Basal thrust
Amphibolites, schists of Pelagonian
Metabasites, schists marbles intercalations Granitoids intrusions
Amphibolites, schists of Pelagonian
Sedimentary cover with marbles and chloritoid-kyanite schists
Granitoids intrusions
Fourni Island
Thymaena Det.
Plagia Thrust
UCB - LCB ?
Chrisomilia Thrust
LCB
Limestones, volcano-sediments
Schists with marbles intercalations, thin quartzites layers
Metabasites Marbles
Massive Marbles
Ikaria Island
e.g. Fanari Det.
Agios-Kirykos SZ
Ophiolitic molasse, limestones & dolomites
Dioritic & amphibolitic rocks
Marbles and metapelites
Interlayered metapelites, quartzites and marbles with rare occurence of metabasites
Miocene granites
Miocene migmatites
B
Samos Island
Vourliotes Thrust
Pythagoras Thrust
VN <=> LN
UCB
LCB
Eastern and Central parts
Schists and marbles intercalations
Metabasites schists and marbles intercalations
Massive dolomitic marbles
Sandstones, serpentinized peridotite lenses, spilites and diabases with red radiolarites and limestone, and massive limestones
Kallithea Det.
LCB
Western part
Amphibolites + quartzites
Dykes
Massive dolomitic marbles
Syn-orogenic HP normal shear zones
Post-orogenic normal shear zones/Detachments
Syn- and/or post-orogenic shear zone ?
Syn-orogenic thrusts
Greenschist
Blueschist
Eclogite
Barrovian

Figure 15r2

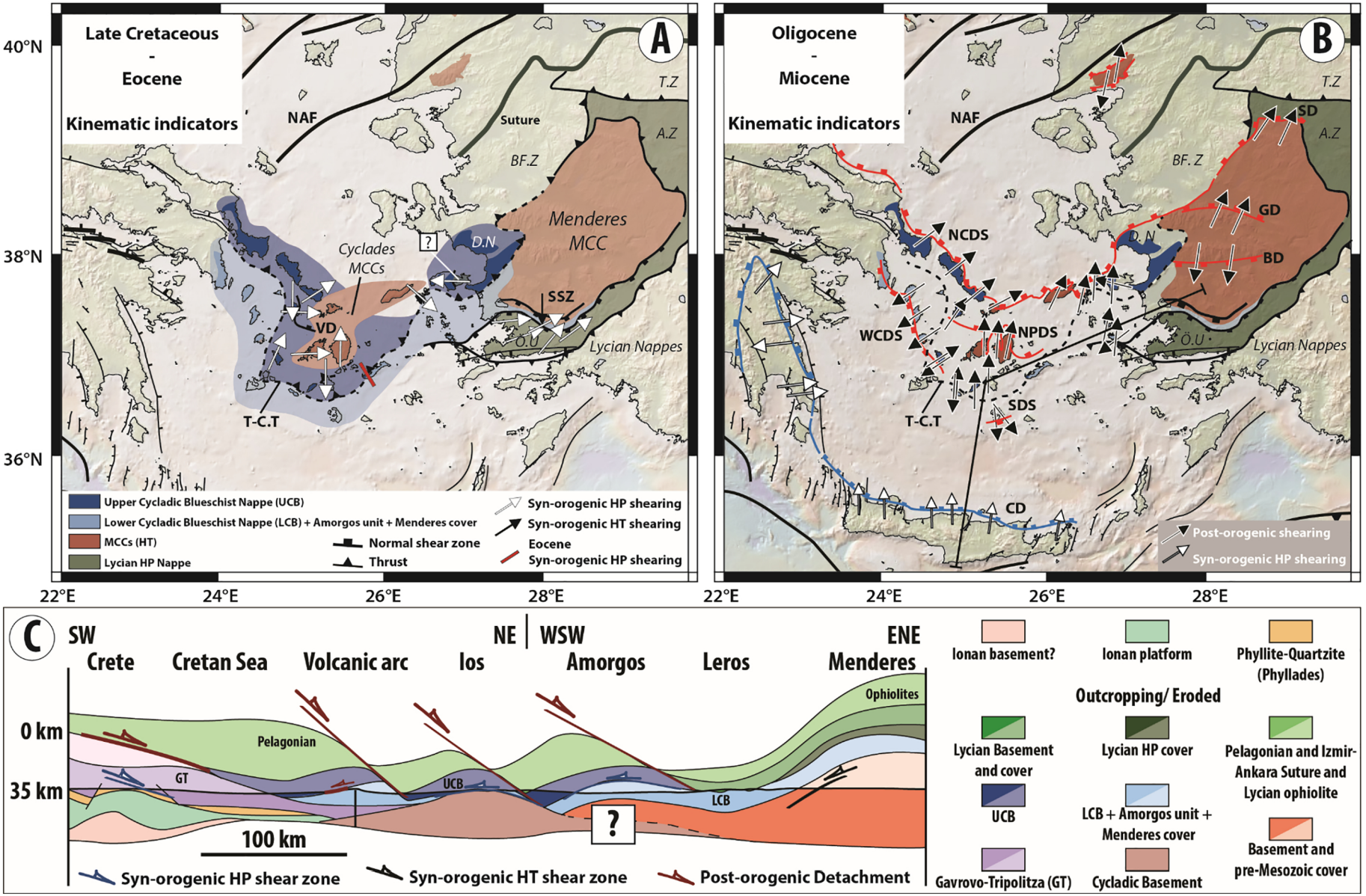
Late Cretaceous
-
Eocene
Kinematic indicators
A
NAF
Suture
T.Z
A.Z
BF.Z
Menderes
MCC
Cyclades
MCCs
D.N
SSZ
VD
T-C.T
Ö.U
Lycian Nappes
Oligocene
-
Miocene
Kinematic indicators
B
NCDS
WCDS
NPDS
SDS
CD
GD
BD
SD
40°N
38°N
36°N
22°E
24°E
26°E
28°E
Upper Cycladic Blueschist Nappe (UCB)
Lower Cycladic Blueschist Nappe (LCB) + Amorgos unit + Menderes cover
MCCs (HT)
Lycian HP Nappe
Normal shear zone
Thrust
Syn-orogenic HP shearing
Syn-orogenic HT shearing
Eocene
Syn-orogenic HP shearing
Post-orogenic shearing
Syn-orogenic HP shearing
C
SW
Crete
Cretan Sea
Volcanic arc
NE
WSW
Ios
Amorgos
Leros
ENE
Menderes
Ophiolites
Pelagonian
GT
UCB
LCB
0 km
35 km
100 km
Syn-orogenic HP shear zone
Syn-orogenic HT shear zone
Post-orogenic Detachment
Ionan basement?
Ionan platform
Phyllite-Quartzite (Phyllades)
Outcropping/ Eroded
Lycian Basement and cover
Lycian HP cover
Pelagonian and Izmir-Ankara Suture and Lycian ophiolite
UCB
LCB + Amorgos unit + Menderes cover
Basement and pre-Mesozoic cover
Gavrovo-Tripolitza (GT)
Cycladic Basement

Figure 16